NEUROPATHOLOGY OF PYRIDOXINE TOXICITY

by

Manuel Melo Pires

A thesis submitted for the degree of

Doctor of Philosophy

in the

University of London

Department of Neuropathology
Institute of Neurology
The National Hospital for
Neurology and Neurosurgery
Queen Square
London WC1N 3BG

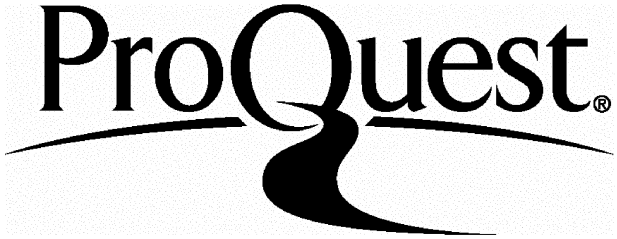

ABSTRACT

Pyridoxine can cause sensory neuropathy in man. Previous experimental studies have demonstrated selective neurofilament accumulation in dorsal root ganglion cells which, in most cases, was associated with axonal damage without causing cell death, but in others produced death of cells.

From these observations the following hypotheses were formulated and tested in this thesis.

1. Pyridoxine interferes with axonal transport of neurofilaments and organelles and would thus cause a dying back neuropathy.
2. As the dorsal root ganglion cells, in many cases, do not die, regeneration should take place.
3. The major action of pyridoxine in causing a dying back neuropathy is due to interference with dorsal root ganglion cell metabolism rather than a local effect on the axon.

A total of 100 rats was used in these experiments. In the first group of animals, rats were dosed daily with pyridoxine for periods of 7-90 days. Following perfusion with fixative, fifth cranial nerve, dorsal root and autonomic ganglia, the saphenous nerve (a purely sensory nerve) were removed and examined by light and electron microscopy. Immunocyto-chemistry was performed using the RT97 antibody against phosphorylated neurofilaments. Axonal degeneration, axonal regeneration, neurofilament

and microtubule numbers and distribution were quantified.

In the second group of animals the sciatic nerve was crushed immediately followed by the intraneural injection of pyridoxine and the degree of axon degeneration and regeneration were quantified.

Damage to dorsal root ganglion cells (used as a measure of toxicity) was very variable so that the effects were only approximately dose-related. The hypotheses set out above were all proved in that:

1. There was distal degeneration of axons tending to affect the largest myelinated nerve fibres but also affecting the unmyelinated fibres. Posterior column axons in the spinal cord showed severe damage.
2. Affected dorsal root ganglion cells showed dispersion and degranulation of rough endoplasmic reticulum (RER), active Golgi bodies and increased neurofilaments. Immunocytochemistry showed increased staining for phosphorylated neurofilaments within small dorsal root ganglion cells compatible with interference with axonal transport.
3. Neurofilaments within axons were reduced and there was clustering of microtubules which probably preceded:
4. Axonal atrophy.
5. Axonal regeneration occurred while dosing continued.
6. Intraneural injection of pyridoxine caused axonal degeneration but paradoxically appeared to stimulate axonal regeneration.

The results of this study suggests that pyridoxine has a direct toxic effect upon dorsal root ganglion cells which interferes with axoplasmic transport and thus results in a "dying back" neuropathy. The biochemical actions involved remain to be elucidated.

ACKNOWLEDGEMENTS

I would like to thank my supervisor, Dr Jean Jacobs, for her teaching and guidance at all stages of the work leading to the completion of this thesis. I am also very grateful to her son Mr S Jacobs for the templates used for the quantitative studies. Professor Leo Duchen gave me the chance to come to London and work in his department. Both he and Professor Francesco Scaravilli supported and encouraged the progress of my work, and I wish to thank them.

Although I am indebted particularly to Mr Andrew Beckett, Mr Paul Carter and Miss Hilary Ayling for their technical support and to Mr Steve Durr for the photographic material, I wish to thank all my colleagues and the technical staff of the department for their collaboration. Mrs M B Bailey and the staff of the Rockefeller Library at the Institute of Neurology were of invaluable help in the search for difficult references.

Miss Janet Simpson should be thanked not only for her skill in the preparation of the manuscript, tables and figures, but also for showing great patience.

I would like to dedicate this thesis to Minal, Malini and Rahul.

CONTENTS

INTRODUCTION

Pyridoxine, together with pyridoxal and pyridoxamine, form the vitamin B_6 group. In their phosphorylated forms, they act as coenzymes in more than 50 enzyme reactions, and are of particular importance in the central nervous system.

Interest in deficiency states has largely been replaced (in the Western world) by concern as to the neurotoxic effects of large, or even modest, doses of pyridoxine. A number of human cases of a purely sensory neuropathy have been reported in recent years, mostly in patients taking pyridoxine regularly for premenstrual syndrome or as a vitamin supplement.

Experimental studies have shown that large doses of pyridoxine also cause a sensory neuropathy in different species. Pyridoxine may cause degeneration of dorsal root ganglion cells - or it may cause an axonopathy due to sublethal damage to the ganglion cells. The details of the pathological processes involved have not been elucidated. The aim of this study was to establish the pathology of the neuropathy produced in experimental animals by the administration of pyridoxine.

The approach was firstly to define the distribution of pathological changes. Pyridoxine is one of the relatively few neurotoxic substances which acts directly, and selectively, on a neuronal cell body in the peripheral nervous system. It was therefore anticipated that the distribution of the pathology was related to vascular permeability, and particular attention was paid to regions known to be without a blood-nerve barrier including dorsal root ganglia, autonomic ganglia and the myenteric plexus.

A second aim was to study dose-related pathology. The earliest experimental studies described degeneration of dorsal root ganglion cells after large doses of pyridoxine. More recent studies suggested that chronic administration of small doses only caused axonal degeneration. Pyridoxine induced neuropathy was likely to represent a model of a "dying back" neuropathy in the sense originally used by Gowers (1886), similar to some naturally occurring diseases.

A third aim was, therefore, to study the pathogenesis of pyridoxine-induced axonal degeneration; to investigate whether the process began distally and moved proximally, to discover whether the axons developed atrophy and, if so, whether this affects all or only a distal part of the axon, to show if there was a selective effect on fibres of different sizes or of different lengths.

As a result of these observations and aims it was possible to test the following hypotheses:

1. Pyridoxine interferes with axonal transport of neurofilaments and organelles and would thus cause a dying back neuropathy.

2. As the dorsal root ganglion cells, in many cases do not die, regeneration should take place.

3. The major action of pyridoxine in causing a dying-back neuropathy is due to interference with dorsal root ganglion cell metabolism rather than a local effect on the axon.

CHAPTER 1. REVIEW OF THE LITERATURE

PYRIDOXINE

Pyridoxine history

Vitamin B_6 was first recognized as a distinct vitamin entity by Gyorgy (1934; 1935) as the rat acrodynia preventing factor, and two years later, by Lepkvosky, Jukes and Krause (1936) as an essential nutrient for chickens. Vitamin B_6 subsequently became known, through the research of Snell et al (1942) with microorganisms, as a complex of active compounds. Isolation of pyridoxine, the principal component, was accomplished in 1938 by five different teams acting independently. It was followed by synthesis by four other teams in 1939.

Pyridoxine as the hydrochloride salt has been in commercial production since the early 1940's. Pyridoxine, 2-methyl-3-hydroxy-4,5-bis pyridine, or 5-hydroxy-6-methyl-3,4-pyridine-dimethanol, has the empirical formula $C_8H_{11}NO_3$. Since then, production of pyridoxine hydrochloride has constantly increased, and the bulk selling price in terms of dollars per kilo has decreased from several thousand to 50 dollars or less. As currently produced, pyridoxine hydrochloride meets all specifications of the U.S. Pharmacopeia XIX (1975) and Food Chemicals Codex II (1972).

Pyridoxine metabolism

Vitamin B_6 is the name which is used to describe the major forms of

3-hydroxy-5-hydroxymethyl-2-methylpyridine(pyridoxine,pyridoxamineand pyridoxal). Each of these forms also exists as the phosphorylated form. Pyridoxine is also found in some plant foods as the 5'-ß-glucoside (Kabir, Leklem and Miller, 1983). To date, this form of vitamin B_6 has not been detected in any animal tissue. The major form found in animal products is pyridoxal, which is probably present primarily as the phosphorylated form (Leklem, 1988). In plant foods, the primary forms are pyridoxine and, in some species pyridoxamine.

Absorption of vitamin B_6 has been less well studied in humans than in other animal species (Henderson, 1985). In the rat, intestinal absorption of pyridoxine and the other two forms occurs via a non saturable, passive process (Middleton, 1982).

While there is interconversion of the three forms of vitamin B_6 in the intestinal cell (Henderson, 1985), the primary forms which leave the intestinal cell and are transported to the liver are the forms which were initially absorbed. Uptake into the liver occurs by facilitated diffusion. The liver is the primary organ for the interconversion and metabolism of the three forms of vitamin B_6. Two metabolic steps are common to all the three forms. These are phosphorylation, in which a phosphate group is attached via pyridoxal kinase, and dephosphorylation by action of a phosphatase (Merril et al, 1986). Two of the phosphorylated compounds, pyridoxine 5'-phosphate and pyridoxamine 5'-phosphate are then converted to pyridoxal 5'-phosphate (PLP) through the action of a phosphate oxidase.

The PLP formed is either utilized in the liver or released to the

circulation. The liver is considered to be responsible for the synthesis of the PLP found in the plasma (Lumeng, Brashear and Li, 1974). However, Leklem and Shultz, 1983, have suggested that muscle reservoirs of PLP may serve as a source of PLP under conditions of caloric deficit. PLP in the circulation is bound primarily to albumin, a mechanism which protects the PLP from hydrolysis and also permits delivery of PLP to other tissues.

Plasma also contains other forms of vitamin B6 in addition to PLP. Under normal conditions, plasma PLP accounts for 60-70% of the total vitamin B6 present. Pyridoxal is the next most abundant form, with lower levels of pyridoxine and pyridoxamine. The role of the erythrocyte in vitamin B6 metabolism consists in converting pyridoxal and pyridoxine in PLP, both pyridoxal and PLP are bound to haemoglobin (Ink and Henderson, 1984). In the rat, pyridoxine can be converted to pyridoxine-phosphate in most tissues, since they have kinase activity (McCormick, Gregory and Snell, 1961). However, conversion to PLP does not occur in many tissues because the oxidase enzyme is absent (Pogell, 1958). The extent to which the kinase and oxidase enzymes are present in tissues other than the human liver (Merril et al, 1984), brain (McCormick and Snell, 1959), and erythrocytes, is limited. In muscle, a majority of the vitamin is present as PLP bound to glycogen phosphorylase (Black, Guirard and Snell, 1978).

There are species differences in the rate of excretion of vitamin B6. Rats excrete 80% of administered pyridoxine per day, in contrast to dogs who excrete 20% (Scudi, Unna and Antopol, 1940).

Functions of vitamin B6

The diversity of biochemical reactions involving the coenzymatic forms of pyridoxine (vitamin B6) is well recognized. There are over 100 PLP dependent enzymes. Most are involved in catabolic reactions of various amino acids.

Neurotransmission: The crucial role played by pyridoxine in the nervous system is evident from the fact that neurotransmitters, like dopamine, norepinephrine, serotonin, gamma-aminobutyric acid and taurine, as well as sphingolipids are synthesized by PLP-dependent enzymes (Reynolds and Leklem, 1985). There is considerable variation in the affinity of different apoenzymes for PLP. This explains the differential susceptibility of various PLP enzymes shown by decreased activity during progression of pyridoxine deficiency (Dakshinamurti, 1977). Of the pyridoxine-dependent enzymes, three, namely glutamic acid decarboxylase, 5-hydroxytryptophan decarboxylase, and ornithine decarboxylase, are critical and can account for most of the neurological effects of pyridoxine deficiency in animals (Coburn and Townsend, 1989).

One of the most extensive vitamin B_6 amino acid inter-relationships is that related to tryptophan-niacin metabolism (Henderson and Hulse, 1978). This in part explains the use of the tryptophan load test to assess vitamin B_6 status. There is only one step in the conversion of tryptophan to nyacin that is a PLP requiring step.

Gluconeogenesis: This is another cellular process in which PLP plays an important role: Glycogen phosphorylase is PLP dependent enzyme,

involved in glucose homeostasis. In muscle the PLP associated with glycogen phosphorylase does not serve as a source for vitamin B6 during its deficiency, except with a calorie deficit (Black, Guirard and Snell, 1978).

Erythrocyte function: Vitamin B_6 also has a role in erythrocyte function and metabolism. Both PLP and pyridoxal bind to haemoglobin and PLP binds to erythrocyte aminotransferases. As a result of this binding, the erythrocyte may serve as an additional reservoir for vitamin B_6. The conditions under which this reservoir may provide vitamin B6 is not known. The binding of PLP to the B chain of haemoglobin S or A lowers the oxygen binding capacity (Maeda et al, 1980).

Steroid function: One of the areas of cellular function in which PLP acts is steroid function (Litwack et al, 1985). Several studies have shown that PLP can be used as an effective tool in extracting steroid receptors from tissues in which the steroid is acting (Compton and Cidlowski, 1986). The physiological significance of this PLP-steroid receptor interaction for humans remains to be determined.

Such diversity and complexity indicates that the vitamin B_6 nutritional status and needs of a person (healthy or diseased) extend beyond the role PLP plays in amino acid metabolism.

PYRIDOXINE NEUROTOXICITY

Medical use and abuse of vitamins

Vitaminotherapy, which began in the 18th century, can be divided into three eras: the prevention and treatment of diseases of deficiency, the treatment of vitamin responsive inborn errors of metabolism and the currently popular "orthomolecular" megadosage (Rudman and Williams, 1983). Vitamins are divided into the nine water soluble and the four fat soluble agents. The water soluble vitamins and their derivatives were eventually found to function as co-enzymes for apo-enzymes.

The minimum daily requirements (MDR) that have been established for vitamins are designed to protect normal, healthy people from deficiency syndromes. The MDR is set at a level above which demonstrable signs of deficiency appear. The recommended daily allowances (RDAs) are set at levels two to six times higher than the MDRs and, therefore, represent an ample intake for the general population. The RDAs of water soluble vitamins range from 0.5 mg to 100 mg a day.

The early 1970s witnessed the popularization of vitamin "megadoses", usually at intakes of 200-600 times the RDA, or 100 mg to 5g a day (Hodges, 1982). Vitamins in megadoses can cause harmful effects. The toxicity of fat soluble vitamins A and D at doses 10 times higher than the RDA has been well established (Woolliscroft, 1983). Previously, megadoses of water soluble vitamins were considered to cause little problem, since it was assumed that they were rapidly cleared from the body.

However, it is now known that large doses of pyridoxine, and even relatively modest doses, can produce neurotoxic effects.

Fat soluble vitamins and neurotoxicity

The fat soluble vitamins (A,D,E and K), unlike the water soluble vitamins, are stored in the body when ingested in excess. As a consequence, the potential for toxicity is greater. However, an individual may ingest toxic doses of a fat-soluble vitamin, and, because there are adequate levels of another fat soluble vitamin, clinical signs and symptoms of toxicity may be avoided. Conversely, deficiency of one or more of these vitamins may exaggerate the toxic effects of others. It has been shown that high or adequate levels of vitamin A protect against vitamin D toxicity and vice versa. Similarly, high levels of vitamin E protect against vitamin A and D toxicity (Stults, 1981). The nature of these interactions remains to be elucidated. However, this may be an explanation as to why some patients appear to be able to ingest toxic doses of fat soluble vitamins without developing either chronic or acute symptoms of toxicity (Woolliscroft, 1983).

Because vitamin A is fat soluble, excess vitamin A is stored in the body, primarily in the liver. Toxicity can be either acute or chronic. The incidence of acute vitamin A toxicity is extremely low; however, the number of patients with chronic vitamin A toxicity is raising (Smith and Goodman, 1976). Increased intracranial pressure is the most common clinical presentation. Children are more prone to develop manifestations of toxicity

than adults. In infants doses of vitamin A of 300,000 IU or more and in adults of 1,000,000 IU or more have been reported to cause toxicity (Korner and Vollm, 1975).

Although Woolliscroft(1983) notes that vitamin D megadoses may cause a polyneuropathy, there is no other reported evidence of it, nor any details of neurotoxicity. Vitamin E and vitamin K are not neurotoxic, other than in infants.

Experimental pyridoxine neurotoxicity

The neurotoxic effects of massive doses of vitamin B_6 (pyridoxine) in experimental animals were reported by Antopol and Tarlov (1942) at the time of its introduction into clinical medicine. Since the amount of pyridoxine needed to intoxicate animals was far in excess of that recommended, at the time, to treat human patients, the results of experimental neurotoxicity did not seem to have any relationship to a possible adverse effect of vitamin B_6 on man.

Pyridoxine has been used as an experimental tool in toxicological research. The LD_{50} of pyridoxine hydro-chloride given orally is 5.5 g/kg in the rat (Unna and Antopol, 1940). Antopol and Tarlov (1942) gave rats doses of pyridoxine close to, and above, the LD_{50} and described degeneration of posterior columns and degeneration or chromatolysis of dorsal root ganglion cells. The absence of changes in autonomic ganglion cells was noted.

Similar changes were found in dogs given rather small doses.

Phillips et al (1978) gave dogs smaller amounts of pyridoxine which caused degeneration in the dorsal columns and in dorsal roots. No mention was made of dorsal root ganglion cell changes. Measurements of pyridoxine were made in various organs including the brain and spinal cord: levels were low in all except the liver, but high in the blood.

Krinke et al (1978) showed degeneration of the primary sensory endings in rats which coincided with the onset of ataxia. There was a corresponding decrease in the number of large nerve fibres. Later, Krinke et al (1980) gave pyridoxine to dogs and showed the selective vulnerability of neurons in the dorsal root and Gasserian ganglia, and the degeneration of their central and peripheral axons. Windebank et al (1985) gave rats relatively small doses of pyridoxine and found specific degeneration of sensory axons. In studies of teased fibres about 25% of fibres showed signs of axonal degeneration in both the proximal and distal nerves. (However, because of sampling problems, quantitative studies are not recommended on teased nerve preparations). A few fibres underwent segmental demyelination and remyelination. There was a striking difference in changes in the ventral and dorsal roots; the ventral roots were unaffected whereas there were many degenerating fibres in the dorsal roots. In the dorsal root ganglion (DRG) of intoxicated animals there was increased separation of cellular elements. Rarely neurons contained an intracytoplasmic vacuole. (The pathological significance of these is not clear, since they may also be found in control animals). This study demonstrated that a toxin capable of causing rapid nerve cell death at high doses can, with chronic lower doses,

cause degeneration of the axons emanating from these same cells while sparing the perikaryon.

Montpetit et al (1988) showed in beagle dogs, four days after initiation of treatment with pyridoxine, that there was an accumulation of neurofilaments (NFs) in the proximal unmyelinated segment of myelinated axons of the DRG cells. In the cytoplasm, the Golgi complexes were abundant and the Nissl bodies together with the Nfs appeared increased in numbers. At 10 days NF and microtubule (MT) aggregates were apparent in both perikaryal and proximal cell processes. These findings suggested that an early morphological correlate of pyridoxine neurotoxicity was the accumulation of Nfs in the unipolar process of the DRG in the absence of extensive vacuolation. It was suggested that this phenomenon could be related to an increased rate of NF protein synthesis together with mechanical defects of transport.

Xu, Sladky and Brown (1989) demonstrated that the manifestations of intoxication in the rat vary according to the dose and rate of pyridoxine administration. High doses provoked decreased volume of large light cells, followed by necrosis. Lower doses implicated a sublethal metabolic injury leading to perikaryal and axonal atrophy.

Yamamoto (1991), using very high doses of pyridoxine in the rat for 1-7 days, showed accumulation of mitochondria, vesicles, multilamellar and dense bodies in the nodal and paranodal regions of myelinated fibres on the second day of injection preceding the degeneration of peripheral and central axons. (This information was obtained from an abstract as the original paper

was in Japanese).

In cultured dorsal root ganglia Windebank (1985) showed inhibition of neuritic outgrowths from dorsal root ganglion cells at a pyridoxine concentration of 10^{-3}M, and no outgrowth occurred at 10^{-2}M. At the latter concentration it appeared that many of the ganglion cells were dying, but if they were returned to the control medium after 6 days, sparse neuritic outgrowth occurred, indicating that some ganglion cells survived. With concentrations of 10^{-1}M all ganglion cells were dead within 3 days. The pyridoxine analogues had different effects on the rate of neurite outgrowth. Pyridoxal and pyridoxamine produced inhibition at a similar concentration to pyridoxine, between 10^{-3} and 10^{-4}M. Pyridoxic acid produced no effect, even at 10^{-2}M, demonstrating that only those compounds that can be phosphorylated to an active coenzyme are neurotoxic.

Pyridoxine neurotoxicity in man

Orthomolecular therapy with megadoses of vitamin B_6 has been employed in several psychiatric disorders (Pauling, Robinson and Oxley, 1973; Rimland, Callaway and Dreyfus, 1978). The effects belong to the field of speculation, as is also the case when used in the treatment of poor memory, nausea, oedema of unclear aetiology and nutritional regimes for body building. Probably the most frequent indication for using high doses of pyridoxine is the premenstrual syndrome (PMS): several publications, including double blind studies, document a partial improvement of the symptoms of this psychoneuroendocrine syndrome (Gunn, 1985). The doses

applied range from 40 to 500 mg/day. However, some patients do not respond to the therapy, which is not surprising in view of the complexity of the syndrome. Advertising, as well as recommendation, often leads to self medication, with the effect that the dose is progressively increased when the measures prove to be ineffective.

Toxic side effects were observed by Schaumburg et al (1983) after long term intake of high doses. The first report comprised six female and two male patients who had taken between 2 and 6g pyridoxine per day for long periods. Four cases involved self medication as a diet supplement and in one case the patient followed the recommendation of a health magazine on treatment of premenstrual oedema. In two cases, the treatment had been prescribed by a gynaecologist for oedema, and in one case it had been prescribed by an orthomolecular psychiatrist. The toxic side effects occurred 2 to 40 months after therapy and consisted of a peripheral sensory neuropathy with progressive ataxia and distal limb impairment of position and vibration sense. All tendon reflexes were diminished or absent and no signs of central nervous system dysfunction were apparent. Nerve biopsies in two patients demonstrated non specific axonal degeneration with moderate or severe loss of myelinated fibres. Discontinuation of pyridoxine led to improvement in 6 months.

Berger and Schaumburg (1984) described a 34 year old lady taking lower doses of vitamin B_6 (200-500 mg/day) over 3 years. She presented with numbness and paraesthesiae of both feet which gradually ascended to her hips. She also had numbness of her hands. On examination she had

marked sensory ataxia, absent reflexes and was unable to walk without assistance. Somatosensory evoked potentials showed prolonged latency between lumbar and cervical sites when both right and left tibial nerves were stimulated. No biopsy was performed. She improved after stopping vitamin B_6.

Parry and Bredesen (1985) described 16 patients who were interviewed by phone after a television report about the treatment of PMS with pyridoxine. Eight of them were also examined. All had symmetrical distal sensory loss. None of the patients had weakness, except one who also had dominantly inherited demyelinating neuropathy: she noted a rapid increase in weakness, which reversed when pyridoxine was stopped. In addition to the symptoms of neuropathy, eight patients showed Lhermitte's sign. Electrophysiologic studies were performed in severe cases and showed that sensory nerve action potentials were absent or severely reduced in amplitude. Compound muscle action potential amplitudes and motor nerve conduction velocities were normal. Sural nerve biopsy was performed in two patients. The myelinated fibre density was reduced and there was some myelin debris indicating axonal degeneration. There was no evidence of segmental demyelination or myelinated fibre regeneration.

Dalton and Dalton (1987) found raised serum B_6 levels in 172 women attending a private practice specializing in PMS and its treatment with pyridoxine. Sixty percent had neurological symptoms which disappeared when B_6 was withdrawn and reappeared in four cases when B_6 was restarted. The mean dose in the 103 patients with symptoms was 117 ±

92 mg/day. No biopsies are reported.

Albin et al (1987) described two patients who developed acute, profound sensory loss after pyridoxine treatment of intoxication caused by the false morel mushroom, Gyromitra esculenta. The rationale of this treatment is that the active toxin, monomethylhydrazine, inhibits a pyridoxine dependent step in the synthesis of the neurotransmitter gamma-aminobutyric acid (Hanrahan and Gordon, 1989). A very large dose of pyridoxine was used (2g/kg) over a 3 day period. The pyridoxine preparation contained chlorobutanol which could explain other features not related to sensory neuropathy, such as weakness, nystagmus and respiratory depression. Autonomic symptoms could possibly be caused by effects of pyridoxine on autonomic ganglion cells which, like DRG cells, lie outside a blood barrier and may therefore be particularly vulnerable. One of these patients was reported in a follow-up study 4.5 years after the initial illness. The sensory deficits were permanent and profound, causing severe disability (Albin and Albers, 1990).

Santoro et al (1991) reported a case of a man with tuberculosis treated with isoniazid (400 mg/day) and pyridoxine (600mg/day) who developed a severe sensory neuropathy, at first thought to be due to isoniazid. Although isoniazid was withdrawn (while pyridoxine was continued) the sensory symptoms persisted. Only after pyridoxine treatment was stopped did the sensory symptoms begin to improve. The rationale for giving pyridoxine in isoniazid therapy is explained in the following section. However, it seems from this case, that the 'protective' pyridoxine therapy

can itself be a cause of neuropathy.

Mechanisms of pyridoxine neurotoxicity

There are very few described mechanisms of the neurotoxic action of pyridoxine. One of them is the formation of a neurotoxic quinone metabolite (Frater-Schröder and Mahrer-Busato, 1975, Frater-Schröder, Alder and Zbinden, 1976). Windebank (1985) suggests that a neurone-specific enzyme is inhibited by an excess of pyridoxine. If the enzyme affected was pyridoxal kinase, a generalized effect should be expected. However, neither in human cases of pyridoxine toxicity nor in animals was there evidence of systemic effects. This suggests involvement of an enzyme other than pyridoxal kinase.

PYRIDOXINE ANTAGONISTS

It is well known that some drugs can impair vitamin absorption, increase vitamin excretion or interfere with vitamin utilization. Isoniazid is the better known pyridoxine antagonist, and will be discussed independently.

Penicillamine, a specific antidote in copper poisoning, is also used in patients with Wilson's disease. Prolonged use or high doses of penicillamine can cause pyridoxine deficiency symptoms (Smith and Gallagher, 1970). The antibiotic cycloserine, used in patients resistant to isoniazid (Roe, 1973), and hydralazine (Roe, 1973), an antihypertensive agent, also act as antagonists. The administration of pyridoxine, along with these drugs helps

to reduce some of the neurological side effects.

Antagonism also exists between the anti-Parkinsonian drug L-Dopa (Yahr et al, 1972) and pyridoxine, reflecting the formation of a Schiff base between an amino acid and pyridoxal phosphate. An example of antagonism in which the enzymatic potential of pyridoxine is diminished is the block in the conversion of pyridoxine to pyridoxal described in alcoholics (Hines and Cowan, 1970). Other vitamin B_6 antagonists are chloroquine (d'Eshougues Gille and Smadja, 1961), mitomycin C (Fujimoto, 1966) and hydrocortisone (Rose and Braidman, 1971). The role of interfering chemicals in the pharmacological aspects of vitamin B_6 has been reviewed by Rosen et al (1964) and (Reynolds (1975).

Oral contraceptive agents have been shown to alter the apoenzyme-coenzyme binding of pyridoxal phosphate and to lower the tissue pyridoxal levels (Lumeng Cleary and Li, 1974), requiring additional vitamin B_6 for correction.

Klosterman (1974), reviewed vitamin B6 antagonists of natural origin. One of the desirable wild mushrooms (Gyromitra esculenta) contains hydrazine and methylhydrazine and when partially cooked can cause poisoning for which pyridoxine is an antidote. Another mushroom (A. bysoris) can also cause hydrazine poisoning; L-dopa is found in the seedlings, pod, and beans of Vicia faba (broad bean) and velvet bean. Other natural antagonists are mimosine, in the seed and foliage of Mimosa and Leucaena species (Klosterman, 1974).

Isoniazid

The neurotoxic effects of isoniazid (isonicotinic acid hydrazide, INH) originate from its disturbance to vitamin B_6 metabolism. Pyridoxine, pyridoxal and pyridoxamine must be phosphorylated in order to form the active co-enzymes involved in many enzymatic reactions, including decarboxylations and transaminations. INH interferes with this phosphorylation by inhibiting pyridoxal phosphate kinase; INH also chelates with pyridoxal phosphate, forming an even more potent inhibitor of pyridoxal phosphate than INH alone.

Since 1956 it has been known that patients on isoniazid therapy could suffer from peripheral neuropathy (Pegum, 1952). This was later confirmed by several workers (Jones and Jones, 1953; Gammon, Bunge and King, 1953). It was also demonstrated that large doses of pyridoxine were protective against developing neuropathy (Biehl and Vilter, 1954). The nutritional state of the patient and genetic factors influence the incidence of peripheral neuropathy. There is variation in the way man inactivates the drug, the slow inactivators being much more susceptible to neuropathy than the rapid inactivators (Hughes et al, 1954). These differences were proposed to be genetically determined by Knight, Selin and Harris (1959). High doses may also produce convulsions, probably resulting from depletion in the brain of the inhibitory neurotransmitter gama-aminobutyric acid (GABA). This depletion is produced by the combined action on glutamic acid of the holoenzyme glutamic acid decarboxylase (apoenzyme) and pyridoxal phosphate (coenzyme). Ataxia, memory disturbance and psychosis

(Weinstein, 1975) are also common clinical presentations.

The first symptoms of neuropathy are paraesthesiae and numbness of the extremities. With continuing dosing, sensory symptoms extend proximally. Vibration sensation in the limbs is reduced (Le Quesne, 1975). Symptoms of motor involvement such as distal muscle weakness, often appear later than the sensory symptoms.

In experimental studies, Cavanagh (1967) showed that, in rats given with high doses of INH for several weeks, the distal parts of the sensory fibres were affected but motor fibre degeneration was more severe, occurring as proximally as the ventral spinal roots. Jacobs et al (1979) showed that single large doses produced ultrastructural changes in axons as early as 24 hours following dosing. These changes consisted of large vacuoles appearing between axons and inner tongues of Schwann cell cytoplasm, sometimes compressing the axon and suggesting that INH produced a multifocal axonal lesion. By the 7th day DRGs showed chromatolysis secondary to peripheral nerve degeneration and regeneration. Axon repair occurred even while the animals were being dosed (Jacobs, Miller and Cavanagh, 1979), further confirming that the primary lesion was in the axon rather than the cell body.

It is clear that pyridoxine deficiency causes an entirely different neuropathy from that associated with increased intake of pyridoxine.

EFFECT OF BLOOD BRAIN BARRIER AND BLOOD NERVE BARRIER IN NEUROTOXICITY

Blood brain barrier

Numerous early studies, including those of Ehrlich (1885) and Doinikow (1913), showed that Trypan blue and Evans blue when injected intravenously stain all the organs except the brain and spinal cord. In 1900 Lewandowsky suggested that capillaries were the site of this barrier. After horseradish peroxidase (HRP) began to be used as a tracer (Reese and Karnovsky, 1965) intravenous HRP could be seen in the lumen of brain capillaries but was prevented, by tight junctions or zonulae occludentes, from penetrating between endothelial cells. Another difference between endothelial cells of brain and those in other organs is the low number of pinocytotic vesicles, which may be used in transport across endothelial cells. This is a further reason to think that their absence is a contributory aspect of this barrier. Essential metabolites are able to pass the brain capillary endothelium in many cases by carrier-mediated transport. Proteins are excluded because of their size and electric charge.

Pyridoxine is an essential constituent of the brain, particularly, in its phosphorylated form, as a coenzyme in the synthesis of neurotransmitters. The few biochemical studies on its entry into the brain date back to the late 1970's (Spector, 1978 a,b) and indicate that its entry (which is carrier-mediated across the blood-brain barrier) is so regulated that it is difficult to increase brain vitamin B_6 (including the interconvertible forms pyridoxine,

pyridoxal and pyridoxamine) levels. There appear to be no comparable studies on the entry of pyridoxine from blood into the permeable dorsal root ganglia (see next section) where regulatory mechanisms present in the brain do not exist.

Blood nerve barrier

The blood vessels of the perineurium and epineurium are permeable, whereas the endoneurial vessels are impermeable. The perineurial sheath acts as a barrier to separate these two regions of differing vascular permeability (Thomas, 1963; Reale, Luciano and Spitznas, 1975). The epineural blood vessels share with other blood vessels in the body the ability to allow passage of serum proteins across their walls, these proteins are reabsorbed into lymphatics which are present in the epineurium but are absent from the endoneurium (Olsson, 1984). The endothelial cells of endoneurial blood vessels have tight junctions joining them; these junctions are possibly less "tight" than those of the CNS capillaries. Olsson (1966) observed that histamine and serotonin increased the permeability of endoneurial vessels to protein tracers, in contrast to cerebral to cerebral capillaries which remain unaffected. Bradbury and Crowder (1976) demonstrated that endoneurial endothelial cells must contain channels greater than 1nm, which are larger than those found in the brain endothelial cells; pinocytotic vesicles are present in their cytoplasm but in fewer numbers than in other tissues.

Peripheral nerve after crush injury or axonotmesis showed increased

permeability due to blood vessels rupturing at the site of injury. Between the first and the fourth day there is also increased permeability distally to the site of the crush, accompanying the growth cones of the regenerating axons (Seitz et al, 1989) and reaching a peak between the first and third week. The endoneurium after nerve injury is infiltrated by an exudate rich in serum proteins which may be a requirement for peripheral nerve regeneration. Proteins which are carried by retrograde axonal transport may stimulate axonal growth (Kiernan, 1979).

Bush, Reid and Alt (1993) demonstrated in a recent study that the enhanced permeability of the blood nerve barrier during degeneration and regeneration was related to the formation of anionic fenestrations in endoneurial vessels of mice. At pH 2.0, the distribution of glycocalyx moieties was disrupted, further increasing the permeability of the blood nerve barrier.

Regions of the nervous system without a blood barrier

Certain regions of the brain have permeable blood vessels; these tend to be grouped around the third and fourth ventricles and include the area postrema, the posterior pituitary and the choroid plexus. The functions of these regions, for example, as hormonal or chemo-receptors, or the production of cerebrospinal fluid, require close contact with blood vessels.

In the peripheral nervous system, also, there are regions lacking blood barriers. Dorsal root and autonomic ganglia have permeable blood vessels. In autonomic ganglia, many of the vessels are fenestrated. Although only

occasional blood vessels in dorsal root ganglia have fenestrated vessels, tracer studies show that there is very rapid leakage from these vessels (Jacobs, Macfarlane and Cavanagh, 1976).

Nerve cells and processes of the myenteric plexus lie in a region of vascular permeability. No blood vessels are present within the plexus, but only a basement membrane separates the elements of the plexus from the surrounding environment. Muscle layers lying adjacent to the myenteric plexuses are vascularized by permeable blood vessels. After intravascular HRP, Jacobs (1977) found rapid leakage of the tracer into the myenteric plexus.

The potential vulnerability to circulating toxic substances of some parts of the nervous system, unprotected by blood barriers, has been pointed out by Jacobs (1980). For example, neuronal degeneration caused by the chemotherapeutic agent adriamycin is restricted to regions without such barriers (Bigotte, Arvidson and Olsson, 1982). The distribution of lipidosis caused by another drug, amiodarone, corresponds precisely to regions without these barriers (Costa-Jussá and Jacobs, 1985). Cisplatin, another chemotherapeutic agent, is known to cause a sensory neuropathy. In some cases, treatment is limited by its neurotoxicity (Roelofs et al, 1984). Recently Gregg et al, (1992) studied 21 one autopsies of patients treated with cisplatin and found that the dorsal root ganglia were the most vulnerable neural structures. Both histopathological and pharmacological parameters were in keeping with a major accumulation of platinum in the DRG. Central structures were spared. These findings correlate with the

clinical picture of a sensory neuropathy in cisplatin intoxication.

Vascular permeability would appear to be the factor determining the localization of these neurotoxic effects.

THE CONCEPT OF DISTAL NEUROPATHIES

The recognition that neuronal disease could become manifest by changes to the distal part of its axon goes back to the time of Gowers (1886), but the term "dying back" was first used by Greenfield (1954). Many naturally occurring human diseases are considered to be of a distal or "dying back" type, though their exact pathogenesis is not known. These include a number of inherited sensory, sensory and motor neuropathies and spinocerebellar degenerative diseases. The distal pattern of nerve fibre degeneration produced by a number of toxic substances led to the hope that they might serve as models for the study of these human diseases. However, most neurotoxic substances proved to have a selective effect upon the axon and were not appropriate as examples of neuronal impairment causing distal degeneration. For example, Bouldin and Cavanagh (1979a) studied cats injected with di-isopropylfluorophosphate (DFP), an organophosphorous compound, showing that in teased nerve preparations of the recurrent laryngeal nerve there was focal axonal degeneration. Prineas (1969a) and Bouldin and Cavanagh (1979b) suggested that the intraaxonal vacuoles seen in the nerves in organophosphorus neuropathy were mainly composed of smooth endoplasmic reticulum.

Schaumburg, Wisniewski and Spencer (1974) showed in cats that the earliest detectable morphological changes of acrylamide intoxication were in the nerve terminals of Pacinian corpuscles, where neurofilaments were seen to accumulate before degeneration started. Focal swellings developed along distal axons during slow intoxication.

The focal nature of the lesions in distal toxic neuropathy caused by hexacarbons was convincingly demonstrated by Spencer and Schaumburg (1978). Teased fibre studies of rats treated with methyl n-butyl ketone or 2,5-hexanedione revealed giant axonal swellings, mainly composed of neurofilaments, appearing multifocally along the axons. Ferri et al (1988) using immuno-methods in rats intoxicated with 2,5-hexanedione showed extensive swellings in autonomic nerve fibres containing accumulations of neurofilaments. Other toxic substances with focal axonal changes include CS_2 and isoniazid (Jacobs and Le Quesne, 1992). Although these are examples of distal axonopathies the lesions are seen to occur multi-focally but tending to be distal.

Sensory or motor neurons were spared when hens (Cavanagh, 1954) or cats (Prineas, 1969a) were intoxicated with tri-ortho-cresylphosphate (TOCP), in spite of the presence of degeneration in the axons of the same neuronal cells. Studies with acrylamide (Prineas 1969b), isoniazid (Cavanagh, 1967) and thallium (Spencer et al, 1973) failed to show nerve cell alterations which could support their involvement in the aetiology of distal axonopathies.

Therefore, in the examples given, these distal axonopathies are due

to a direct effect upon the axon rather than a primary insult to the nerve cell body, the mechanism suggested by Cavanagh to be the cause of distal or toxic "dying back" neuropathies.

One of the main purposes of the present study was to investigate pyridoxine neuropathy as a possible model of a "dying back" neuropathy in the original sense of the term as used by Gowers, Greenfield and Cavanagh.

NORMAL MORPHOLOGY OF PERIPHERAL NERVOUS SYSTEM

Dorsal Root Ganglia

The spinal and autonomic ganglia are part of the peripheral nervous system. Almost all of the afferent fibres, both somatic and visceral, have their cell bodies in the spinal ganglia. These aggregations of unipolar nerve cells form spindle-shaped swellings on the dorsal roots. Each ganglion is surrounded by a connective tissue capsule that is continuous with the epineurium of the spinal nerves. Cells of the spinal ganglia have a peripheral location beneath the capsule, and bundles of nerve fibres entering and leaving the ganglia form a central core. In the trigeminal ganglion the cells and fibres are more loosely arranged. In spinal ganglia the interneural spaces contain large and small axons, satellite cells, Schwann cells and blood vessels.

Dorsal root ganglion cells can be divided into two main groups, "large pale" and "small dark", and show ultrastructural differences (Lieberman, 1976; Lawson, 1979). Many more subdivisions of sensory cell types have

been proposed on the basis of the localization of neurotransmitters and of the expression of cell surface oligosaccharide antigens, both of which are present in the cell bodies and central terminals of primary afferent fibres in the spinal cord (Jessell and Dodd, 1986).

In the small dark cells there is a high concentration of rough endoplasmic reticulum (RER) which is organized in parallel cisterns forming a ring around the cell. In the large light cells the RER forms aggregates of varying sizes between which are neurofilaments sometimes in large numbers (Lieberman, 1976). The Golgi apparatus, Golgi-associated smooth endoplasmic reticulum (GERL) and lysosomal bodies appear to be more developed in the small dark cells. The nuclei are large in relation to perikaryal volume, particularly in the small cells, and they normally occupy a central position in the cell body, generally spherical with a smooth outline and few indentations. The large size attained by many DRG cells reflects the very great volume of axoplasm which is maintained by these cells, which have both peripheral and central processes.

The number of cells per ganglion varies enormously from the few hundred in the spinal ganglion of lower vertebrates to thousands in the corresponding human ganglia. The thoracic ganglia contain significantly fewer cells than cervical or lumbar ganglia. Rat cervical ganglia contain about 11,000 cells whereas thoracic ganglia contain approximately 7,000 cells (Hatai, 1902). The cells of lumbar ganglia in rats range from 18-75μm (Andres, 1961), in humans in sacral ganglia the diameter ranges between 15 and 110μm (Ohta, Offord and Dyck, 1974).

The large size attained by many DRG cells reflects the very great volume of axoplasm which is maintained by these cells, which have both peripheral and central processes.

Satellite cells

Satellite cells are derived from the embryonic neural crest and, in the adult, form a concentric layer which closely invests the perikaryon of dorsal root ganglion cells and its unmyelinated axonal coils (Wyburn, 1958). The round or elongated nuclei of the satellite cells are more dense than the adjacent perikaryon, and are identified easily with the light microscope. They have ultrastructural features that distinguish them from Schwann cells. Satellite cells display plasma membrane redundancy in the form of folds on the surface that faces the neuron. Such folds and processes may form layers and interdigitate with the surface evaginations of the perikaryon. The outer surface of the satellite cells is invested with a basal lamina which is continuous with that investing the myelin at the first internode (Pineda Maxwell and Kruger, 1967). The capsule of satellite cells separates the perikarya from adjacent ganglionic capillaries, and must be involved in fluid transport mechanisms. They can increase in number after birth, and may play a role in the metabolism of ganglion cells.

Peripheral nerve

An axon is an extension of the nerve cell bounded by a prolongation of its cell membrane, the axolemma. The axonal cytoplasm, the axoplasm,

does not show any structures associated with protein synthesis and this has an important consequence for their maintenance and growth, involving transport mechanisms.

In the formation of the sheath of a peripheral myelinated nerve there is an extension of the Schwann cell plasma membrane which wraps spirally around the axon. The myelin sheath consists of a series of cylindrical segments called internodes, each of them deriving from a single Schwann cell. The myelin sheath is interrupted at the nodes of Ranvier. There are specializations of the myelin sheath in which lamellae separate and contain Schwann cell cytoplasm. They occur frequently along each internode, and are called Schmidt-Lanterman incisures.

Myelinated nerve fibres in humans range in diameter between 2 and 22μm. In the sural nerve of a middle aged man they range between 2 and 13 μm (Jacobs and Love, 1985) and axon diameter between 1 and 9 μm. Myelin thickness is related to axon diameter. The ratio $\frac{\text{axondiameter}}{\text{fibrediameter}}$ is called the 'g' ratio. Friede and Samorajski (1967) showed an approximate value for 'g' of about 0.6 - 0.7 over the whole diameter range. This is not true when the internodal length is below the normal range for a particular axon diameter, as happens at the initial segments of dorsal root ganglion neurons (Lieberman, 1976) and in regenerated nerves in adult animals (Hildebrand et al, 1987).

The unmyelinated axons are totally enveloped by Schwann cell cytoplasm and the entire fibre is invested by a single basal lamina (Schwann

cell unit). The ratio between numbers of myelinated and unmyelinated axons is 1:1 in muscle nerves and 1:4 in cutaneous nerves (Ochoa, 1976). The axons of unmyelinated fibres range in diameter from 0.4 to 2μm in man and their distribution is unimodal about a mean value of approximately 1.0μm (Jacobs and Love, 1985). Unmyelinated fibres show in their axoplasm the same components as the myelinated fibres.

The structure of the axoplasm is simple when compared with the cytoplasm of the neuron. The main component is an electron lucent amorphous matrix in which is suspended a population of longitudinally orientated organelles and mitochondria. Microfilaments (5-7nm in diameter) are thought to be composed of paired helical chains of actin and they possibly have contractile functions.

Neurofilaments, 8-11nm in diameter, are longitudinally orientated and of indefinite length. They are linked by lateral structures forming a polygonal lattice. In normal nerves, neurofilament density is of the order of 100-300 filaments/μm^2 (Thomas, Landon and King, 1992). Neurofilament (NF) content has been correlated with area of axons: in the peripheral and central nervous system (Friede and Samorajski, 1970; Friede, Miyagishi and Hu, 1971; Smith, 1973), in unmyelinated and myelinated fibres (Friede, Miyagishi and Hu, 1971; Berthold, 1978) and in various regions of the same axon. Neurofilaments are the axonal organelles most associated with axonal calibre: under normal conditions, NF density remains relatively stable and axonal area changes proportionately to the NF content of an axon (Friede, Miyagishi and Hu, 1971; Berthold, 1978). Morphometric studies of

myelinated axons in rats showed that the number of NF correlate closely with their areas (Friede and Samorajski, 1970; Griffin et al 1982).

NFs consist of three protein sub-units which have molecular weights of 68KDa (NF-L), 155 KDa (NF-M) and 200 KDa (NF-H), collectively referred as the neurofilament triplet (Hoffman and Lasek, 1975). They appear in late embryonic life when neurites have not reached their targets (Carden et al, 1987). Expression of genes for NF-M and NF-L precedes NF-H expression (Lindenbaum et al, 1988), suggesting that NF-H may have a more independent and dynamic function than the other subunits. The ultrastructural locations of individual components of the triplet in the neurofilament structure have been examined using antibodies raised against individual components of the triplet. These studies indicate that NF-L makes up the core of the filament, while NF-M is wound helically around the core with a pitch of 100 nm and NF-H forms side arms which can connect filaments (Tokutake, 1990).

The cell body synthesizes the neurofilaments as soluble proteins and they are rapidly assembled into stable, insoluble proteins in 8 to 12 hours (Lasek, Oblinger and Drake, 1984, Nixon et al, 1989). They are poorly phosphorylated in neurons and highly phosphorylated in axons. Mata, Kupina and Fink (1992), using quantitative electron microscopy immunocytochemistry with colloidal gold, found a decrease in 200kDa and 160kDa neurofilament subunit peptides at the node of Ranvier, suggesting that the degree of phosphorylation of these neurofilament subunits is reduced at this site in comparison to the internode. It is reported that

neurofilaments which are highly polymerized and form cytoskeletal structures are highly phosphorylated, particularly in the C-terminal region of NF-H and NF-M (Lee et al, 1988). It is considered that the phosphorylation of the side arms of NF-H has a significant role in the interaction of filaments (Nixon et al 1989).

During the slow component of axonal transport, neurofilaments are delivered to the axon (Hoffman and Lasek, 1975, Black and Lasek, 1980). Nerve cells, specially those with long axons, deliver most neurofilament proteins into axons within 6-12 hours after synthesis (Nixon et al, 1989). The early stages of neurofilament axonal transport are quite eventful in modifications as they are transformed into mature organelles that can react with other axonal proteins. This transformation is evident shortly after the entrance of neurofilaments into the axon (Sternberger and Sternberger, 1983), and reaches its maximum within 24 to 48 hours (Nixon et al,1989), the state of phosphorylation of NF-L decreases but phosphates on the amino terminal end of NF-M continue to turn over (Sihag and Nixon, 1987). NF-L and NF-M dephosphorylation increases the binding of cytoskeletal proteins and may modulate the interaction of neurofilaments with other structures (Nixon, 1993).

The phosphorylation of the highly charged carboxyl terminal tail regions of NF-M and NF-H, corresponding to the filament periphery, is possibly related to the sidearms of neurofilaments (Julien and Mashynski, 1983). The phosphorylation of these areas in the neurofilaments starts after neurofilaments advance 200-300 μm along the axon (Oblinger, 1988). There

is a zone of transition from neurofilaments with weakly phosphorylated sidearms to others with highly phosphorylated ones; this zone is 200-300 μm wide and can be immunocytochemically detected in optic axons of mice (Nixon et al, 1989). This area corresponds to an increase in number of neurofilaments and an increased distance between neurofilaments and an enlarged axonal diameter (Nixon et al, 1991).

Although some modification of NF proteins occurs in the axon (Nixon, Brown and Marotta 1982), actual degradation of NFs takes place usually in the axon terminal (Roots 1983). There are, however, some axonal neurofilaments which are turned over locally during axonal transport, it being possible to find breakdown products along the axons. Phosphorylation seems to protect neurofilaments against proteolysis by proteases associated with cytoskeletal preparations (Goldstein, Sternberger and Sternberger, 1987) and by calpains (Litersky and Johnson, 1992). Phosphorylation is also associated with the speed of neurofilament transport; after treatment with IDPN, there is a decrease in transport velocity of neurofilaments (Watson et al, 1989). In 2,4 hexanedione-treated rats there is an opposite effect (Watson et al, 1991).

Local accumulation of NF possibly due to defective slow transport, can produce axonal swelling as in hereditary giant axonal neuropathy (Asbury et al, 1972; Maia, Pires and Guimarães, 1988; Ouvrier, 1989), or after exposure to several toxins including carbon disulfide (Seppäläinen and Haltia, 1980) and 2,5-hexanedione (Spencer and Schaumburg, 1975). Monaco et al (1989), studying 2,5-hexanedione toxicity in the optic

pathway, showed that proximal optic axons were smaller and contained fewer neurofilaments than controls. The distance between neurofilaments and microtubules was increased and these changes were thought to be provoked by increased neurofilament transport, without their synthesis or supply being affected from the cell body.

Other filamentous structures in the axoplasm are microtubules or neurotubules. They are arranged longitudinally and occur singly or in parallel arrays. Observed at EM, they appear to be unbranched 25-35nm "hollow" cylinders of indefinite length. They are thought to be composed of globular subunits of the protein tubulin. The number of tubules in the terminal branches of some large mammalian axons is many times greater than the number found in the parent axon (Zenker and Hoberg, 1973), suggesting local synthesis, since branching has not been seen to occur. Unmyelinated axons contain proportionately larger numbers of microtubules than myelinated axons; there are between 50 and 100/μm^2 of axonal cross-sectional area in unmyelinated axons, in contrast to large myelinated axons in which there may be only 10-20/μm^2 (Friede and Samorajski, 1970).

Smooth endoplasmic reticulum (SER) is composed of a mesh of tubules which is thought to extend from the neuron to the distal end of the nerves. The arrangement of SER has been demonstrated by Droz, Rambourg and Koenig (1975) using special high voltage EM and metal impregnation techniques. SER may appear as flattened expansions of smooth membranes, and subaxolemmal sacs. Vesicles, including the synaptic vesicles may originate from SER. The axoplasm also contains long and thin mitochondria.

AXONAL TRANSPORT

Intra-axonal transport has been reviewed by Ochs and Brimijoin (1993); it is divided into slow and fast components (Table 1). Its importance in neurological disease has been reviewed by Griffin and Watson (1988). In the anterograde direction, slow transport moves most of the cytoskeletal and axoplasmic constituents. Fast transport is bidirectional and carries small vesicles and other organelles (Ellisman and Lindsey, 1983; Tsukita and Ishikawa, 1980).

COMPONENTS OF ANTEROGRADE AXONAL TRANSPORT		
Component	Velocity in mammals (mm/day)	Materials transported
Fast	200-400	Membranous organelles, proteins, glycoproteins, glycolipids, phospholipids, vesicle-associated enzymes, neurotransmitters
Slow component 'b'	3-5	Soluble proteins(e.g. actin, calmodulin, CPK, PFK, LDH, enolase, choline acetyltransferase)
Slow component 'a'	1.5-2.5 0.5-1.5	Soluble tubulin, 'Insoluble' tubulin, neurofilament triplet, neurofilament-associated proteins

Table I - Components of anterograde axonal transport (Tomlinson, 1988)

Fast anterograde transport

Fast anterograde transport is energy dependent, utilizing ATP. It transports mainly mitochondria and transmits storage vesicles (50-80nm) (Ellisman and Lindsey, 1983). Vale, Reese and Sheetz (1985) and Schnapp et al (1985) isolated from neural tissues a protein (kinesin) which forms tight complexes with microtubules and is able to translocate vesicles along single microtubules. A similar protein was also described in the mammalian brain (Vale, Reese and Sheetz, 1985). Kinesin must be one of a wide family of proteins capable of translocating vesicles within cells.

Fast retrograde transport

This consists mainly of transport of membrane bound structures from the periphery back to the cell body at a speed of around 200mm/day. These structures include secondary lysosomes, multivesicular bodies and small vesicles ready for recycling or destruction (Holtzman, 1971). Nerve growth factor also reaches developing sympathetic nerve cell bodies and DRG's via retrograde transport (Hendry et al, 1974).

Defective turnaround of materials at nerve terminals and reduction in the rate of retrograde transport have been suggested as primary defects in some experimental neuropathies, such as those caused by zinc pyridinethione (Sahenk and Mendell, 1981).

Slow transport

The slow anterograde transport has two components. Slow

component "a" consists of tubulin and neurofilament proteins which travel at a speed of 0.25-1μm/day (Tytell et al, 1981). Slow component "b" consists of actin monomers, soluble enzymes and small oligomers which travel together at a speed of 2-4μm/day. The neurofilament proteins are transported in the form of polymerized neurofilaments (Lasek, 1982). Alterations in slow transport produce changes in the axonal cytoskeleton which may cause alterations in axonal calibre.

REACTION OF PERIPHERAL NERVE TO INJURY

Degeneration after crush: Wallerian degeneration

After a peripheral nerve crush or a complete transection of the nerve tissue, degeneration of the distal segment of the nerve occurs. The events after nerve injury were first described by Waller (1850) and later studied and extensively documented by Ramon Y Cajal (1928).

By light microscopy the early changes in myelinated fibres consist of disruption of the myelin sheath, usually beginning at the Schmidt-Lanterman incisures, with later interruption of the axon and breaking down of the myelin sheath into ovoids containing axonal debris. Originally it was thought that the ovoids of myelin were first taken up by a proliferating subpopulation of Schwann cells, but more recent studies suggest that the debris are transferred to macrophages which appear in the endoneurium.

The importance of macrophages was elegantly demonstrated by Beuche and Friede (1984) who showed that there was no proliferation of

Schwann cells and no myelin breakdown when macrophages were prevented from entering an isolated degenerating peripheral nerve. At the same time that breakdown is occurring, macrophages appear in the nerve and there is Schwann cell proliferation in the distal segment beginning from two to three days after nerve injury, reaching a peak at three to four weeks (Abercrombie and Johnson, 1946; Bradley and Asbury, 1970). By this time most of the myelin debris has been removed.

By electron microscopy, the basement membrane of the degenerated myelinated fibres encloses many processes of Schwann cells called Bands of Bungner. After a few hours of nerve injury unmyelinated axons appear dilated and swollen and later on there is a gradual disappearance of the normal axonal structures. The axoplasm may become filled with mitochondria, vesicles and lamellar bodies, and finally the axons disappear. There is some Schwann cell proliferation (Clemence, Mirsky and Jessen, 1989), but it is less striking than for myelinated fibres (Dyck and Hopkins, 1972; Aguayo and Bray, 1975). Electron microscopy shows that unmyelinated degenerating axons are surrounded by Schwann cell processes. When the axons disappear these processes form flattened bands encircled by basement membrane.

Regeneration of Peripheral Nerve After Crush

The degenerative changes that take place in peripheral nerves, produced either by transection of the nerve or by crush, are similar. There is a significant difference, however, concerning nerve regeneration. After

nerve crush, there is an interruption of axons but the structural continuity of the basement membrane is maintained, guiding the growth of the regenerating axons to their original terminations. Therefore, the regenerative process after nerve crush is more effectively accomplished than after nerve transection. After the axons have reached their original termination there is further increase in size, although the fibre diameter never reaches its original dimension (Gutmann and Saunders, 1943).

During the 6 hours after injury axonal sprouts can be detected (Ramon y Cajal, 1928) but many of these appear to be abortive. As axons regenerate, Schwann cells become spaced along the axons at intervals of about 200-300μm, which is the length of the regenerated internode in the adult. The definitive sprouts seem to appear a few days after nerve transection (Duce and Keen, 1976) and slightly earlier after nerve crush (Haftek and Thomas, 1968). They may arise from the terminal axons or as collateral sprouts from a proximal node of Ranvier. After nerve crush, the sprouts are guided to the periphery through basement membrane lined bands of Büngner, and the axons which establish connections survive and mature (Aitken, Sharman and Young, 1947).

Schröder (1972) found that the thickest regenerated nerve fibres were thinner than the largest control fibres, and some large regenerated nerve fibres had a relatively thin myelin sheath 24 months after nerve crush in rat. Smith et al (1982) suggested that there was a direct relationship between the volume of myelin and the area of the axon to cover; for that reason, the regenerated fibres with short internodes have a thinner myelin sheath and

they never recover a normal diameter. Similar findings are reported by Friede and Beuche (1985) and Beuche and Friede (1985). They suggest that this is an adaptation of the myelin sheath to the shorter internodes, to optimize the conditions for transmission of impulses.

It is well known that central nervous system fibres have less capacity to regenerate. Ramon y Cajal (1928) suggested the absence of Schwann cells as a cause. Aguayo et al (1982) confirmed this when they achieved axonal regeneration from the central nervous system, provided they grew in a graft of peripheral nerve trunk which contained bridges of Schwann cell processes, emphasizing the role of Schwann cells in axonal regeneration.

If Schwann cell response is blocked by intraneural injection of mitomycin C, then axonal outgrowth will only occur if the immediate cellular environment of the proximal stump is rich in Schwann cells (Hall, 1986) which can migrate into the distal segment. Hall (1989) emphasized the function of macrophages in peripheral nerve repair. In a normal peripheral nerve fibre, resident macrophages constitute less than 5% of the total endoneurial cell population (Oldfors, 1980). Recruited macrophages during degeneration remove myelin debris from the Schwann cell tubes and they probably interact with Schwann cells during the injury response, e.g. by presenting mitogens and cytokines. There is no nerve growth factor (NGF) or NGF receptor in normal adult nerve. But after degeneration NGF and NGF receptor appear to be synthesized in the Schwann cells of the distal stump. The subsequent persistent elevation of $mRNA^{NGF}$ levels may be mediated by reactive macrophages, via the secretion of interleukin-1 (Lindholm et al,

1987).

Drugs influencing regeneration of peripheral nerves

Some publications mention the positive effect of gangliosides, the mode of effect of which, however, is yet unknown. Gangliosides are reported to promote the growth of neuronal processes, to activate the protein synthesis within the neuron and to have a stabilizing effect on the cytomembrane (Tuellner, 1987). This was never shown convincingly and further studies are necessary.

Becker, Kienecker and Dick (1990) investigated the degenerative and regenerative changes in the saphenous nerve of the rabbit following systemic treatment with a combination of the vitamins B_1, B_6 and B_{12}, with a control group that was treated with saline. Cold lesion was used to cause a secondary degeneration. Results after 4, 10 and 21 days showed that the number of regenerating axons was higher; however, problems with the interpretation of these results are pointed out in the discussion.

Stelmack and Kiernan (1977) injected rats subcutaneously with triiodothyronine sodium (T_3) and studied its effects on regenerating facial nerve after crush. The axonal diameters were smaller in T_3-treated than in control animals, but the myelin thickness were greater. These authors suggested that T_3 stimulated myelination of regenerating axons by acting upon the Schwann cells.

Seckel (1990) reviews several factors and drugs which promote peripheral nerve regeneration, amongst them other hormones like

oestrogens, adrenal hormones and insulin. Isaxonine has also been shown to enhance axonal sprouting in rats, but does not increase the rate of regeneration (Pécot-Déchavassine and Mina, 1985).

CHAPTER 2. MATERIALS AND METHODS

ANIMALS

One hundred healthy male Sprague-Dawley rats, weighing about 250g, aged between 2 and 3 months were used in this experiment. Rats were received from B & K Universal Ltd, Grimston Aldbrough Hull. They were kept in cages in groups of 4 and fed with a B & K rat and mouse standard diet containing wheat, barley, soya, wheatfeed, fish meal, fats and oils, minerals and vitamins. The average content of pyridoxine was 14 mg/kg.

Twenty five healthy male Balb-C mice, bred at the Institute of Neurology, weighing about 20 g and aged 6 months were used at the beginning of the experiment and were fed with the diet mentioned above.

PYRIDOXINE HYDROCHLORIDE

Pyridoxine hydrochloride was received from BDH chemicals (Merck) as a white crystalline powder, 99-100% pure. Pyridoxine is a stable compound and may be heated for 30 minutes at 120° without decomposition (Bauernfeind and Miller, 1976). The compound was dissolved in distilled water at concentrations ranging from 0.01% to 20%. It was necessary to raise the water temperature to 40-45°C when preparing 10% and 20% solutions. The solutions were prepared daily and kept in sterile containers.

Oral administration

Under light ether anaesthesia a flexible catheter attached to a syringe was inserted into the stomach of rats and mice. Concentrations of pyridoxine were calculated so that volumes not exceeding 1 ml (rats) and 0.2ml (mice) were used. Controls were given water in each case.

Intraperitoneal injection (i.p)

Under light ether anaesthesia pyridoxine was injected i.p. Again concentrations were varied so that the volume did not exceed 1.1ml in rats and 0.2ml in mice.

Intraneural injection

Animals were sedated with isoflurane and anaesthetized with a mixture of hypnorm and midazolam (mixture of 1 part midazolam and 1 part water and 1 part hypnorm and 1 part water). The dose administered was 2.0 ml/kg i/p. The pH of the solutions varied between 2.0 at 1M (20% solution) and 3.96 at 60 mM (0.01% solution). The right sciatic nerve was exposed using retractors through an oblique incision of the skin and by blunt dissection between the muscles of the thigh. The nerve was held as tautly as possible and the injection was made through the perineurium into the endoneurial space using a Hamilton syringe with a 36G needle. The injection of approximately 20μl pyridoxine was directed proximally and, because of anatomical variation, the site of injection was sometimes in one branch or in a single nerve. The point of bifurcation of the sciatic nerve was used as

a landmark. In later experiments, a suture was used to mark the site of injection. Having injected the nerve, muscle and skin were sutured and the wound protected by using a sprilon spray.

NERVE LESIONS

Crush

The crush was made by fine forceps with flattened tips; these were held together for 5 seconds. Muscle and skin were sutured and protected as above. The site of crush was noted either by the landmarks of the division of the nerve or by suture.

Crush plus intraneural injection

The sciatic nerve was exposed as described above and crush was performed at a distance of 1cm above the division of the sciatic nerve into tibial and peroneal branches. Immediately afterwards, injection of 20μl pyridoxine was made into the tibial fascicle was directed proximally. Both sites of injection and crush were marked in the adjacent tissues with a suture. Nerves were examined at a level just distal to the crush and at another level just proximal to the injection of pyridoxine.

CLINICAL EXAMINATION

The animals given pyridoxine by mouth or i.p. were examined for loss of grip of the hindlimbs by observing their behaviour when placed on a wire

mesh grid. Loss of splay reflex was judged on a flattened surface. Animals held by the tail were observed for evidence of crossing of the hindlimbs, a sign of ataxia. All the animals were inspected on a daily basis, just before being given the pyridoxine.

Intraneurally injected animals were also observed for loss of grip and motor function, since the intraneural injection was given in the sciatic nerve produced in most cases paralysis of the limb.

PREPARATION OF TISSUES

Fixation

Rats and mice used for morphological studies requiring fixation were killed by intracardiac perfusion of fixatives under deep pentobarbitone anaesthesia. The animals were pinned out in the supine position. The rib cage was opened, and the right atrium and the left ventricle were incised. The apex of the heart was held with blunt forceps and a cannula was inserted and tied into the aorta. In rats fixative was delivered mechanically using a peristaltic pump at a pressure of about 100mm of mercury. In mice, fixative was delivered through a 20ml syringe fitted with a metal cannula. The interval between opening the thorax and the beginning of perfusion was kept to a minimum. Successful perfusion was recognisable by rapid stiffening of the body and discolouration of the viscera.

Fixatives

The main fixative for paraffin histology was Formal-calcium (40% formaldehyde: 10ml; distilled water : 90ml; Calcium chloride: 1g), and the post-fixation was done with FAM (40% formaldehyde: 10ml; glacial acetic acid: 10ml; absolute methanol: 80ml). Another fixative used was Bouin's Fluid (saturated aqueous picric acid solution: 75ml; 40% formaldehyde: 25ml; glacial acetic acid: 5ml).

A modification of Karnovsky's fixative (paraformaldehyde: 2%; glutaraldehyde: 3%; 0.08M sodium cacodylate buffer at pH 7.3 - 7.4) was used for electron microscopy (Karnovsky, 1965). This fixative was freshly prepared and used at 4°C.

PARAFFIN HISTOLOGY

Serial sections were used to identify axon degeneration, particularly in the distal part of lower limbs and tail. After perfusion with formal-calcium at room temperature the skin was removed, the lower limbs were post-fixed in FAM overnight and then decalcified in formic-nitrate (65 parts of 20% solution of trisodium nitrate in distilled water and 35 parts of 98% formic acid). Following dehydration and clearing, the tissue was impregnated with paraffin wax. Before final embedding serial blocks were taken and embedded in sequence using the technique of Beesley and Daniel (1956). Sections were cut at 5μm and stained with haematoxylin and eosin, Luxol fast blue/Nissl. Some sections were cut at 10μm and impregnated with silver for demonstration of axons using the method of Marsland, Glees and

Erikson (1954).

IMMUNOCYTOCHEMISTRY FOR PHOSPHORYLATED NEUROFILAMENTS

A modified avidin-biotin immunoperoxidase method was used for detection of phosphorylated neurofilaments. The monoclonal antibody (RT97) was donated by Prof. Brian Anderton and stored at -20°C. RT97 is a mouse monoclonal antibody produced against a Triton X-100 insoluble extract of rat brain, as described by Wood and Anderton, 1981. It reacts with the 200K dalton protein subunit of neurofilaments.

The method used consisted of different steps:

1. Removal of wax from sections in xylene for 30 min. They were immediately placed in absolute alcohol.
2. Block of endogeneous peroxidase using 0.1% hydrogen peroxide in methanol for 10 min.
3. Wash running tap water for 10 min.
4. Transfer to warmed distilled water for 10 min in the 37°C oven.
5. Wash in running tap water for 10 min.
6. Application of trypsin.
7. Wash in tris buffered saline (TBS).
8. Application of antibody (1/10 solution in TBS) on sections - 1 hour. Negative controls kept in TBS.
9. Wash in TBS, three times 5 min each.

10. Application of biotinylated secondary antibody, (rabbit anti-mouse immunoglobulin diluted 1/200 in TBS with 40μl/ml of normal human serum added) for 30 min at room temperature.
11. Wash in TBS - 3 washes 5 min each.
12. Application of avidin-peroxidase conjugate diluted 1/500 in TBS for 30 min at room temperature.
13. Preparation of diaminobenzidine (DAB) chromogen solution (see below).
14. Three washings in TBS, 5 min each.
15. Treatment of sections with activated DAB (see below) for 10 min.
16. Wash in running tap water.
16. Counterstain nuclei with haematoxylin for 30 seconds and quick differentiation in 1% acid alcohol.
17. Wash in running tap water until nuclei are blue.
18. Dehydration through graded alcohols, clear in xylene and mount.

The solutions used were the following:

DAB chromogen solution: 20-30mg DAB were dissolved in 80ml TBS using a stirrer with mild heating. When dissolved cool to room temperature and filter.

Activate DAB solution: Add 1ml of 10% H_2O_2 to 75ml distilled water. Make up immediately before use and add 1ml of this per 80ml DAB solution.

Trypsin solution: calcium chloride 0.05g; trypsin 0.05g; distilled water 100ml; adjust pH to 7.8

Tris buffered saline (TBS): 1 part tris buffer pH7.2 added to 9 parts of normal saline.

Tris buffer pH 7.2: 0.2M Tris: 250ml; N/10 HCl: 450ml; distilled water 300ml; adjust pH to 7.2.

RESIN EMBEDDED SECTIONS

After perfusion with modified Karnovsky's fixative, the spinal cord, sciatic and saphenous nerves were exposed immediately and the whole animal was immersed in the same fixative for 24 hours. Blocks were taken from the medulla, cervical, thoracic and lumbar cord. From the peripheral nervous system blocks were taken from dorsal root ganglia (4th, 5th lumbar), Gasserian ganglia, superior cervical ganglia, coeliac ganglia and sciatic and saphenous nerves (proximal and distal levels) approximately 2.5cm apart. From the nerves transverse and longitudinal sections were studied. Dorsal root ganglia were also embedded in both transverse and longitudinal sections. The nerves and dorsal root ganglia were studied in both transverse and longitudinal sections. To examine the myenteric plexus, two blocks, one transverse and the other longitudinal were taken from the proximal and distal ileum in each animal.

The material was post-fixed for one hour in 1% osmium tetroxide in 0.1M sodium cacodylate buffer, dehydrated in ethanol and propylene oxide and embedded in Araldite CY212 resin (TAAB). 1um thick sections were cut on

a LKB ultramicrotome and stained with toluidine blue.

In some cases following intraneural injection the nerves were carefully removed, placed on cards and held at either end with fine forceps to prevent shortening. After allowing a few seconds for the nerves to adhere to the card, they were immersion fixed overnight in the modified Karnovsky fixative at 4°C. Blocks were taken from regions proximal and distal to sites of intraneural injection and to levels of crush. (See text for methods used to mark sites of crush and injection).

TEASED FIBRE PREPARATIONS

Approximately 1cm lengths of some nerves were used for teased fibre studies and these were processed into araldite resin without hardener and stored in a refrigerator. After removing the perineurium, small bundles of nerve fibres were transferred from non-polymerised resin to a slide with a drop of resin with hardener. Using fine needles fibres were separated and a permanent preparation was obtained after placing a coverslip over the teased fibres and allowing the resin to polymerise.

ULTRATHIN SECTIONS

Ultrathin sections from selected blocks were cut in the silver grey area of interference colour with either a glass or a diamond knife using a LKB ultramicrotome. They were collected on copper grids, stained with saturated uranyl acetate in 50% ethanol and lead citrate (Reynolds, 1963), and examined in a Jeol 100CX electron microscope at an accelerating

voltage of 80kV.

MORPHOMETRY AND QUANTITATIVE METHODS

Measurement of diameter of dorsal root ganglion cells

Serial 7μm paraffin sections were taken of L_4 dorsal root ganglia and stained with RT97 antibody. The diameter of all ganglion cells was measured in every section, regardless of the degree of antibody staining. At a second stage only those cells staining positively for RT97 were measured, the antibody in some cases tended to slightly stain the small cells, but it was clear the difference between the two cell types. Only those nerve cells with a clearly defined nucleolus were measured, using a light microscope with a drawing tube attached. The tube extended over the bit-pad of a mini MOP linked to an IBM computer. At the tip of the MOP cursor was a small light emitting diode, which was to be seen superimposed on the image under the microscope. By moving the cursor, the point of light could be traced round the perimeter of the ganglion cell and the area measured. The computer was programmed to convert areas to diameters assuming circularity of the measured profiles. Histograms were prepared showing the distribution of diameters of the total number of cells and also of those cells staining positively for RT97. The independent (two-sample) t-test was used to compare DRG's mean diameters in the experimental and control groups in one, two and three months dosed animals. A significance level of 0,005 was considered in each test.

Number and density of myelinated and unmyelinated axons in the saphenous nerve

It was felt necessary to use electron microscopy in order to clearly differentiate early degenerating axons from normal axons. The density of myelinated axons was obtained from ultrathin sections of the proximal and distal ends of the saphenous nerve. Sections were mounted on grids with narrow grid bars and all complete myelinated fibres were counted. Electron micrographs were taken at an initial nominal magnification of 3,300 and micrographs were printed to a final magnification of about 9,900. A grating replica, 2160 lines/mm was used for calibration at each EM session. The total area counted was estimated from the area of each print multiplied by the number of prints. Normal myelinated fibres, degenerated myelinated fibres and unmyelinated axons were counted. Bands of Büngner were counted as examples of later stages of myelinated fibre degeneration.

Measurement of myelinated fibre diameters and axons

The electron micrographs used to obtain myelinated fibre density were also employed for measurement of myelinated fibre and axon diameters. Transverse sections were taken from the proximal and distal ends of the saphenous nerves and at least 400 (proximal) or 200 (distal) fibres were measured. Total fibres and axon areas were measured from the micrographs with a mini-MOP interfaced to an IBM computer programmed to calculate the axonal and total fibre diameters from respective area measurements assuming circularity. The 'g' ratio (axon diameter divided by fibre diameter)

was calculated and the relationship between 'g' and fibre diameter displayed as scatterplots.

Correlation between numbers of myelin lamellae and fibre diameter

Electron micrographs of the saphenous nerve were taken and enlarged to a final magnification of 19,800 (calibrated by means of a grating replica, 2160 lines/mm). Myelin lamellae were counted using a dissecting microscope, and fibre diameters were calculated from measurement of areas assuming their circularity (Karnes et al, 1977) using the Mini-MOP. Scatter plots were prepared. Linear regression was performed considering the number of myelin lamellae as the dependent variable and the fibre diameter as the independent one. In each case, the slope of the regression line and the Pearson's correlation coefficient were computed.

Distribution of axonal microtubules and neurofilaments

Myelinated axons were photographed at an initial magnification of 16,000 and enlarged to a final magnification of 49,680. The distribution of microtubules and neurofilaments was assessed in 12 control myelinated axons and 26 myelinated axons from two pyridoxine-injected rats whose nerve fibres showed disorganisation of axonal organelles but no fibre degeneration. Because of the high magnification required for this procedure only axons of 2.2-4.6μm diameter were examined.

Microtubule distribution was quantified by placing over each micrograph of an entire or almost entire axon, a transparent template marked

to give a grid of squares. At the magnification of x49,680, each square was equal to 0.098μm^2. All microtubules lying within each square were counted, and numbers of squares containing 0,1,2,3 ... microtubules respectively, were calculated. Results were displayed graphically expressing microtubule numbers as percentages.

The method for quantifying neurofilament distribution was based on that described by Price, Lasek and Katz (1990). A transparent template marked with regularly spaced hexagons was superimposed over micrographs of entire, or almost entire, axons of myelinated fibres. At the magnification of x49,680, each hexagonal area was the equivalent of 0.023μm^2 and the hexagons were spaced 0.2μm apart. All of the neurofilaments/hexagon were sorted and the results displayed graphically, expressing numbers as percentages.

Counts of microtubules and neurofilaments

The total number of microtubules was counted in 712 squares covering 12 control myelinated axons and 1410 squares covering 26 experimental axons. The total area measured was 8.9 μm^2 in the controls and 20.8 μm^2 for the experimental axons. From area measurements of the axons, it was possible to estimate the microtubule densities.

Since the hexagons only covered a fraction of the total axonal area, results of neurofilament counts were expressed simply as total numbers of filaments in the total number of hexagons counted.

STATISTICAL METHODS

Student's t test was used to assess the results obtained when measuring dorsal root ganglion cells. This parametric test was chosen since there was a normal distribution of the data and it has a greater power, thus helping to avoid Type 1 and 2 errors. The 95% confidence intervals were also calculated.

CHAPTER 3. RESULTS

PYRIDOXINE NEUROTOXICITY IN MICE

Pilot study using mice

Preliminary studies were performed using mice injected or fed with pyridoxine at different doses and killed at different intervals.

Clinical examination

All the animals were weighed and inspected daily. Mice dosed with 900 mg/kg on the first day and killed at 7 days or 600 mg/kg/day for 14 days did not show significant difference in weight when compared to controls. Mice injected with 300 mg/kg/day for 8 weeks were also weighed (Table I) and the same results were observed. None of the animals in the different groups showed loss of grip or signs of ataxia.

TABLE I **Weight of mice (g) given i.p. pyridoxine 300 mg/kg/day**

0 weeks	1 w	2 w	3 w	4 w	5 w	6 w	7 w	8 w
21	20	21	21	25	23	23	22	23
22.5	21	22	22	25	23	23	21	22
23	22	23	23	23				
23	23	22	21					
26	21							
Controls								
23	22	23						
21	22	21	21	22	22	23	23	23

Examination of tissues

Animals were fixed as described in Materials and Methods and semithin sections were examined and results shown as indicated in Tables II and III. Table IV includes findings for paraffin embedded material.

Table II **Pathological findings in mice given 900 mg/kg per 1 day and killed at 7 days**

Animal n°	DRG cells	Saph.ner	Route
20/88	(-)	(-)	Oral
21/88	(-)	(+)	I/P
22/88	(-)	(-)	Oral
23/88	(-)	(+)	I/P
(-) No pathology			
(+) Some degenerated fibres			

Table III **Pathological findings in mice given 600 mg/kg/day for 7 days and killed at 7 days**

Animal No.	DRG cells	Saphenous	Route
48/88	(-)	(-)	Oral
51/88	(-)	(-)	Oral
65/88	(-)	(-)	I/P
67/88	(-)	(-)	I/P
(-) No pathology			

Table IV **Pathological findings in mice given 300 mg/kg/day (i.p.) for 30 and 60 days**

No.	DRG cells	Saphenous	Tail	Lower hind limbs	Section	Dosing
99/88	(-)	(-)	0	0	semi-thins	30 d
CM4	(-)	0	(±)	(±)	paraffin	60 d
CM6	(-)	0	(±)	(±)	paraffin	60 d
(±) also seen in control						
0 Not examined						

Interpretation of the appearances seen in Glees stained preparations was sometimes difficult due to occasional patchy impregnation of axons in some bundles, giving a false impression of axonal degeneration. However comparison with controls confirmed that this was an artefactual appearance. These results, compared with the ones obtained using rats (see later), suggested that mice are less susceptible and consequently the use of mice was discontinued for further experiments.

PYRIDOXINE NEUROTOXICITY IN RATS

Pilot study to compare administration of pyridoxine by feeding and i.p. injection

12 rats were used to compare routes of administration of pyridoxine (oral or intraperitoneal): 3 in each group were given 600 mg/kg/day for 7 days; another 3 in each group were given a single dose of 900 mg/kg and killed at 7 days. Examination of DRGs, tibial and saphenous nerve resulted in more pathological changes in the animals that had i.p. injection than the ones that had been given pyridoxine by the oral route. It was decided to continue the study using i.p. dosing.

Intraperitoneal injection of pyridoxine

Dosing schedule

50 rats were injected and killed at different intervals as shown in Table V. Control animals were also killed at the same periods of time.

Table V **Dosing schedule**

Duration of dosing (days)	7	10	27	35	44	60	90	120
300 mg/kg/day			6		5	6	6	2
600 mg/kg/day	11	3	2	1	2			

Six animals received a single dose of 900 mg/kg/day and were killed after 7 days.

Clinical examination

The animals were weighed and inspected daily and tested for loss of grip and signs of ataxia (Fig. 1) and hind limb crossing (Fig. 2). There was a substantial variation in the timing and presentation of clinical signs, even in the groups dosed with the same amount of pyridoxine. A few (2/25) rats dosed with 300 mg/kg/day showed ataxic gait after the 1st month, although hind limb grip was reduced by the end of the second week. Rats injected with 600 mg/kg/day started showing ataxia much sooner than seen in Table VI and occasional animals were found on dissection to have developed megacolons and others had peritoneal swellings possibly caused by needle trauma to the peritoneal wall. The table also shows that very few animals showed clinical signs and that the initial signs were quite variable.

Table VI **Clinical examination of rats (initial signs) injected with 600 mg/kg/day (19 rats)**

Time of initial sign (weeks)	1 w	2 w	3 w	4 w
Loss of grip	1/19	2/19		
Ataxia		2/19		1/19
Other signs (abdominal swelling)		2/19	1/19	

Weights

Animals dosed with 300 mg/kg/day tended to loose weight for 5-6 weeks but a significant loss was only seen after 9 weeks of dosing. Those given 600 mg/kg/day all tended to weigh less than controls from the first week of

Fig. 1 Rat injected with 600mg/kg/day for 2 weeks, showing sprawling of hind limbs and ruffled fur.

Fig. 2 Rat injected with 600/mg/kg/day for 2 weeks, showing the typical crossing of hind limbs when held by the tail.

dosing, but the difference did not become significant until the 5th week (Fig. 3).

DRG cell immunocytochemistry

Six rats were used in this study. They were given 300 mg/kg/day pyridoxine and killed at 30, 60 and 90 days. Three controls were also examined. Sections were stained with an antibody for phosphorylated neurofilaments (RT97). Normally just the large "pale" neurons stain for this antibody (Fig. 4a).

Differences in staining patterns of DRG cells were not observed until after two months during which time there was an increase in depth of staining of some large cells and of many small cells (Fig. 4b), which normally tend to remain unstained or only faintly stained (Fig. 4a). In some cases the cells showed eccentricity of the nucleus (Fig. 5) although the majority of cells showed no other obvious abnormality. The staining tended to be diffuse throughout the cytoplasm, although in some cells with an eccentric nucleus staining was darkest in the centre of the cell (Fig. 5). Increased numbers of satellite cells were seen surrounding some neurons (Fig. 5).

Quantitative studies included measurement of the diameter of cells in which the nucleolus was in the plane of section. Firstly, all cells were measured from semi-serial sections (**TOTAL cells**). In most cases from 200-400 cells were measured. Secondly, those cells which stained clearly with RT97 were measured (**STAINED cells**) in semi-serial sections. Histograms of cell diameter distribution showed a unimodal pattern in all cases (Figs.

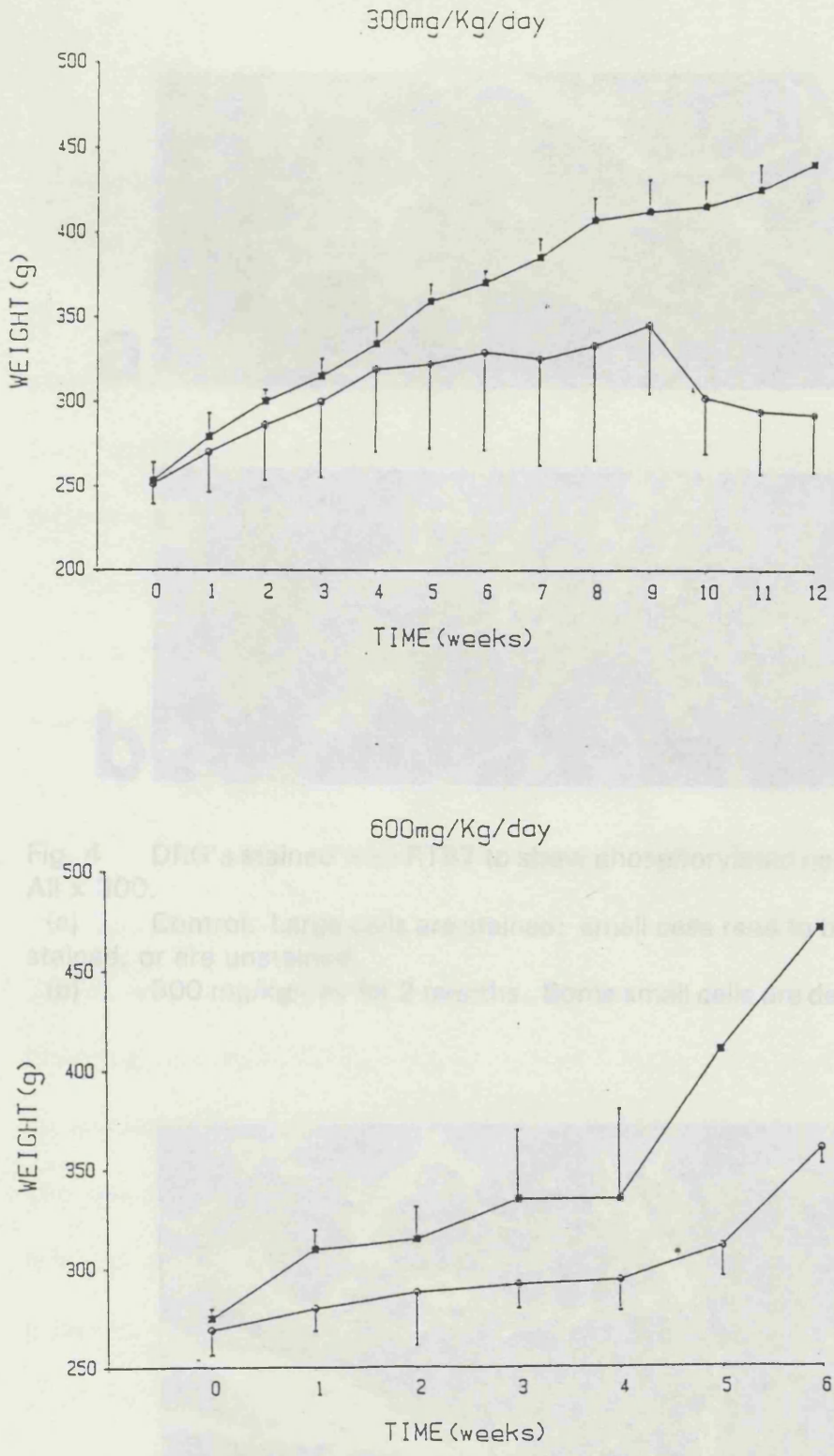

Fig. 3 Graphs showing mean weight and standard deviation of rats dosed with 300 and 600 mg/kg/day. Squares = controls; circles = experimental animals

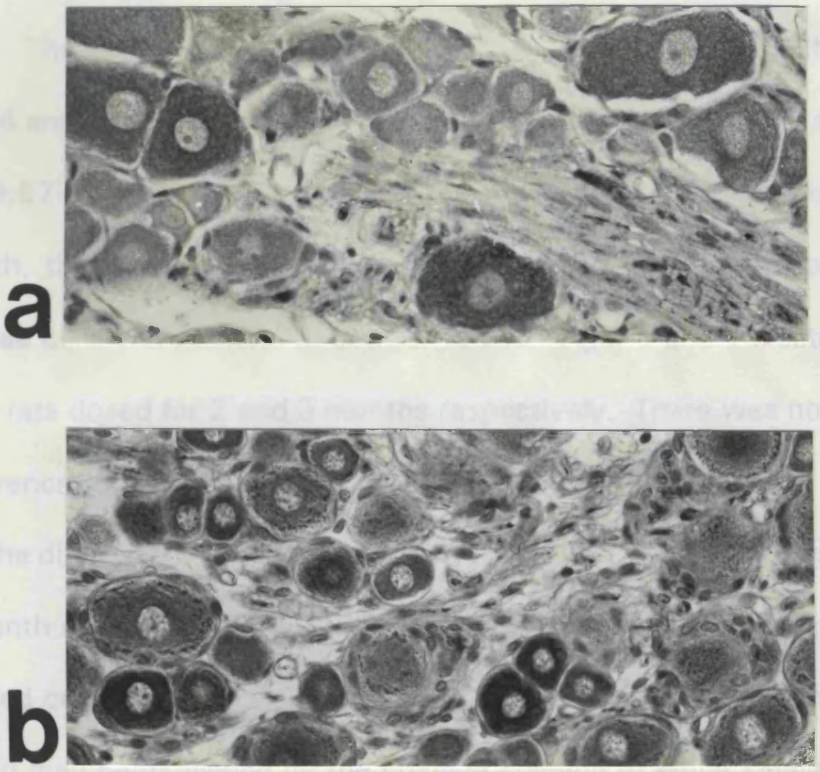

Fig. 4 DRG's stained with RT97 to show phosphorylated neurofilaments. All x 300.
(a) Control. Large cells are stained; small cells tend to be only faintly stained, or are unstained.
(b) 300 mg/kg/day for 2 months. Some small cells are deeply stained.

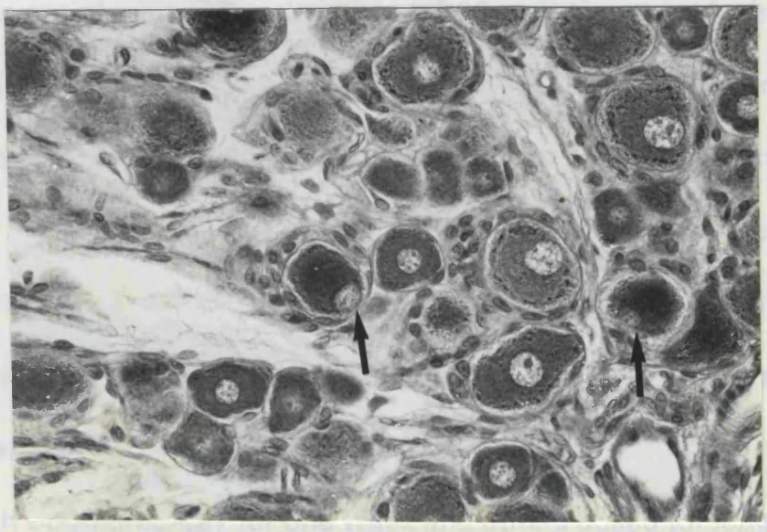

Fig. 5 300 mg/kg/day for 3 months. Several cells have eccentric nuclei (arrows); some showing deep staining of the cell centre. Many satellite cells are seen surrounding the DRG cells.

6,7). Three **total** cell controls showed ranges of 10-80 μ, with means of 38,44 and 45μm. Three **stained** controls had a similar range but with means of 49,57 and 59μm. In experimental rats dosed with 300 mg/kg/day for 1 month, the ranges and means (40 and 49μm respectively) for **total** and **stained** cells were similar to control values. Figs. 6 and 7 illustrate results from rats dosed for 2 and 3 months respectively. There was no significant difference between ranges and means of **total** cell sizes (t-test; $p = >0.1$), but the difference between means of **stained** cells was highly significant for 2 month dosing and for three months dosing $p < .0001$. The distribution of **stained** cells suggests an increased number of cells of 30-50μm diameter, which may be explained by the positive staining of some smaller cells.

DRG Cell Morphology

There was a significant variation in the degree of morphological abnormalities seen in DRG cells of animals injected with pyridoxine. Only six animals out of twenty five dosed with 300mg/kg/day pyridoxine showed changes in the DRG cells, in five of these only one or two cells were affected out of a minimum of 80 cells. The 6th animal was more severely affected. Six animals out of eighteen dosed with 600mg/kg/day showed abnormalities. These were not qualitatively different but there were quantitative differences and the effect of time of dosing did not seem to be a major factor; there were animals with major pathological changes when dosed with 600mg/kg/day for one week and others dosed for longer periods with significantly less pathology. It was therefore decided to describe the

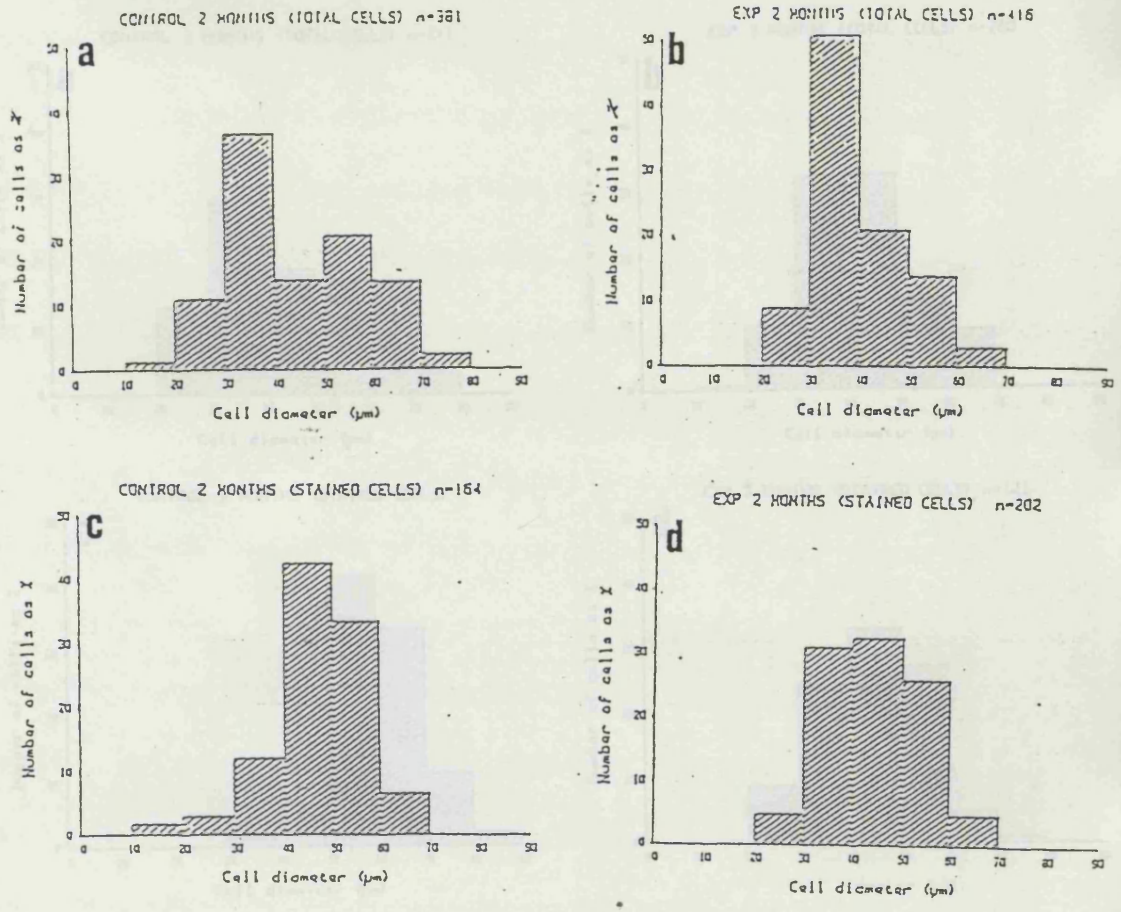

Fig. 6 Histograms showing distribution of DRG cell diameters (μm) in a, b of total cells (see text), and c, d of cells staining positively with RT97. a and c, control; b and d 300 mg/kg/day for 2 months. In b and d there is a slight shift to the left compared with the controls.

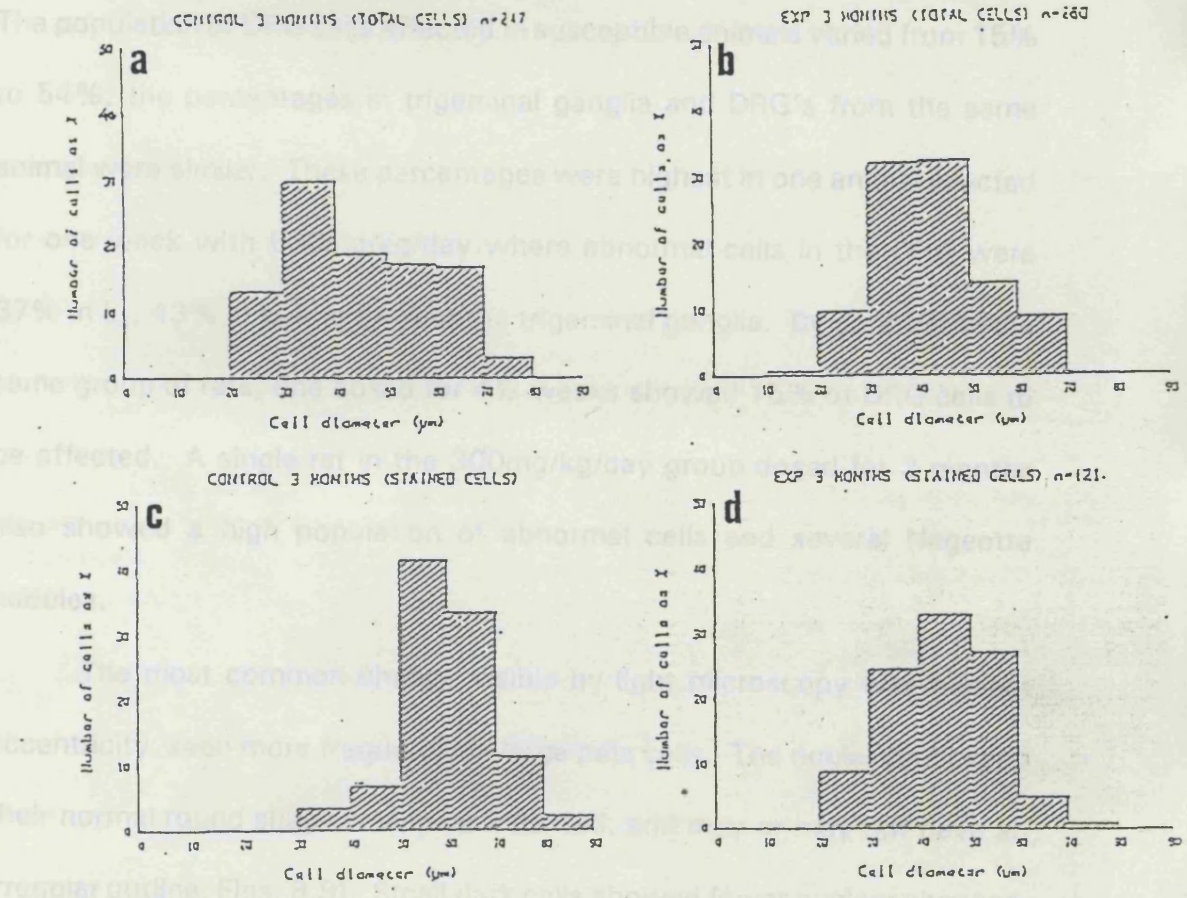

Fig. 7 Histograms showing distribution of DRG cell diameters (μm) in a, b of total cells (see text), and c, d of cells staining positively with RT97. a and c, control; b and d 300 mg/kg/day for 3 months. In b and d there is a slight shift to the left compared with the controls.

light and ultrastructural changes only in affected DRGs giving dosing schedules and noting particular individual animals.

Light microscopy

The population of DRG cells affected in susceptible animals varied from 15% to 54%, the percentages in trigeminal ganglia and DRG's from the same animal were similar. These percentages were highest in one animal injected for one week with 600mg/kg/day where abnormal cells in the DRG were 37% in L_4, 43% in L_5 and 54% in the trigeminal ganglia. By contrast in the same group of rats, one dosed for 4½ weeks showed 15% of DRG cells to be affected. A single rat in the 300mg/kg/day group dosed for 3 months also showed a high population of abnormal cells and several Nageotte nodules.

The most common change visible by light microscopy was nuclear eccentricity, seen more frequently in large pale cells. The nuclei could keep their normal round shape or appear indented, and may or may not have an irregular outline, Figs. 8,9). Small dark cells showed fewer nuclear changes, but these were seen occasionally (Fig. 9).

The cytoplasmic changes in DRG cells in some cases consisted of pallor, of large (Fig. 10), and small (Fig. 11), cells. There were also cells showing peripheral bands of paler staining (Fig. 12). In other cells the distribution and amount of Nissl bodies was affected with evidence of dispersion of Nissl substance (Fig. 10). There were also aggregates of other densely staining organelles (Fig. 9), not seen in control animals. Vacuolation

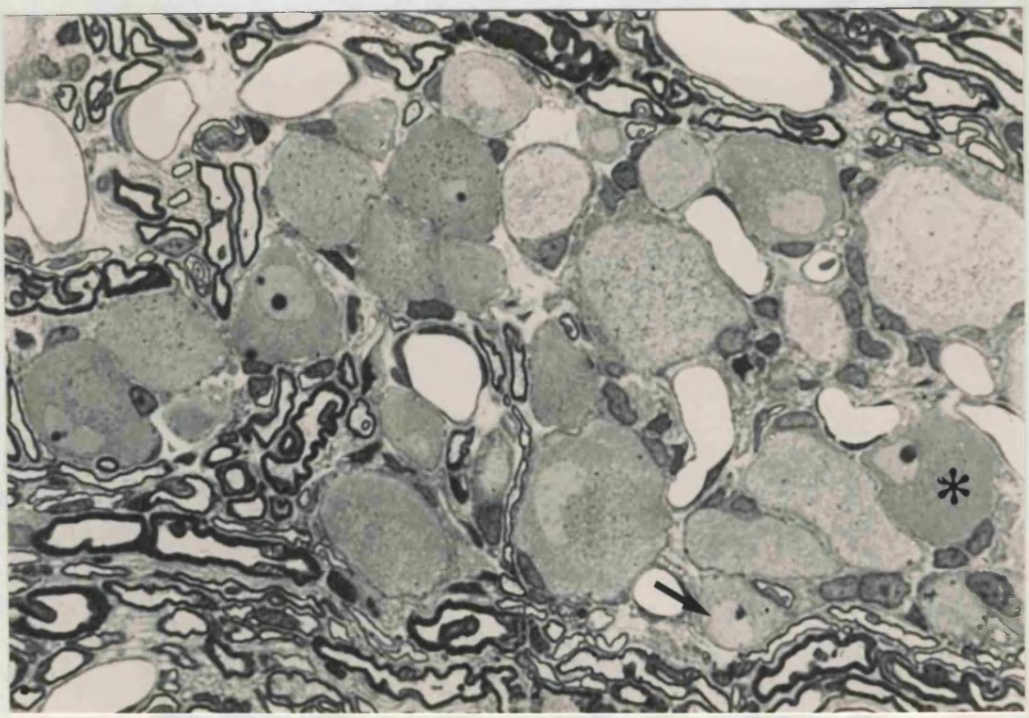

Fig. 8 DRG cells 600 mg/kg/day for 7 days. 1μm resin section showing several large cells and 1 small cell (arrow) with eccentric nuclei. Some of these nuclei are very irregular in shape. The cytoplasm of some cells stains more densely than normal (asterisk). x 470.

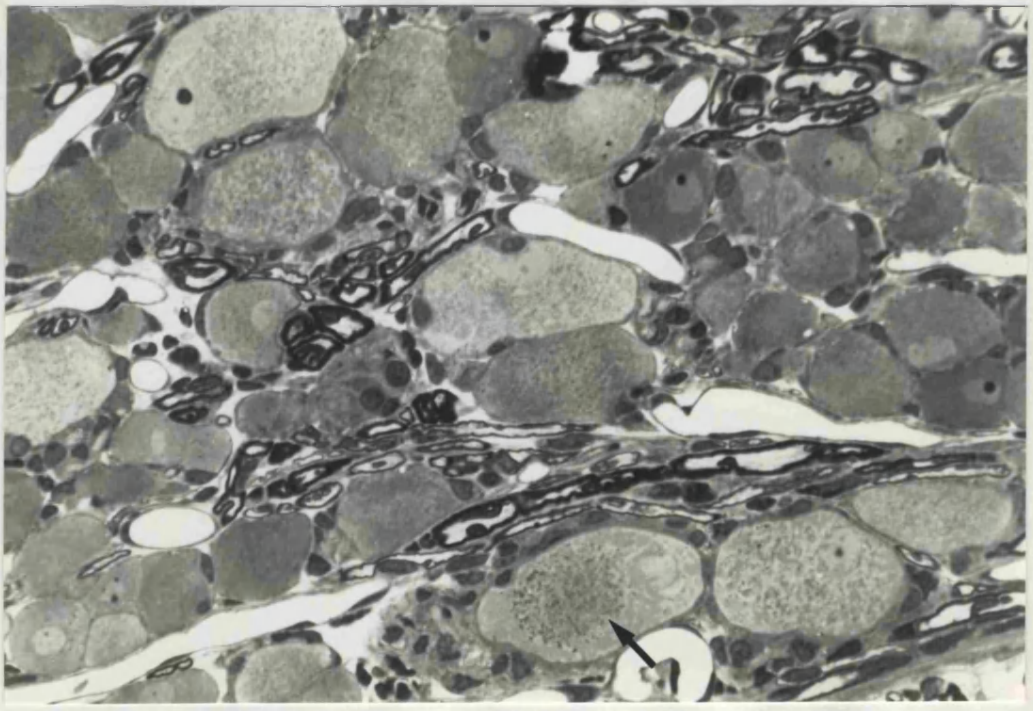

Fig. 9 DRG cells 600 mg/kg/day for 7 days. 1μm resin section showing several large and small cells with eccentric nuclei. A collection of granular bodies is seen in the centre of a large cell (arrow). x 470.

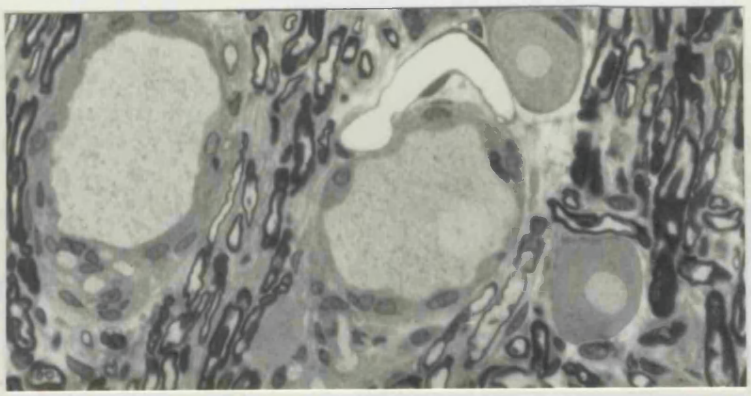

Fig. 10 DRG cells 300 mg/kg/day for 3 months. 1μm resin section showing pallor of the cytoplasm of two cells with dispersion of Nissl bodies. Satellite cells surrounding these ganglion cells are very prominent. x 470.

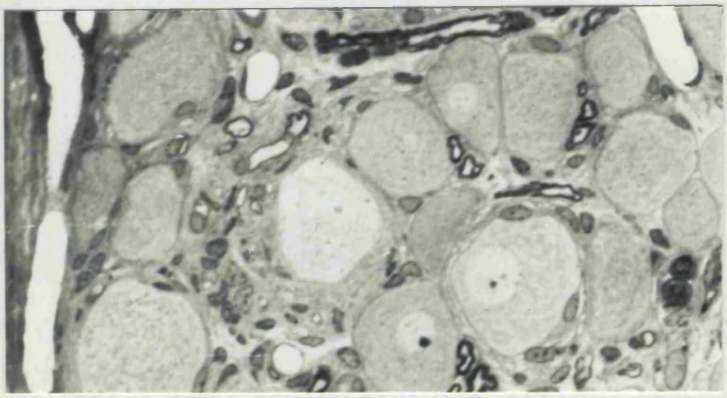

Fig. 11 DRG cells 300 mg/kg/day for 3 months. 1μm resin section showing pallor of the cytoplasm of a small ganglion cell. x 470.

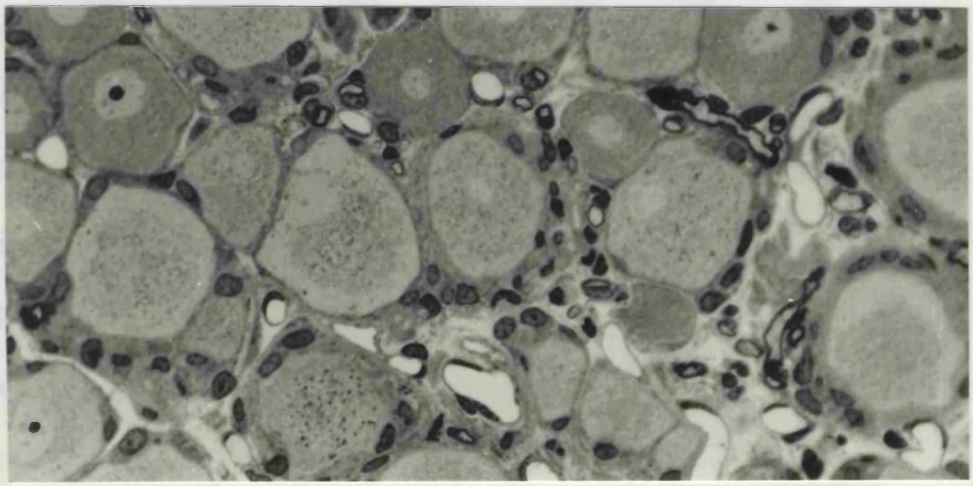

Fig. 12 DRG cells 300 mg/kg/day for 3 months. 1μm resin section showing large ganglion cells with a peripheral band that remains unstained. There is an eccentric nucleus in one of these cells. x 470.

of DRG cells was seen occasionally; the vacuoles were often very large occupying much of the cell cytoplasm (Fig. 13). The significance of these vacuoles is uncertain, since they are also seen occasionally in control animals. The impression was that they were seen more frequently in the pyridoxine dosed animals. However, more of these animals were examined than controls.

The satellite cells, mainly those surrounding abnormal ganglion cells were increased in number and tended to form a ring of nuclei around single DRG cells (Fig. 10). In one instance a satellite cell was seen in mitosis (Fig. 14). In the more severely affected ganglia, occasional ganglion cell death resulted in the formation of Nageotte nodules, collections of satellite cells replacing the degenerated neuron (Fig. 15).

The proximal, non-myelinated axon, was prominent in some cells (Fig. 16a), but this was also the case in some control cells (Fig. 16b).

Electron microscopy

Rough endoplasmic reticulum

Cytoplasmic alterations in the presence or absence of eccentric nuclei, involved marked changes to the rough endoplasmic reticulum (RER). In some cells dispersion and degranulation of RER has led to the excessive accumulation of free ribosomes throughout the cytoplasm (Fig. 17). In other cells, there has been marked loss of RER, so that at low power the cytoplasm appeared pale (Fig. 18a), at higher power the paucity of RER is seen (Fig. 18b). At its most extreme, there was complete absence of RER

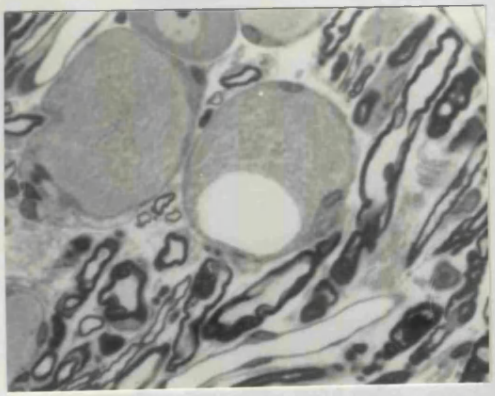

Fig. 13 DRG cells 300 mg/kg/day for 3 months. 1μm resin section showing a large, clear vacuole within the cytoplasm of a large ganglion cell.x 470.

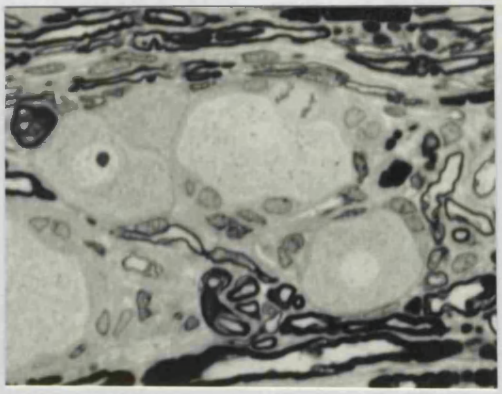

Fig. 14 DRG cells 300 mg/kg/day for 2 months. 1μm resin section showing a satellite cell in mitosis. The ganglion cell with which it is associated appears normal.x 470.

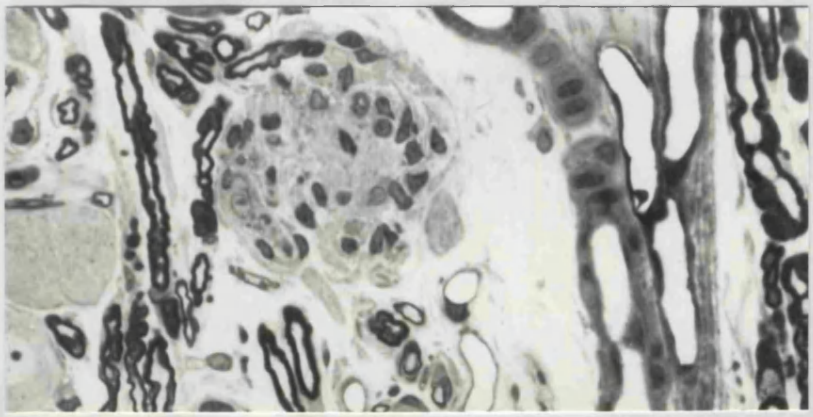

Fig. 15 DRG cells 300 mg/kg/day for 3 months. 1μm resin section showing a collection of satellite cells forming a Nageotte nodule, replacing a degenerated ganglion cell. x 470.

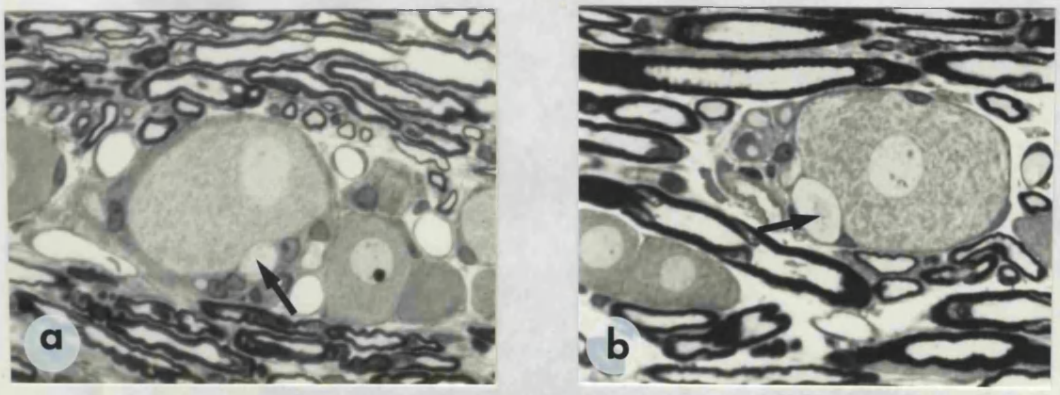

Fig. 16 1μm resin section showing DRG cells from:
(a) A rat given 300 mg/kg/day for 3 months.
(b) A control rat.
Prominent initial segments of the axon (arrows) are seen in both (a) and (b). x 470

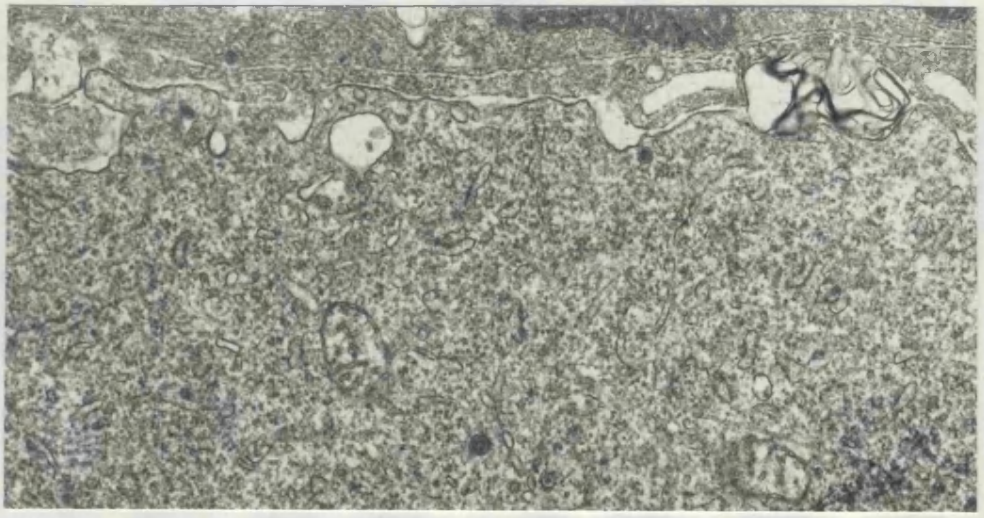

Fig. 17 DRG: 600 mg/kg/day for 10 days. Electron micrograph showing part of a ganglion cell with short strands of degranulated RER and large number of free, single ribosomes in the cytoplasm. x 30,000.

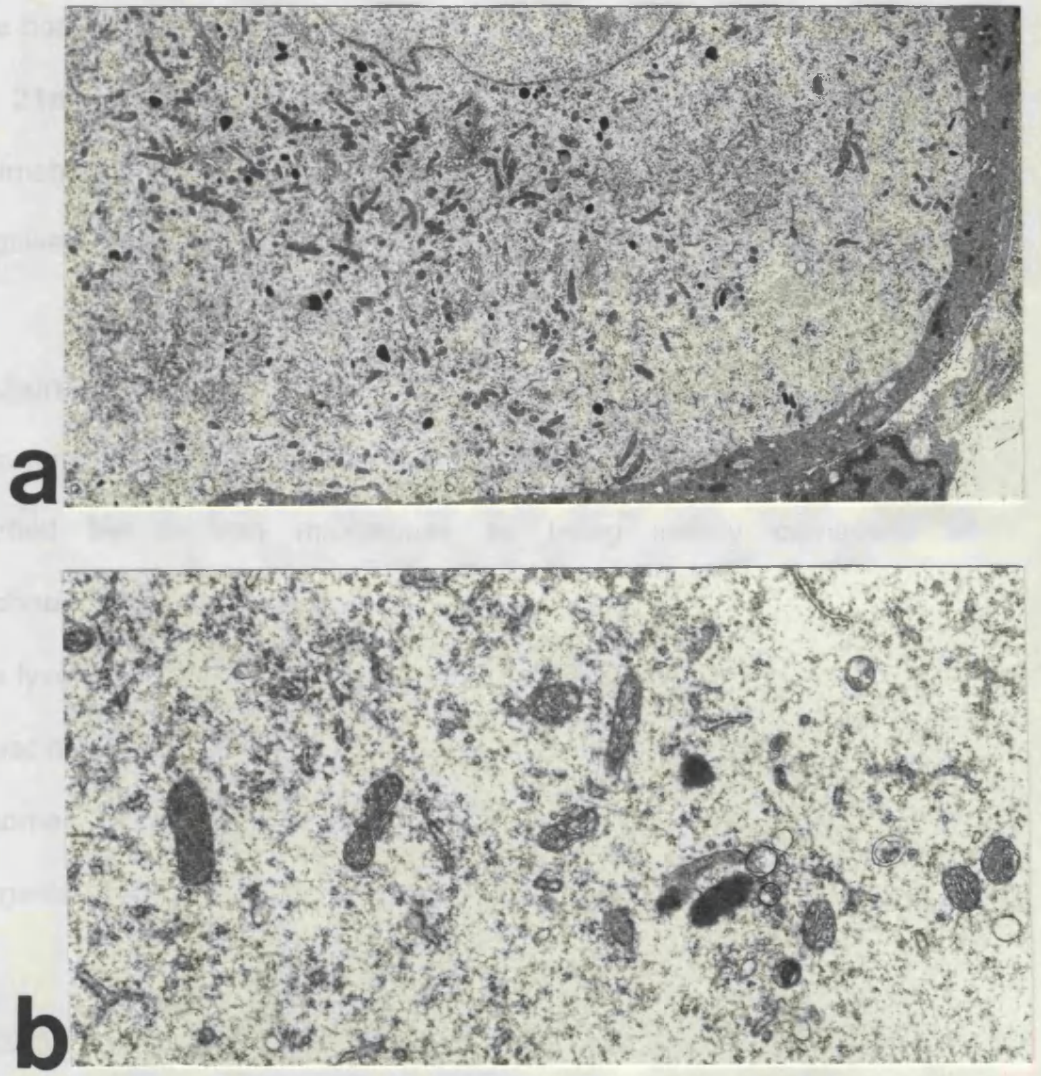

Fig. 18 DRG: 600 mg/kg/day for 27 days.
(a) Low power electron micrograph showing patchy loss of Nissl bodies, leaving pale staining areas. The nuclear has an irregular profile. x 3,900.
(b) High power of the same cell showing patchy loss of RER. x 19,800.

and ribosomes, giving the cell the extreme pallor, seen at light microscopic level (Fig. 10; Fig. 19a,b). In occasional small cells, there was also marked dispersion and loss of RER (Fig. 20). Irregularity of the nuclear membrane was not usually associated with the presence of RER, as is sometimes the case in chromatolysis.

Golgi

The Golgi apparatus tended to be conspicuous in many cells; vesicles and dense bodies were numerous and prominent in the vicinity of Golgi bodies (Fig. 21a). Occasionally massive collections of smooth membranes, presumably derived from Golgi, were seen (Fig. 21b). Golgi bodies could be recognised in the cells showing marked pallor due to loss of RER (Fig. 19b).

Mitochondria

The large accumulations of organelles seen in occasional cells (Fig. 9) were identified by electron microscopy as being mainly composed of mitochondria, which were sometimes of considerable size (Fig. 22a), and some lysosomes. However aggregations of mitochondria, lysosomes and lipofuscin may occasionally be seen in normal ganglion cells.

In some cells with dispersed RER, mitochondria showed severe disorganisation of the internal cristal structure (Fig. 22b).

Filaments

Filaments are numerous in the cytoplasm of DRG cells, mainly in large pale

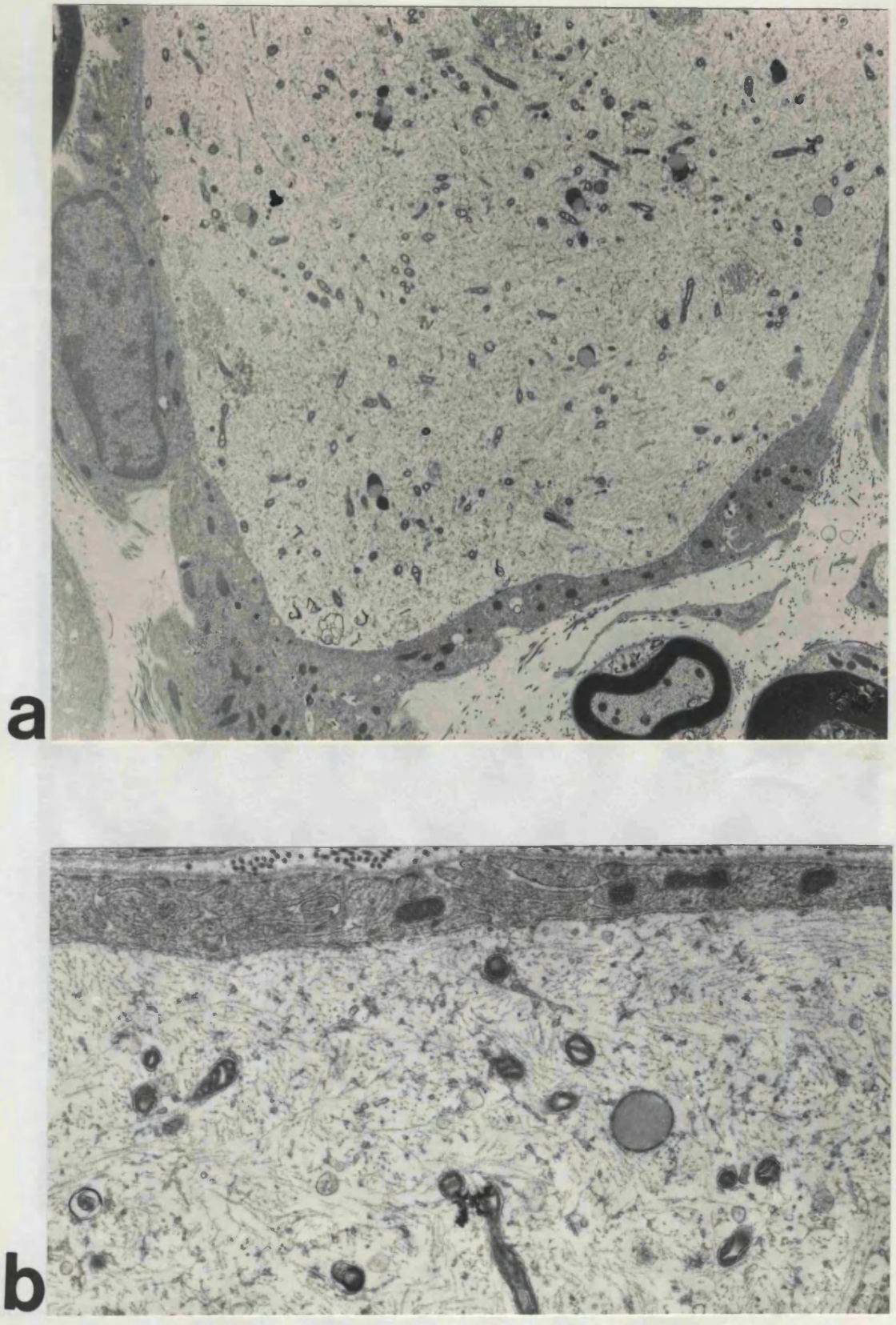

Fig. 19 DRG: 600 mg/kg/day for 10 days.
(a) Low power electron micrograph showing part of a ganglion cell with complete absence of RER, producing marked pallor. x 5,200.
(b) Higher power of the same cell showing absence of RER and large number of loosely packed neurofilaments. x 19,800.

Fig. 20 DRG: 600 mg/kg/day for 27 days. Low power electron micrograph of a small ganglion cell showing patchy loss of RER and increased numbers of neurofilaments. The nucleus is irregularly shaped. x 7,800.

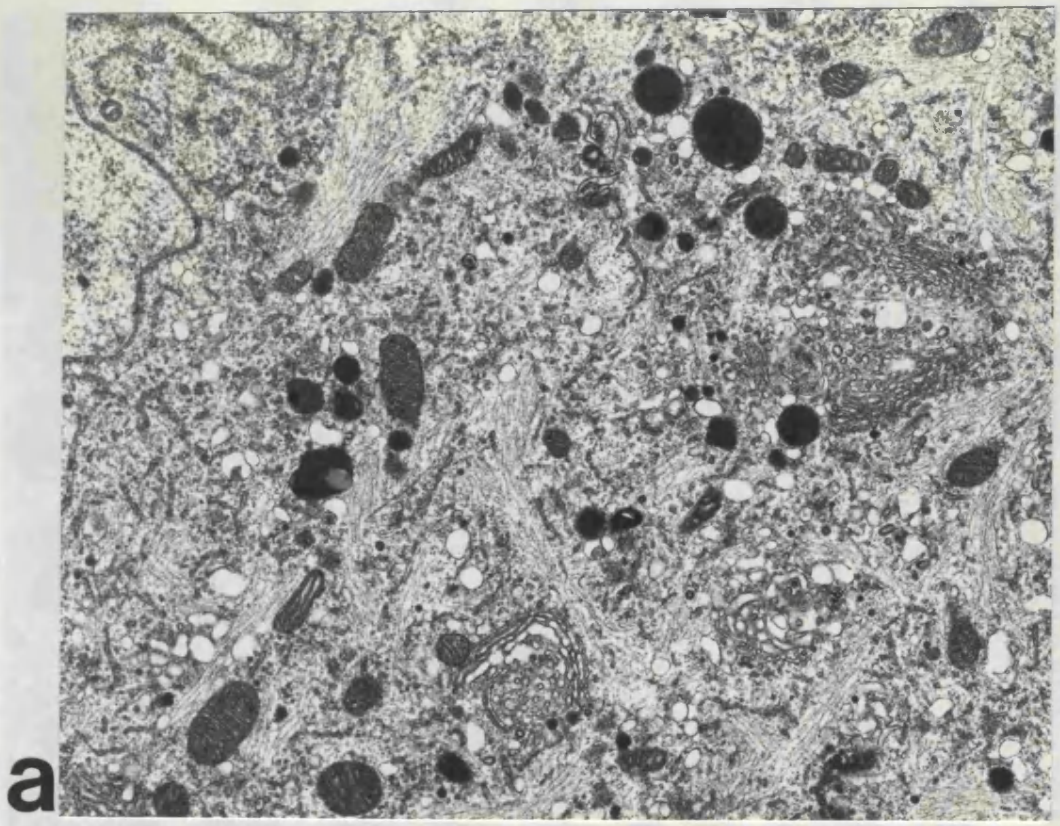

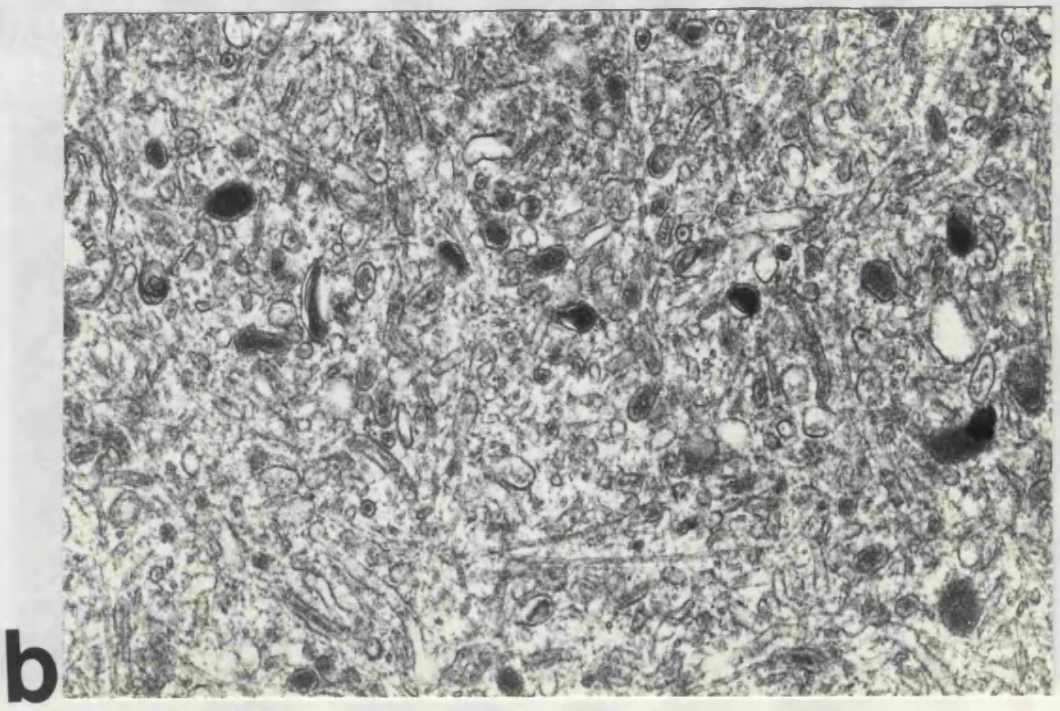

Fig. 21

(a) DRG: 600 mg/kg/day for 10 days. Electron micrograph showing several Golgi bodies with nearby vesicles and dense bodies. x 15,900.

(b) DRG: 600 mg/kg/day for 7 days. Electron micrograph showing collections of smooth reticulum and some bodies with dense cores, possibly lysosomal. x 39,000.

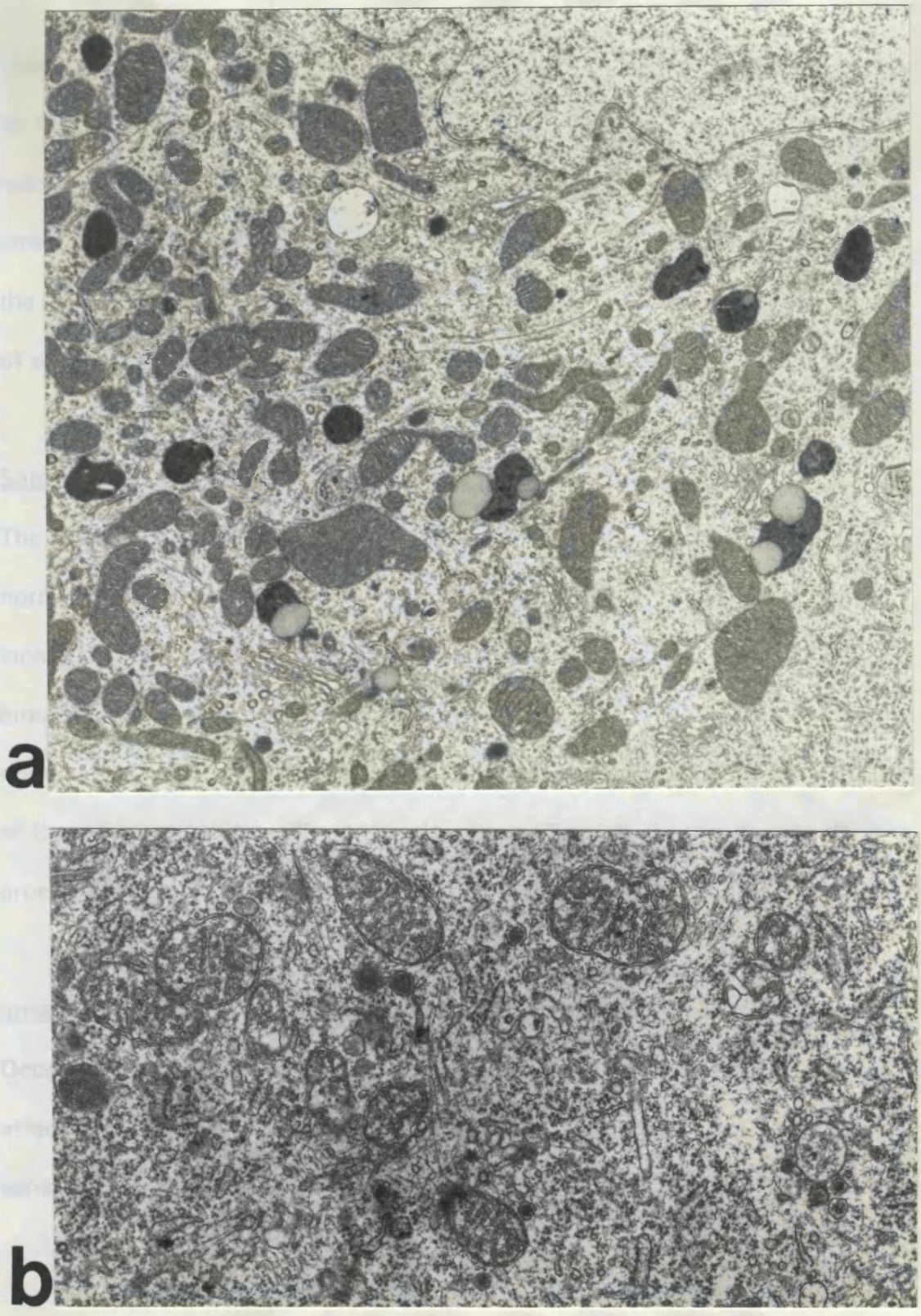

Fig. 22

(a) DRG: 600 mg/kg/day for 44 days. Electron micrograph showing a large accumulation of mitochondria of varying sizes adjacent to the nucleus. x 15,900.

(b) DRG: 300 mg/kg/day for 2 months. Electron micrograph showing disorganisation of cristae of mitochondria. x 32,400.

cells, forming bundles of varying size. In some affected DRG cells there was an obvious increase in number of neurofilaments, which tended to be more marked in the larger cells, but good examples of filament accumulation in small dark cells were also found. There were cells in which filaments were the most conspicuous of the cytoplasmic components, forming large bundles of well orientated (Fig. 23) or randomly arranged filaments (Fig. 19b).

Satellite cells

The perineuronal satellite cells showed normal shaped elongated nuclei and normal cytoplasmic organelles. Around some ganglion cells there was an increase in number of satellite cells and cell processes formed dense interdigitations between cells. There was no obvious correlation between the number of satellite cells and/or their processes, and the severity of damage of the ganglion cell (see Fig. 19b). However (Fig. 24) illustrates multiple processes of satellite cells round a very abnormal ganglion cell.

Intraganglionic sensory axons

Occasional clearly degenerated myelinated fibres were seen in severely affected ganglia. In the most severely affected animal, some of these sensory axons contained accumulations of filaments (Fig. 25).

Autonomic Ganglia

Superior cervical and coeliac ganglia were examined by light and electron

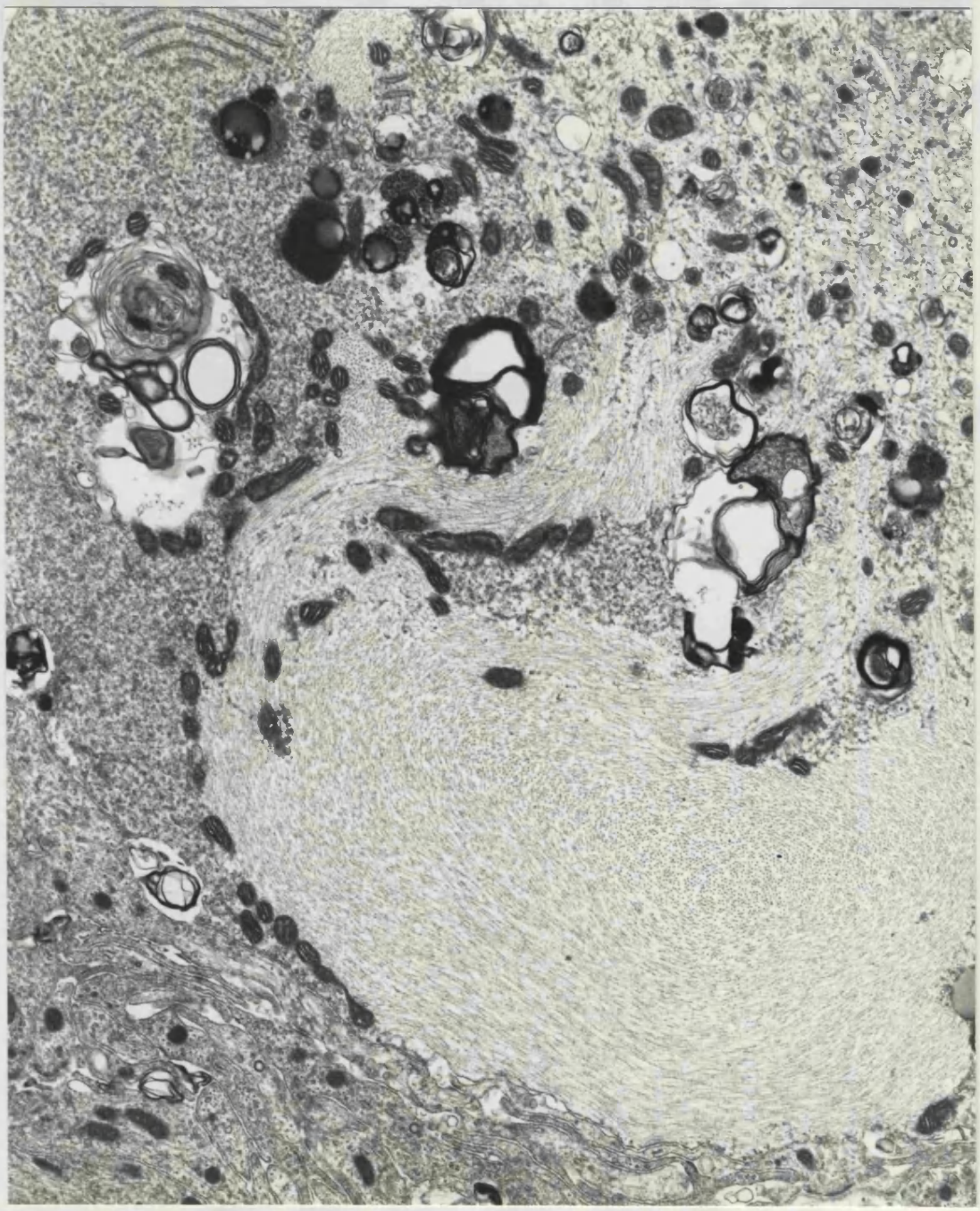

Fig. 23 DRG: 600 mg/kg/day for 10 days. Electron micrograph showing an accumulation of neurofilaments at the periphery of the cell, possibly part of the axon hillock. The surrounding cytoplasm is very abnormal, with large numbers of free ribosomes. Several collections of whorled membranes or myelin like bodies are seen as well as lipofuscin bodies. x 15,900.

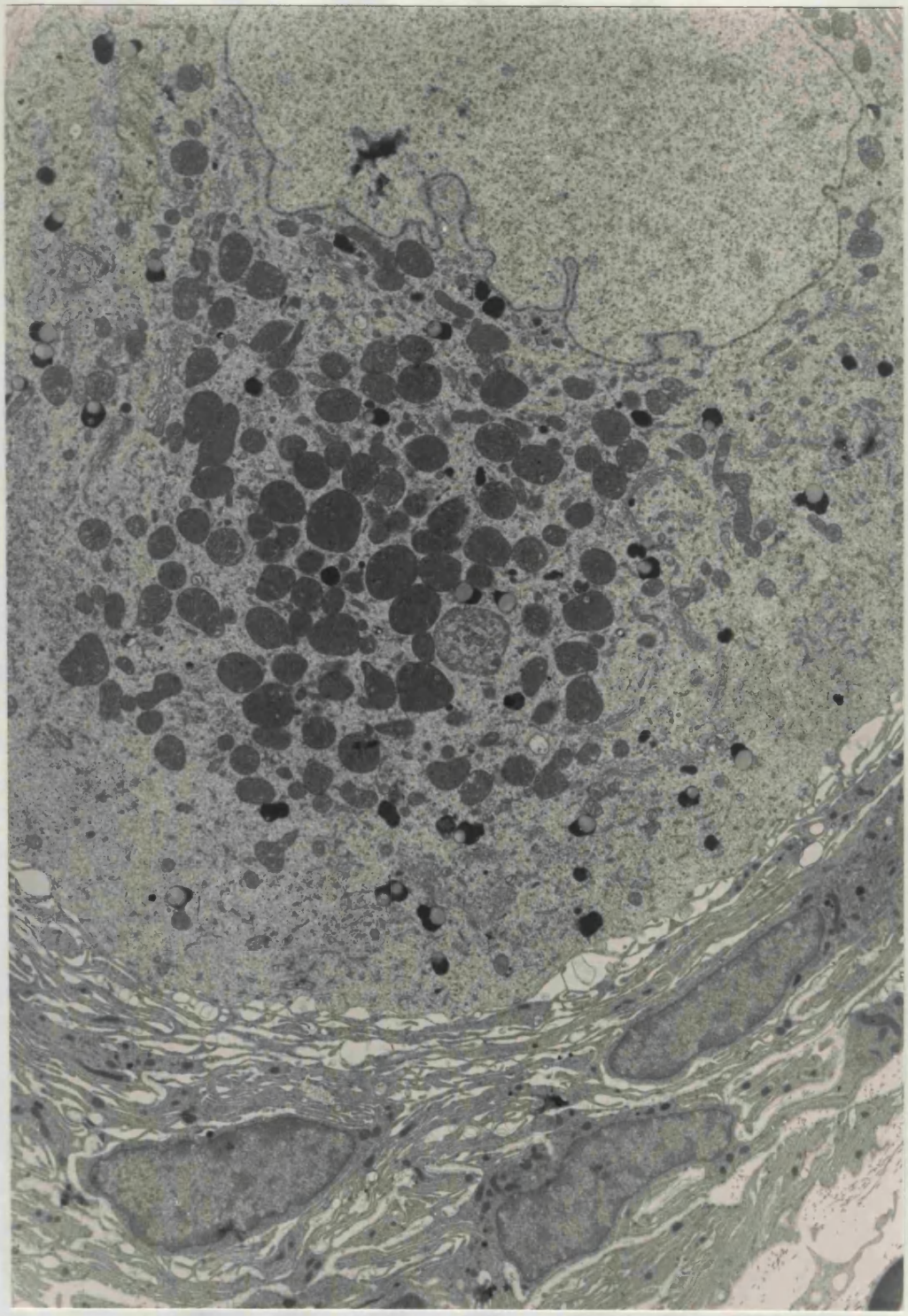

Fig. 24 DRG: 300 mg/kg/day for 3 months. Low power electron micrograph showing an abnormal cell with dispersed RER and an accumulation of mitochondria surrounded by multiple satellite cell processes. Some of the separation of these processes may be artefactual. Three satellite cell nuclei are seen. x 6,500.

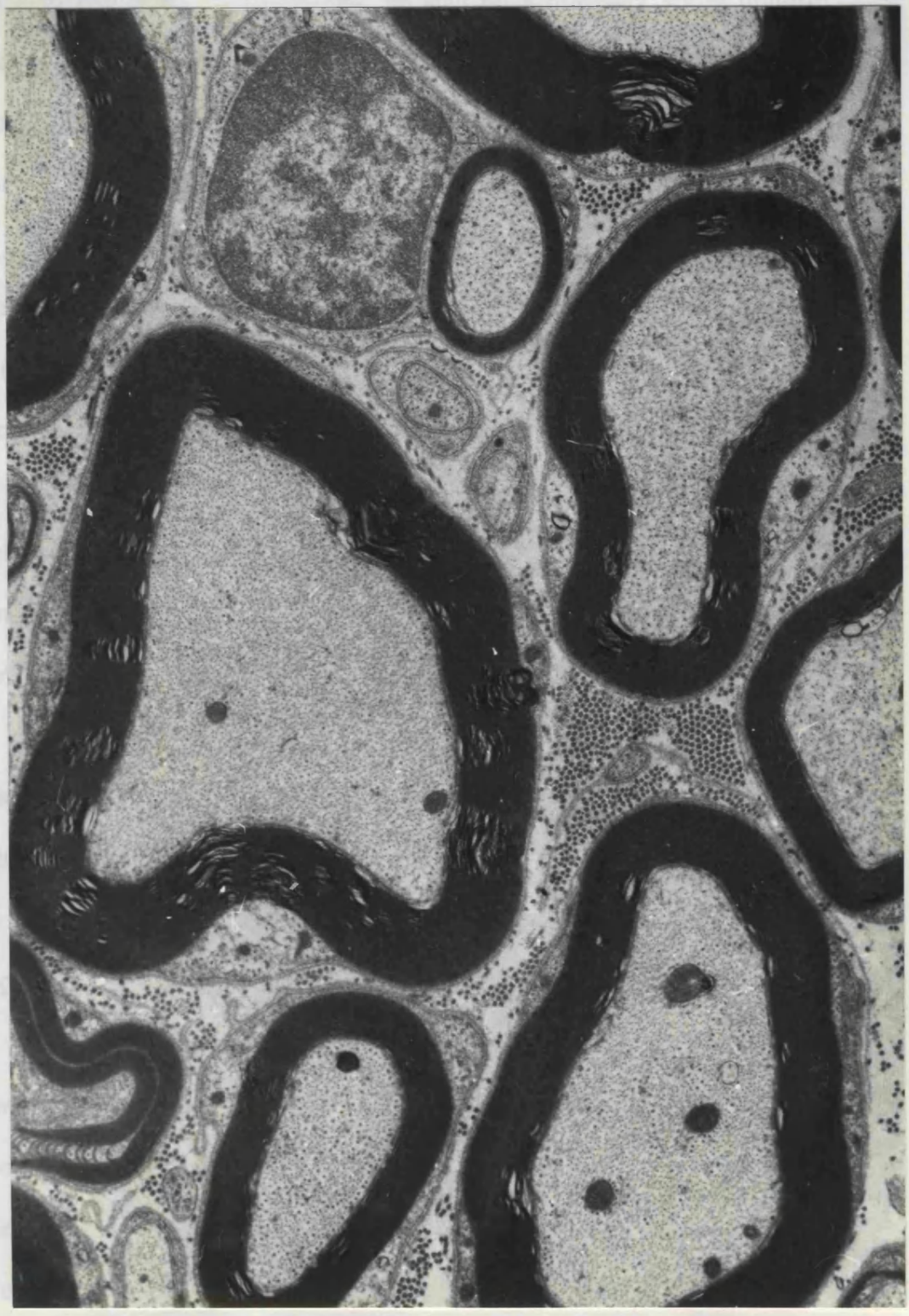

Fig. 25 Intraganglionic sensory fibres: 600 mg/kg/day for 10 days. Electron micrograph showing myelinated fibres containing excessive numbers of axonal neurofilaments. The smallest myelinated axon has a normal complement of axonal organelles. x 13,200.

microscopy in all groups of animals. Ganglion cells of the myenteric plexus were also examined. Sympathetic ganglia cells normally show uniform cytoplasmic staining with central nuclei and sometimes more than one nucleolus. Pre and post ganglionic fibres separate the neurons. The only abnormality seen was the very rare presence of some pale cells on the semi-thin sections, apparently with a peripheral nucleus (Fig. 26). Ultrastructurally there were no significant pathological findings although it has not been possible to study any of the pale neurons by electron microscopy. No degeneration of axons, myelinated or unmyelinated was seen within the ganglia or in small nerves afferent and efferent of the ganglia.

Myenteric plexus neurons showed normal morphology, even in animals with severe affected DRG.

Spinal Cord

Lumbar and cervical levels of spinal cord were examined by light microscopy in all groups of animals. In those animals showing abnormalities of dorsal root ganglion cells, there was degeneration of the dorsal columns at cervical level and to a lesser extent at lumbar, suggesting a pattern of distal degeneration (Fig. 27, a,b,). The fasciculus gracilis showed myelin debris associated with axonal degeneration. In the fasciculus cuneatus the degenerative changes were less severe.

The anterior horn cells, ventral roots and corticospinal motor tracts were well preserved.

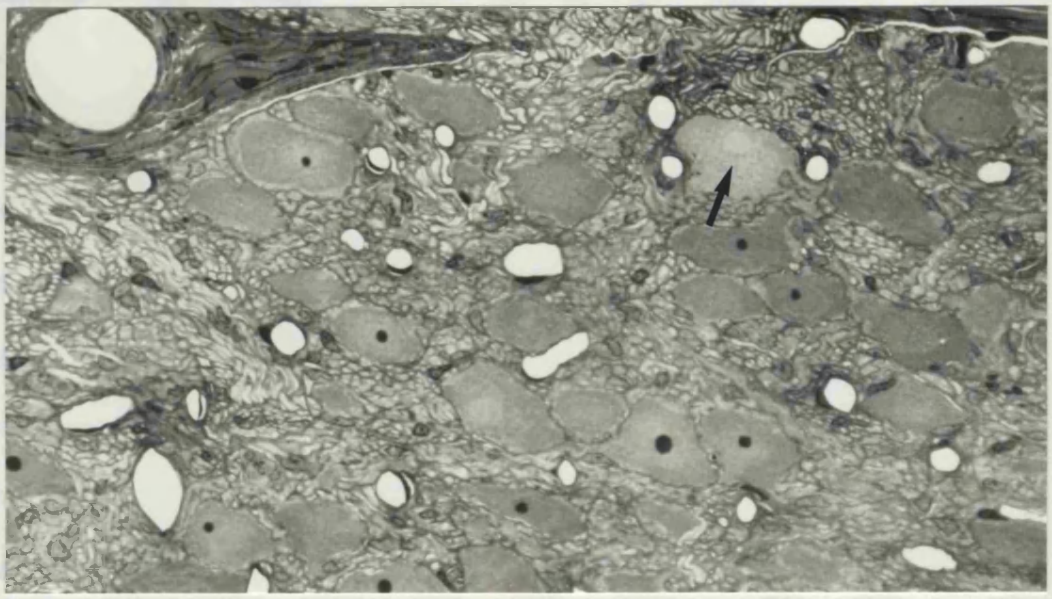

Fig. 26 Coeliac ganglion. 600mg/kg/day for 44 days. 1μm resin section showing a pale neuron with an eccentric nucleus (arrow). x 300.

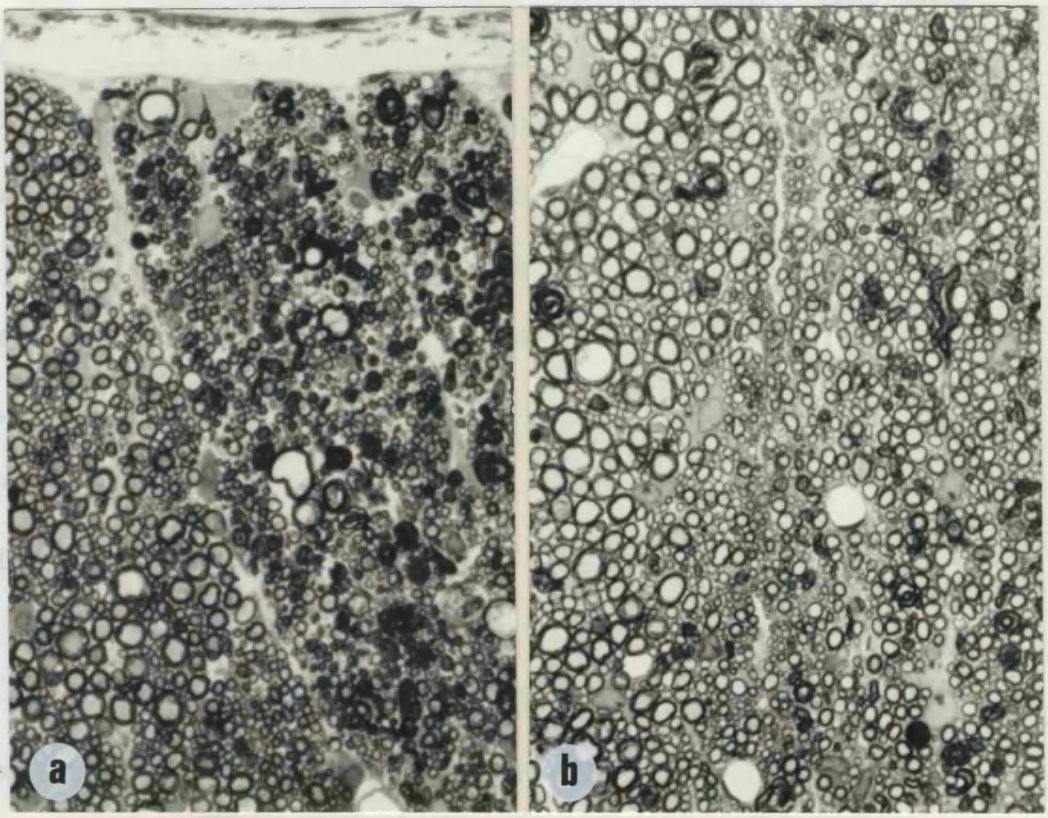

Fig. 27 1μm resin sections showing posterior columns of spinal cord from a rat given 600mg/kg/day for 10 days.

a) Cervical level. Fasciculus gracilis shows severe axonal degeneration. The fasciculus cuneatus is better preserved. x 300.

b) Lumbar level. Both fasciculus gracilus and cuneatus are less affected than at cervical level. x 300.

Saphenous nerve pathology

Light microscopy

In the saphenous nerves, as with the DRG cells, there was no clear relationship between dose and effect. The findings in rats given different doses of pyridoxine are described;-

<u>300 mg/kg/day for periods of 30 days - 90 days.</u>

Only 1 out of 9 animals showed nerve fibre degeneration. (Quantitative findings shown in Table VII). Of the remaining 8 rats, 7 showed changes in the axons of myelinated fibres which were not detectable by light microscopy, but which were apparent as disorganisation of axonal organelles (see below) by electron microscopy.

<u>600 mg/kg/day for periods of 10 days - 44 days.</u>

Of 11 rats, 6 showed no fibre degeneration or DRG cell changes, and of these 6, only 1 showed axonal abnormalities in myelinated fibres. In this one case, some axonal changes were visible by light microscopy as a slightly increased density of staining(Fig. 28), usually towards the centre of the axon, and confirmed by electron microscopy to be due to altered distribution of axonal organelles.

<u>900 mg/kg/day for 7 days</u>

Of 2 rats examined, degeneration of nerves and DRG abnormalities were seen in 1, whilst in the other axon changes were only visible by electron microscopy in otherwise normal-looking myelinated fibres.

Electron microscopy

Changes affecting the numbers and distribution of axonal organelles in otherwise normal-looking myelinated fibres

The axonal changes in myelinated fibres referred to above consist of alterations in the distribution and numbers of organelles. Not all fibres in any one animal showed this change but it did affect fibres of all sizes. Fig. 29 shows marked central clustering of microtubules, which was visible by light microscopy (see Fig. 28). In general there was clustering of microtubules at or near to the middle of the axon, with reduced numbers of filaments and a peripheral region with no, or few, recognisable organelles (Figs 30 A,B,C,D).

Distribution of axonal microtubules in myelinated fibres

This were studied quantitatively using square templates superimposed over electron micrographs, as described in Methods.

Myelinated axons were measured from 26 selected fibres from two experimental animals (300 mg/kg/day for 30 days) and 12 randomly selected control axons of similar size. Fig 31 shows that in control axons, the maximum number of microtubules/square was 7, and the percentage of squares with no microtubules was 16.7%. In experimental axons, the maximum number of microtubules/square from one nerve was 26, and 54.3% and 62.3% (from the two nerves respectively) of squares had no microtubules. These findings confirm the observed change in organelle

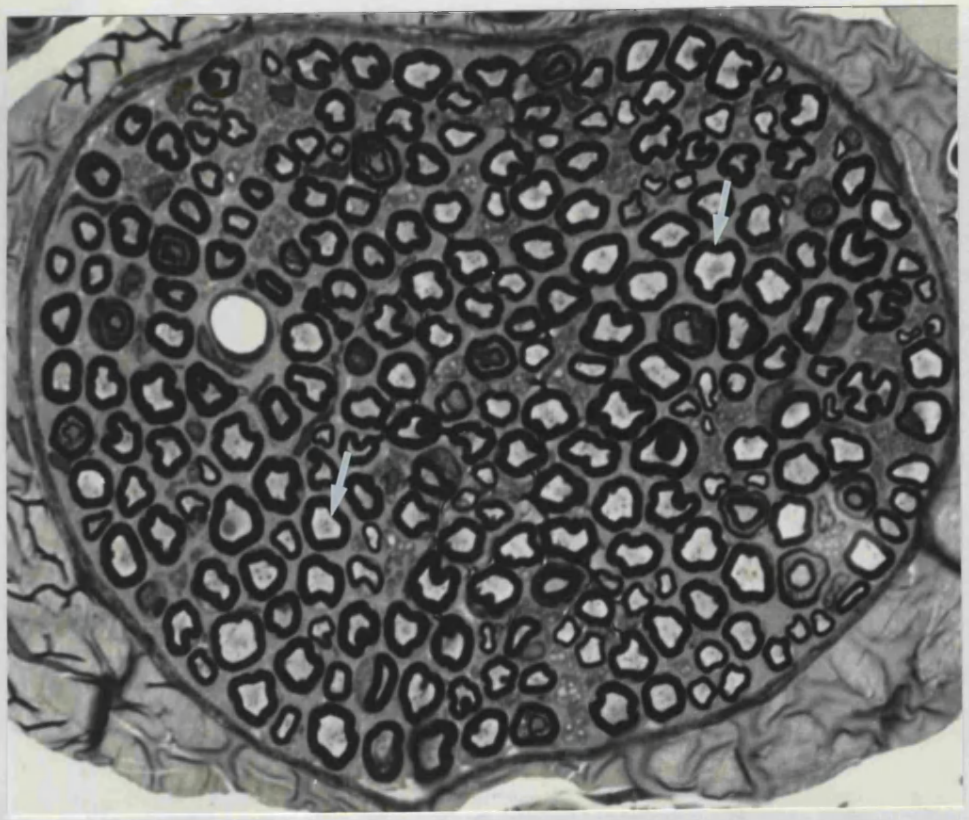

Fig. 28 1μm resin section showing the saphenous nerve of a rat given 600 mg/kg/day for 27 days. There is no degeneration. Many axons show increased central density of staining. Arrows indicate two such axons. x 1040.

Fig. 29 Electron micrograph of axon of fibre from nerve shown in Fig. 28 showing central clustering of microtubules and reduced number of neurofilaments. The peripheral zone of the axon contains few recognizable organelles. x 25,300.

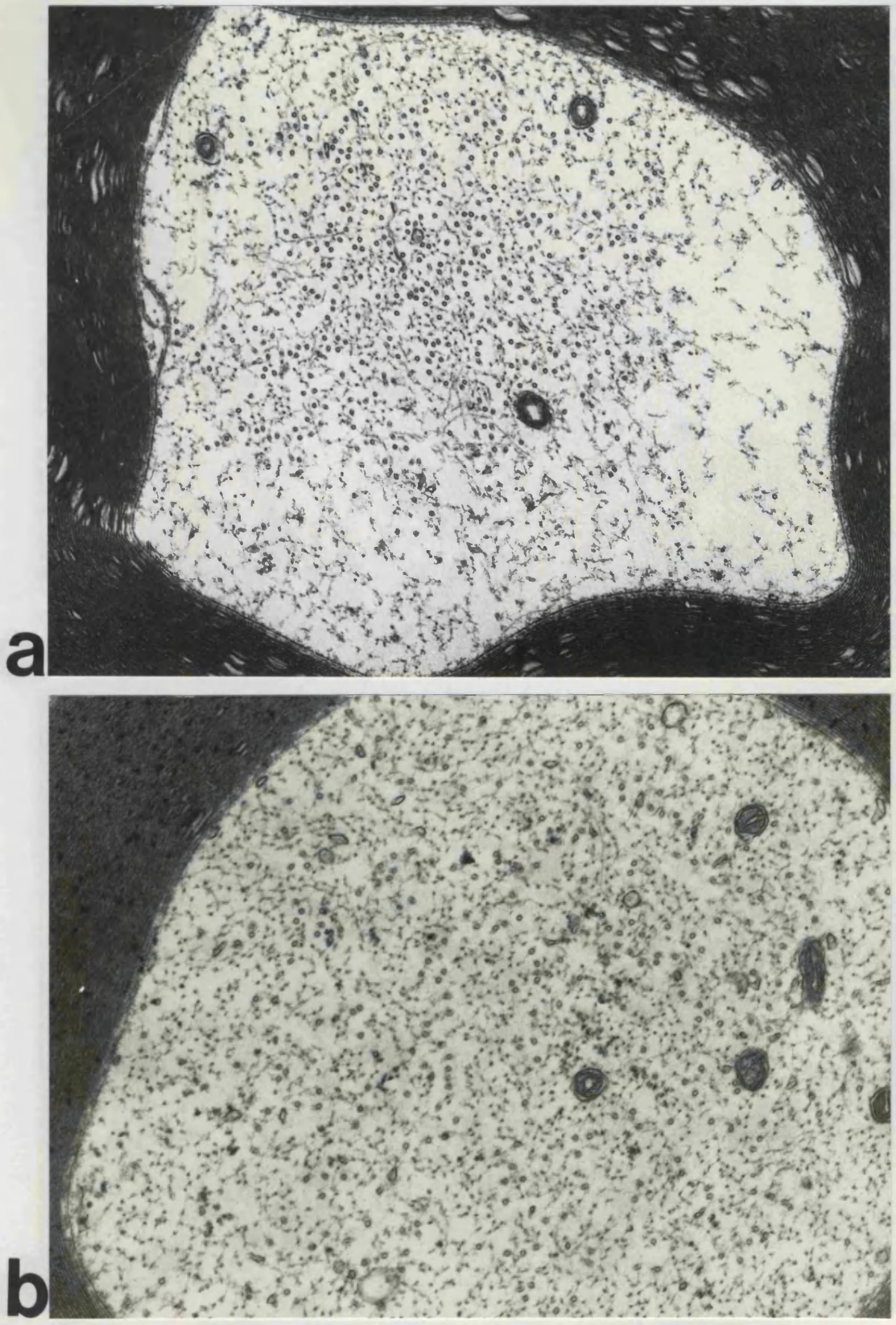

Fig. 30

a)Saphenous nerve. 300mg/kg/day for 60 days. Electron micrograph showing disorganisation of organelles in a large myelinated fibre with clustering of microtubules and a peripheral region of rarefaction. x 29,600.
(b)Control saphenous nerve. Large myelinated fibre showing the normal distribution of organelles. x 38,400.

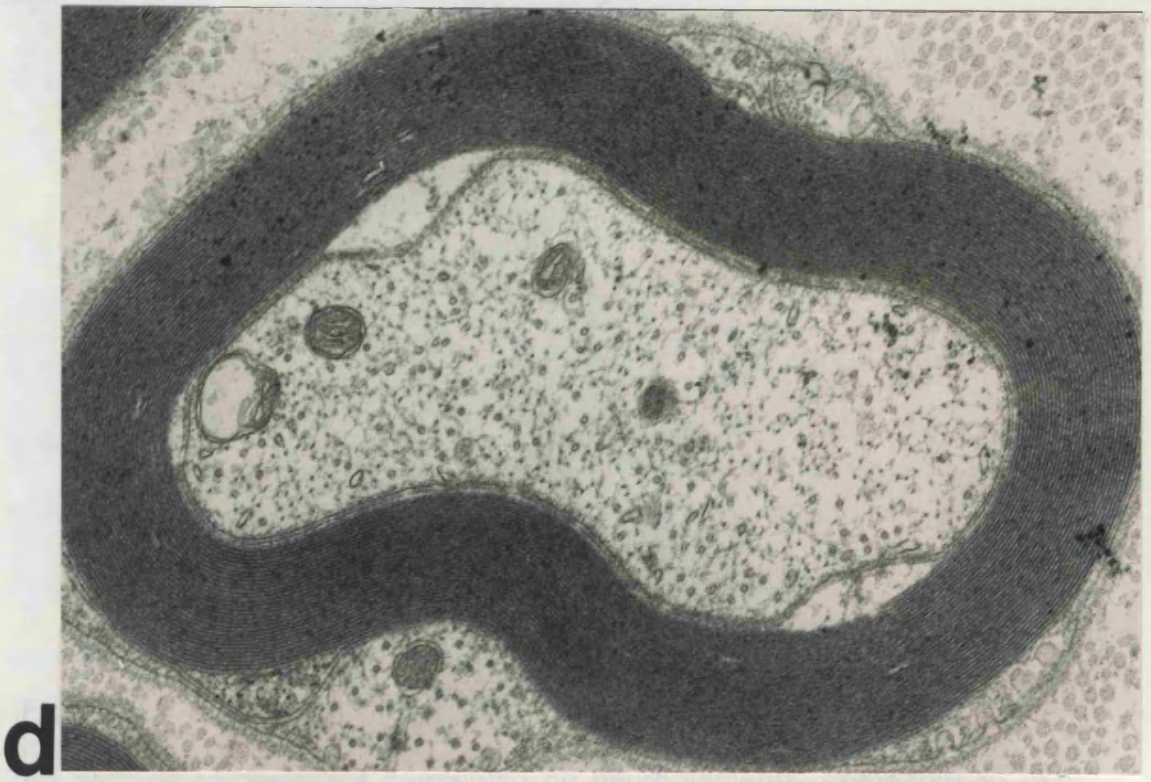

Fig. 30
(c)Saphenous nerve. 600mg/kg/day for 27 days. Electron micrograph showing clusters of microtubules, reduced number of filaments and peripheral rarefaction in a small myelinated fibre. x 37,300.
(d)Control saphenous nerve. A small myelinated fibre showing the normal distribution of organelles. x 40,000.

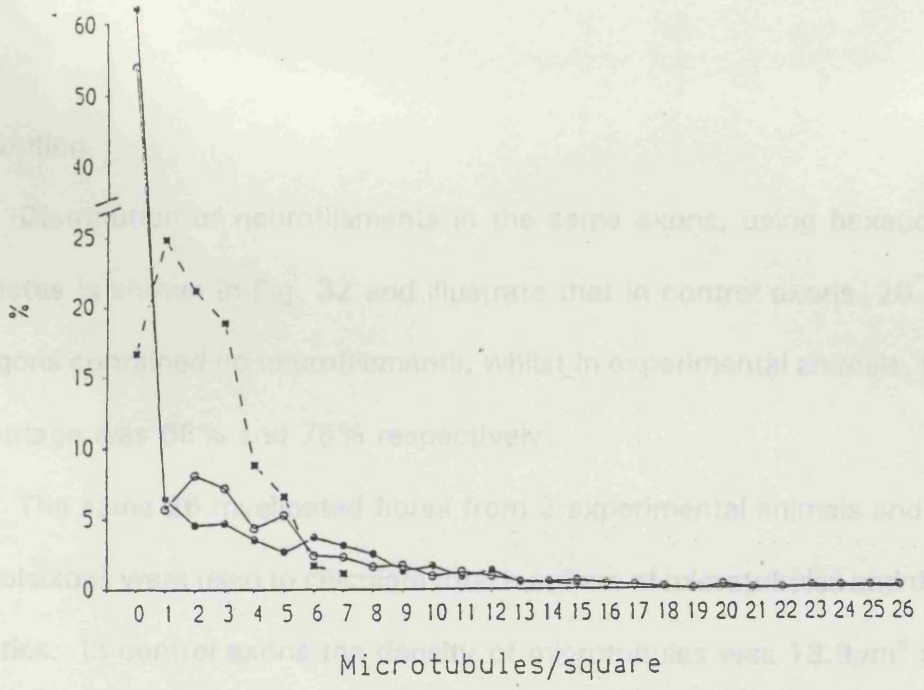

Fig. 31 Graph showing microtubule distribution in otherwise normal-looking myelinated fibres. In control axons (dotted line) the maximum number of microtubules/square was 7 and the percentage of squares without microtubules was 16.7%. In two experimental rats (continuous lines) given 300mg/kg/day for 30 days there was a high percentage of empty squares and the number of microtubules/square reached 26.

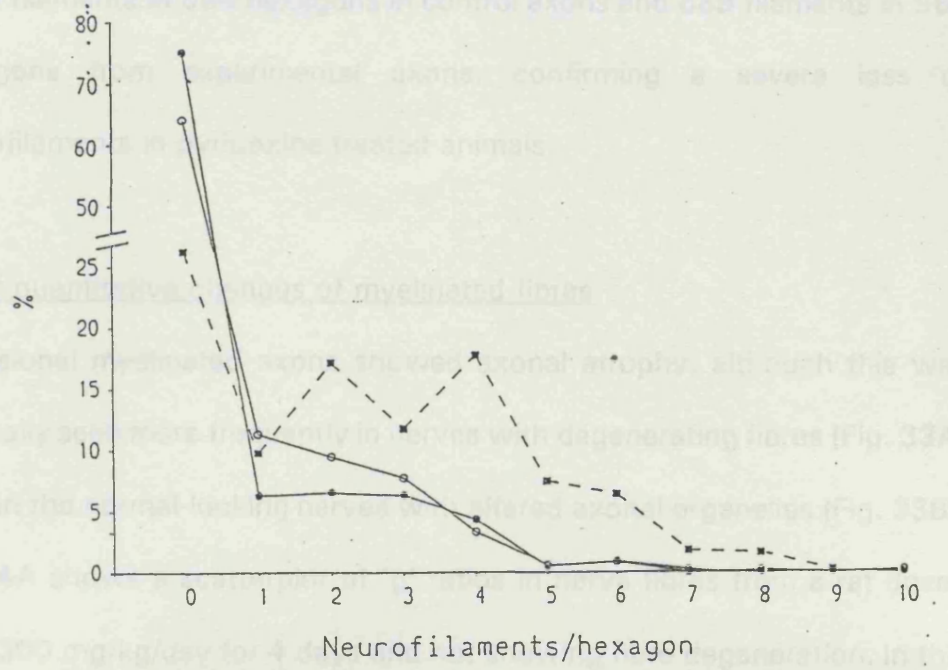

Fig. 32 Graph showing distribution of neurofilaments in otherwise normal looking myelinated fibres. In control (dotted line) axons there was a small percentage of hexagons containing no neurofilaments, compared to two experimental animals (continuous line) dosed with 300mg/kg/day for 30 days in which there was a high percentage of empty hexagons.

distribution.

Distribution of neurofilaments in the same axons, using hexagonal templates is shown in Fig. 32 and illustrate that in control axons, 26.2% hexagons contained no neurofilaments, whilst in experimental animals, this percentage was 66% and 75% respectively.

The same 26 myelinated fibres from 2 experimental animals and 12 control axons were used to calculate total numbers of microtubules and their densities. In control axons the density of microtubules was 18.9μm^2 and 20.8/μm^2 in experimental animals. This confirmed that clustering of microtubules was not associated with their loss. Numbers of neurofilament hexagons were counted and a total number was calculated. There were 1429 filaments in 564 hexagons in control axons and 689 filaments in 963 hexagons from experimental axons, confirming a severe loss of neurofilaments in pyridoxine treated animals.

Other quantitative changes of myelinated fibres

Occasional myelinated axons showed axonal atrophy, although this was generally seen more frequently in nerves with degenerating fibres (Fig. 33A) than in the normal-looking nerves with altered axonal organelles (Fig. 33B). Fig 34A shows a scatterplot of 'g' ratios in nerve fibres from a rat dosed with 300 mg/kg/day for 4 days and not showing fibre degeneration. In this animal 'g' was calculated from electron microscopy measurement of fibres. Using the methods described, it is very unusual for 'g' ratios of less than .5 to be found in normal animals (Fig 34B). An arbitrary line drawn at the 0.5

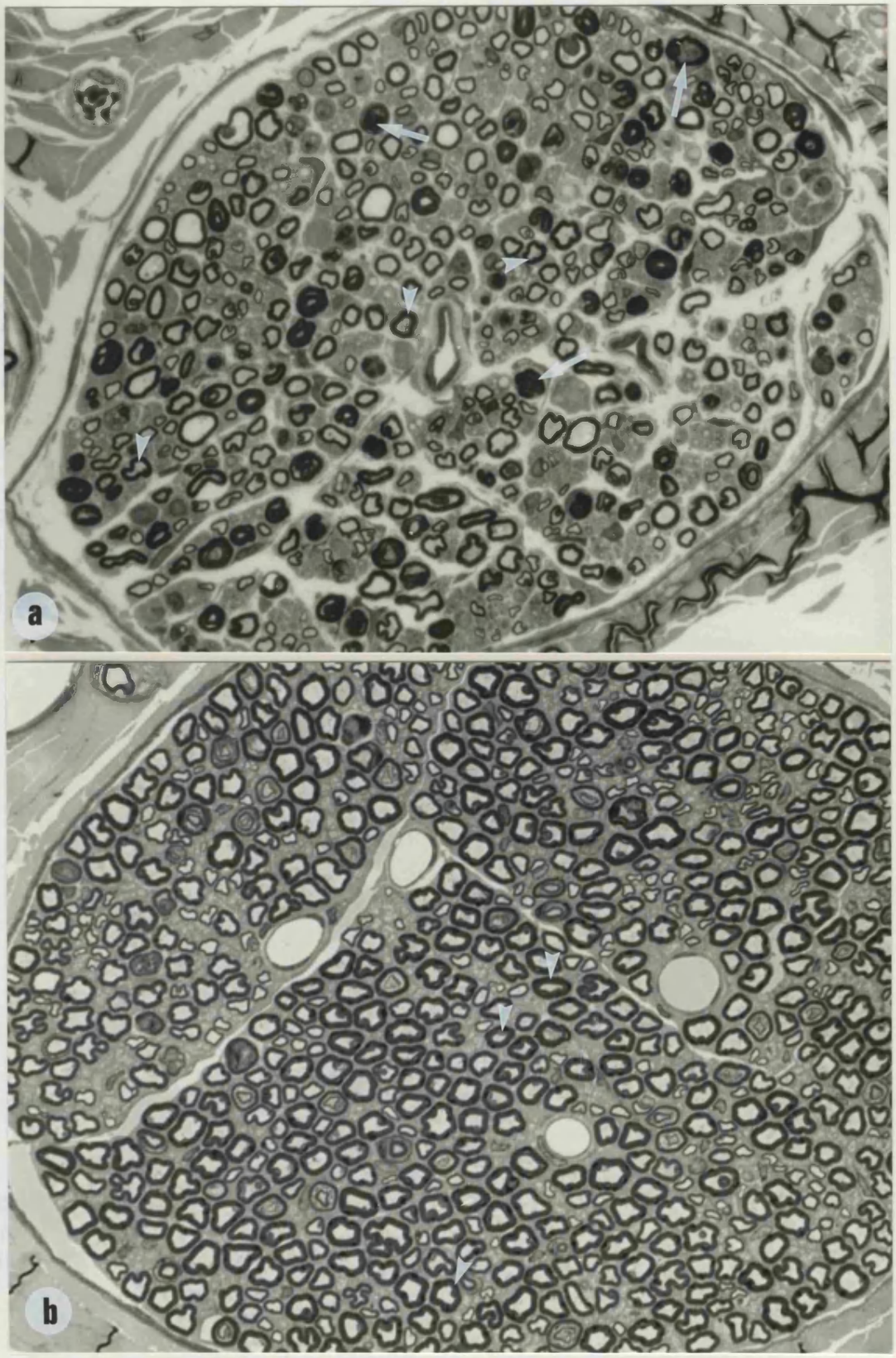

Fig. 33

(a)Saphenous nerve. 600mg/kg/day per 10 days. 1μm resin section showing several atrophic myelinated fibres (arrowheads) in a nerve with many degenerating fibres (arrows). x 450.

(b)Saphenous nerve. 300mg/kg/day for 90 days. 1μm resin section showing atrophic myelinated fibres (arrowheads) in a nerve without degeneration. x 450.

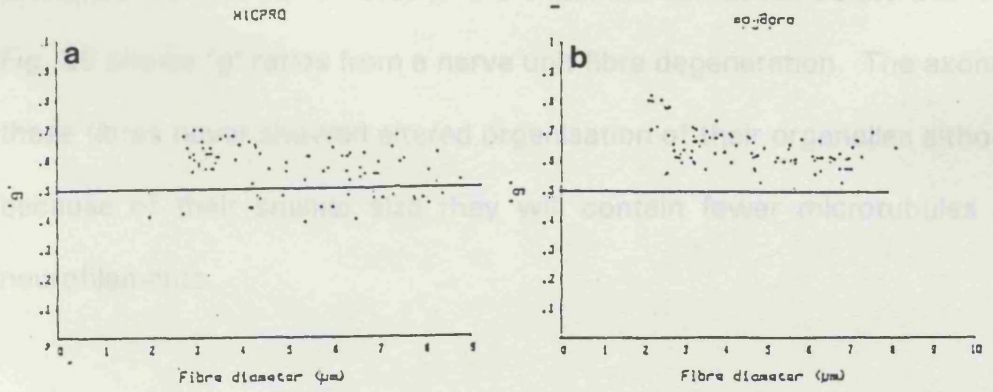

Fig. 34 Scatterplots of 'g' ratios
(a)Saphenous nerve. 600mg/kg/day for 27 days. A nerve without fibre degeneration showing several atrophic fibres with g ratios less than 0.5
(b)Control saphenous nerve. All the fibres show 'g' ratios above 0.5.

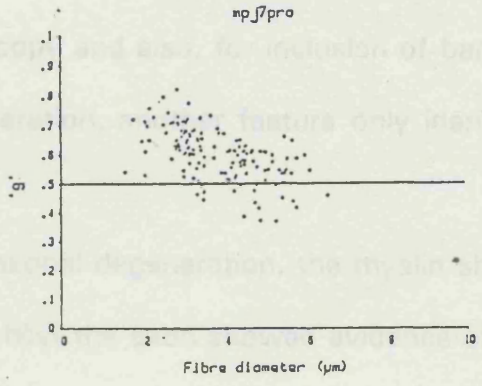

Fig. 35 Saphenous nerve: 600mg/kg/day for 44 days. scatterplot of 'g' ratio in a nerve with fibre degeneration. There are several atrophic fibres with 'g' ratios of less than 0.5.

levels shows that some fibres in the experimental rat fall below this level. Fig. 35 shows 'g' ratios from a nerve unit fibre degeneration. The axons of these fibres never showed altered organisation of their organelles although because of their smaller size they will contain fewer microtubules and neurofilaments.

Nerves with fibre degeneration

These were identified by light microscopy, when the presence of degenerating fibres was clearly visible (see Fig. 33A). Quantitative methods were applied to all nerves showing degeneration. As explained in Methods, quantitation was done on electron micrographs partly because of the difficulty of recognising myelinated fibres at an early stage of degeneration by light microscopy and also, for inclusion of bands of Büngner as a late stage of degeneration, another feature only identifiable at ultrastructural level.

In early axonal degeneration, the myelin sheath was often seen to remain intact whilst the axon showed evidence of degeneration (Fig. 36), often with loss of all recognisable organelles, or its total disappearance, leaving an empty space. In other fibres the axon had collapsed and contained only granular material (Fig. 37). The process of degeneration showed no features different from those of non-specific Wallerian type degeneration.

Bands of Büngner consisted of numerous Schwann cell processes bounded by a basement membrane; lipid globules were sometimes present

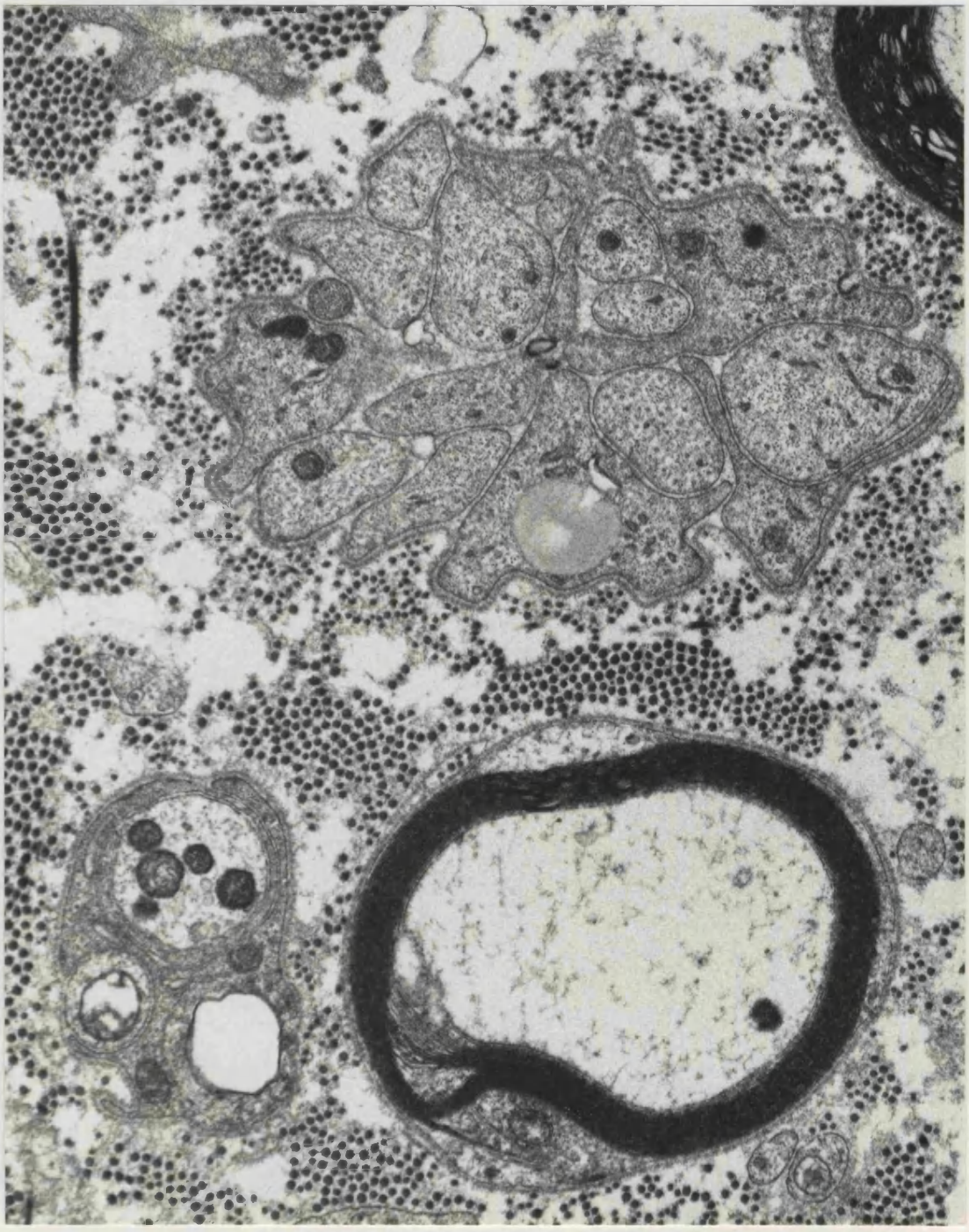

Fig. 36 Saphenous nerve. 600mg/kg/day for 10 days. Electron micrograph showing a myelinated fibre with intact myelin sheath and an axon almost completely devoid of organelles. A band of Bungner consisting of Schwann cell processes surrounded by basement membrane is also present. x 24,000.

Fig. 37 Saphenous nerve. 600mg/kg/day for 35 days. Electron micrograph showing a myelinated fibre with a collapsed axon containing dense granular material (arrow) and 2 bands of Bungner, one of them containing lipid material. Microtubule clustering is also seen in the remaining myelinated fibres. Unmyelinated fibres appear normal. x 9,900.

in the Schwann cell cytoplasm (see Fig. 36). Histograms showing the fibre diameter distribution of remaining fibres in each of these nerves showed a shift to the left compared with controls, indicating a tendency for the selective degeneration of the larger fibres. Figs. 38 and 39 illustrate the shift to the left at proximal and distal levels of nerves from rats given 600 mg/kg/day for 35 and 44 days respectively.

Atrophic fibres with axons small for myelin sheath thickness have been mentioned above, and are illustrated in electron micrographs in Figs. 40, 41 and 42. In some fibres the myelin sheath is more or less circular, having apparently accommodated to the reduced size of its axon (Figs. 40 and 41); in other fibres the myelin sheath is irregular in shape (Fig. 42). In most cases the schwann cell has an irregular contour and the basement membrane is folded (Figs. 40, 41 and 42). Fig. 42 shows regenerating axons, one of which is myelinated, in very close association with an atrophic myelinated fibre. Only a few remnants remain of what was possibly a common basement membrane. This may indicate that the fibre has degenerated distally, and sprouting has occurred from a proximal node of Ranvier.

Scatterplots of 'g' ratios are shown in Figs. 34A and 35A. In the nerves with fibre degeneration examined by electron microscopy, the 'g' ratios were calculated from measurements made on electron micrographs. To confirm the accuracy of these measurements, myelin lamellae counts were done; these showed a close correlation with measurements made by tracing axon and fibre contours (Fig. 43).

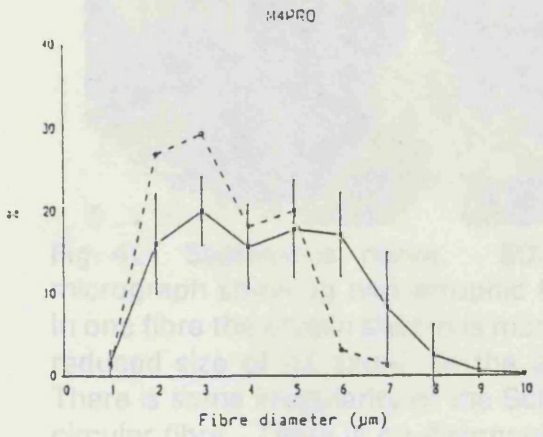

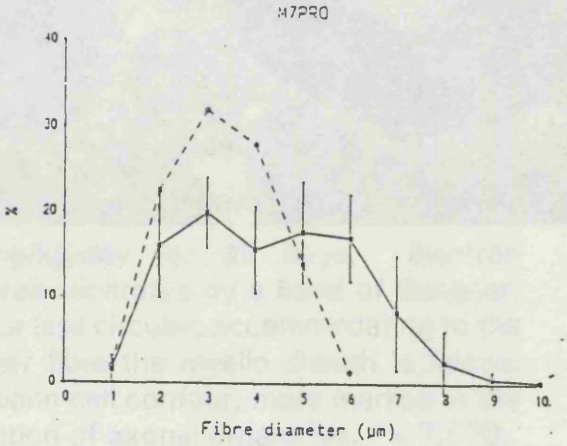

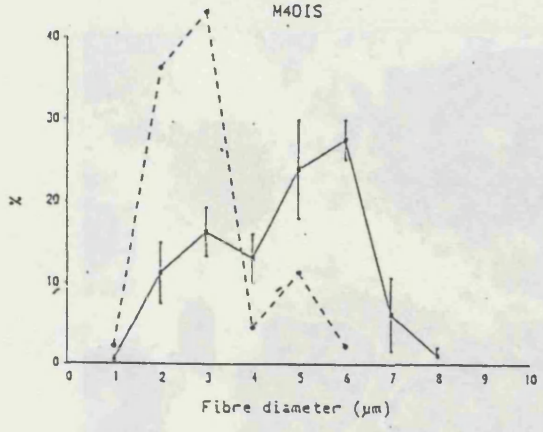

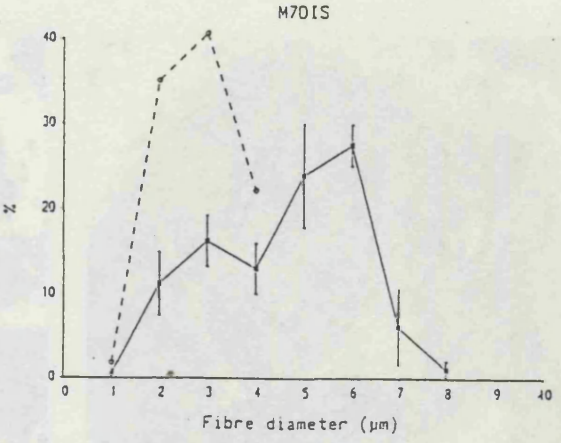

Fig. 38 Fibre diameter distribution graph from proximal (above) and distal (below) ends of a saphenous nerve of an animal given 600mg/kg/day for 35 days (dotted line). The continuous line shows means and standard deviations from 4 controls. there is a clear shift to the left of experimental fibres, compared with controls, which is more pronounced distally.

Fig. 39 Fibre diameter distribution graphs from proximal (above) and distal (below) ends of a saphenous nerve of an animal given 600mg/kg/day for 44 days. The continuous line shows means and standard deviation values from 4 controls. There is also a clear shift to the left in the experimental animal (dotted line) more evident distally.

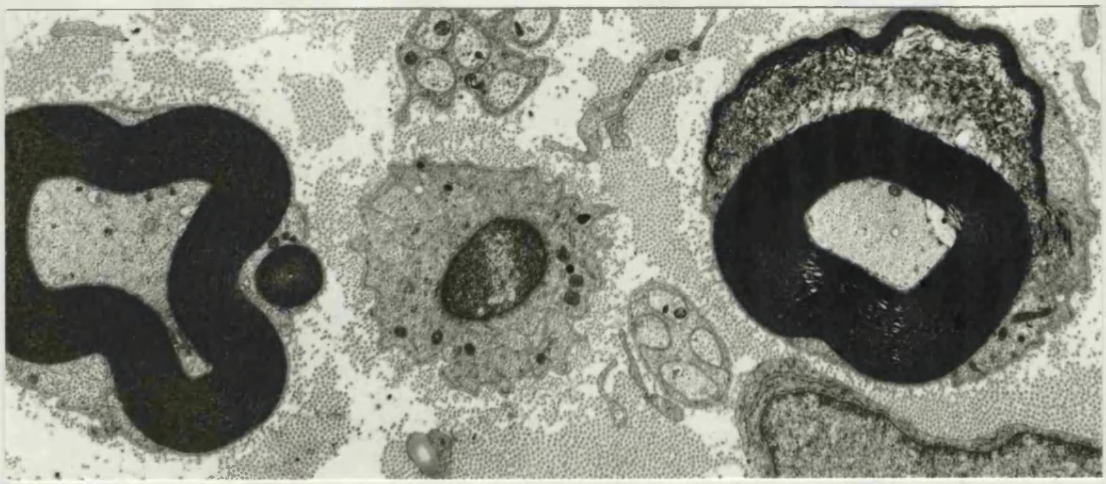

Fig. 40 Saphenous nerve. 600mg/kg/day for 35 days. Electron micrograph showing two atrophic fibres separated by a band of Bungner. In one fibre the myelin sheath is more or less circular, accommodating to the reduced size of its axon. In the other fibre the myelin sheath is folded. There is some irregularity of the Schwann cell contour, more marked in the circular fibre. There is no disorganisation of axonal organelles. x 7,500.

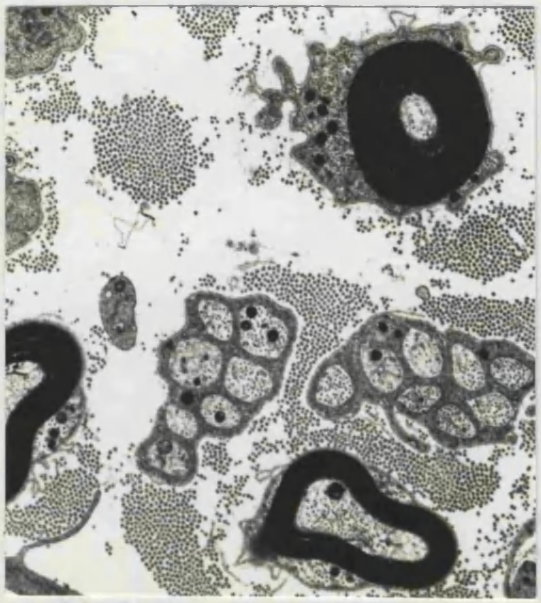

Fig. 41 Saphenous nerve. 600mg/kg/day for 35 days. Electron micrograph showing a small atrophic fibre with an extremely small axon relative to the thickness of the myelin sheath. There is marked irregularity of the Schwann cell contour. x 9,900.

Fig. 42 Saphenous nerve. 600mg/kg/day for 44 days. Electron micrograph showing an atrophic myelinated fibre of irregular shape. Two axons, one of which is myelinating, seen in very close association with this fibre, and almost certainly represent regenerating sprouts arising from a proximal node of Ranvier. x 9,900.

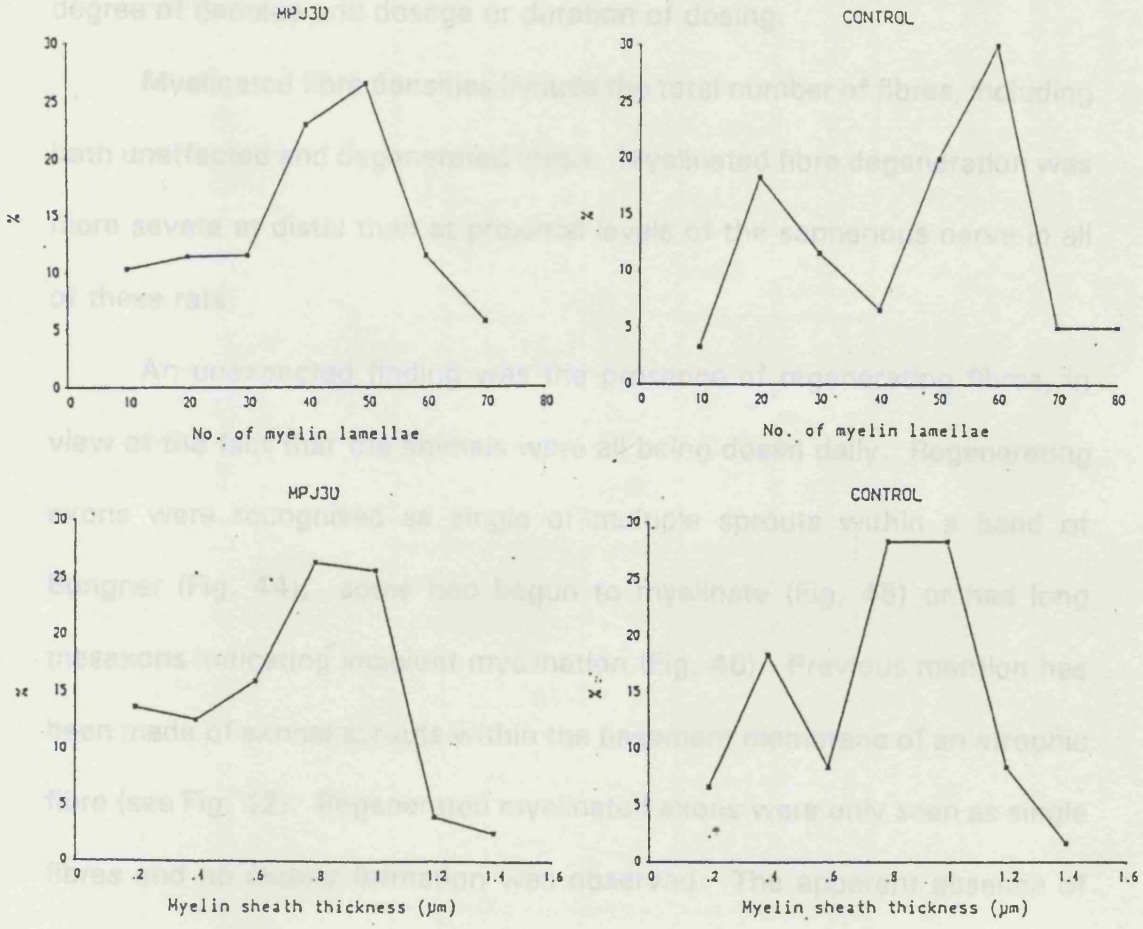

Fig. 43 Graphs comparing methods of measurements of the myelin sheaths by counts of myelin lamellae (above) and myelin sheath thickness measured by tracing axon and fibre contours (below). Left, saphenous nerve, 600mg/kg/day for 27 days. Right, control saphenous nerve.

Quantification of myelinated and unmyelinated axon degeneration

Table VII shows the results from rats given either 300mg/kg/day pyridoxine for 90 days (1 rat) or 600mg/kg/day (6 rats) for periods from 10-44 days. As previously observed there is no clear relationship between degree of damage and dosage or duration of dosing.

Myelinated fibre densities include the total number of fibres, including both unaffected and degenerated fibres. Myelinated fibre degeneration was more severe at distal than at proximal levels of the saphenous nerve in all of these rats.

An unexpected finding was the presence of regenerating fibres, in view of the fact that the animals were all being dosed daily. Regenerating axons were recognised as single or multiple sprouts within a band of Bungner (Fig. 44); some had begun to myelinate (Fig. 45) or had long mesaxons indicating incipient myelination (Fig. 46). Previous mention has been made of axonal sprouts within the basement membrane of an atrophic fibre (see Fig. 42). Regenerated myelinated axons were only seen as single fibres and no cluster formation was observed. The apparent absence of regenerating fibres in the 90-day dosed rat may be due to the difficulty in recognising a small, single regenerating fibre from an original small fibre.

Table VII shows a higher percentage of regenerating fibres in proximal levels of the nerve than at distal levels.

Unmyelinated fibres were affected in all animals with nerves showing myelinated fibre degeneration (Table VII). The axons sometimes appeared swollen and devoid of organelles (Fig. 47). However, in many cases their

TABLE VII Quantitation results in proximal and distal ends of 5 saphenous nerves of rats dosed with 600 mg/kg/day from 10-44 days and one dosed for 90 days with 300 mg/kg/day.

	10 days	27 days			27 days			35 days		44 days		90 days		Controls	
	P	P	D	FD	P	D	FD	P	D	P	D	P	D	P	D
Fibre density/mm^2	20,795	17,073	17,893	15,626	19,329	26,135	18,176	21,384	25,990	18,545	22,658	19,983	18,689	25,624 23,310	19,095 21,350
% Degenerated fibres	38.9	26.7	37.7	49.6	14.2	27.6	35.12	30	52.4	30.6	37.2	19.2	47.5	0	0
% Regenerated fibres	0	0	0	0	3.8	3.2	0	2.75	0	16.3	12.73	0	0	0	0
Unmyelinated axon density/mm^2	14,381	36,640	60,520	50,815	100,720	82,355	53,088	59,754	58,320	83,243	27,610	22,872	19,829	87,034 85,132	87,162 87,565

P = proximal D = distal FD = far distal

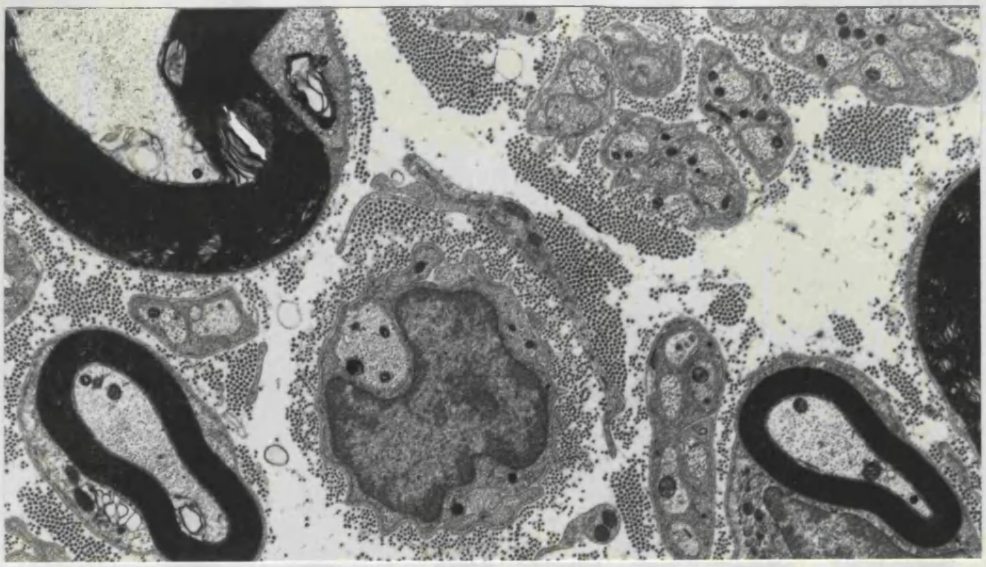

Fig. 44 Saphenous nerve. 600mg/kg/day for 27 days. Electron micrograph showing a single regenerated sprout in a band of Bungner. This is seen to be considerably larger than the adjacent unmyelinated axons. x 9,900.

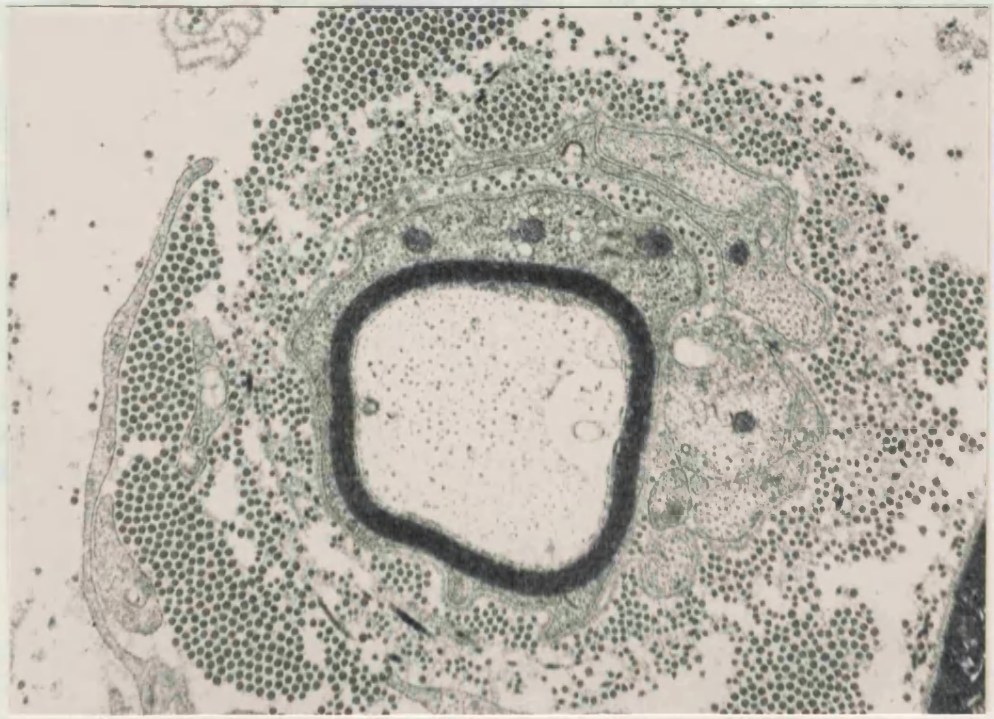

Fig. 45 Saphenous nerve. 600mg/kg/day for 27 days. Electron micrograph showing regenerated fibre with thin myelin sheath. Many Schwann cell processes are also seen within a common basement membrane, confirming that this is a regenerating fibre. x 20,500.

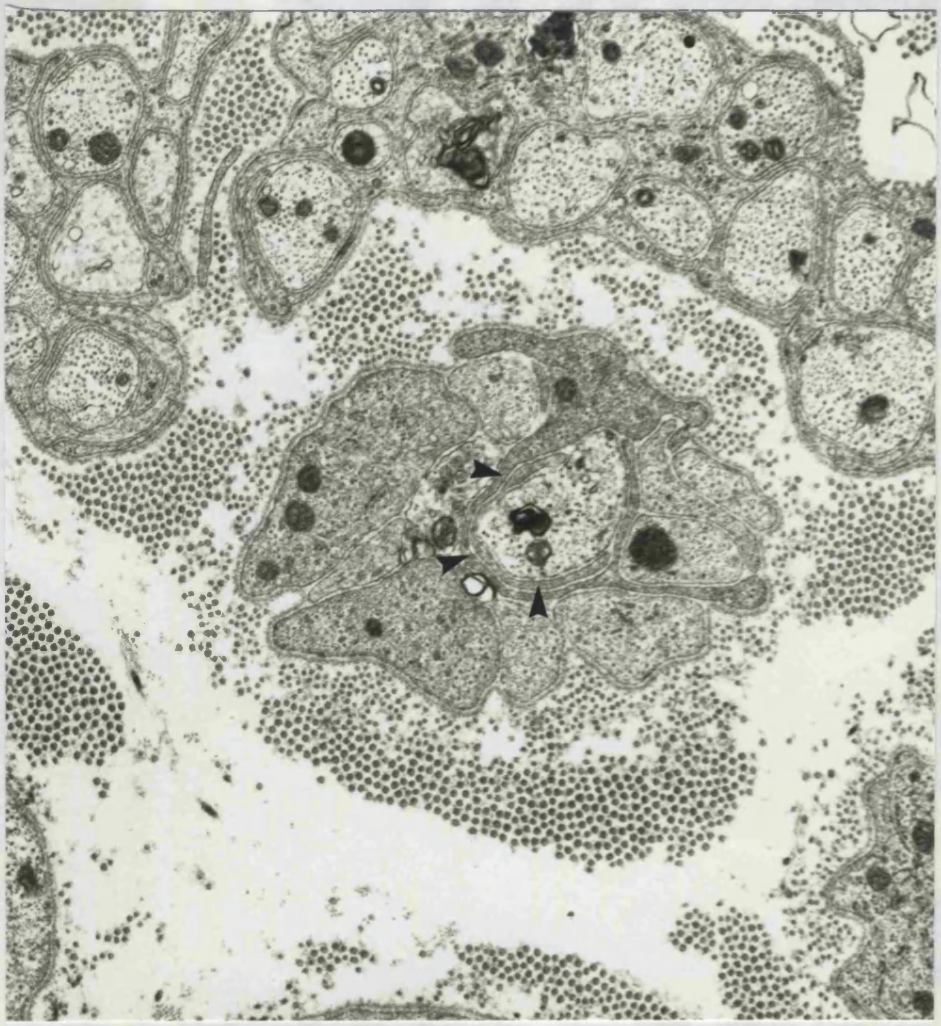

Fig. 46 Saphenous nerve. 600mg/kg/day for 35 days. Electron micrograph showing a band of Bungner containing a single axonal sprout which is partly encircled by elongated mesaxon (arrowheads), indicating incipient myelination. x 16,500.

Fig. 47 Saphenous nerve. 600mg/kg/day for 10 days. Electron micrograph showing three swollen unmyelinated axons without recognizable axonal organelles. The arrangement of Schwann cell processes suggests that there has been loss of several axons from this fibre. x 26,400.

loss was inferred from the appearance of the denervated Schwann cell processes (Fig. 48) and confirmed by quantitation. The banding of Schwann cell processes, usually regarded as evidence of loss of unmyelinated axons was not seen. The unmyelinated counts were sometimes difficult to interpret since they seemed to vary very widely from one level to another.

The sample area counted was very small, possibly giving rise to variable results, but this was also the case for the controls in which the axon density was very consistent. Another explanation for higher densities at more proximal levels is that regeneration had occurred. This is very difficult to identify. Measurement of unmyelinated axon size in these nerves showed a unimodal peak at about 1 μm, with no sign of a peak of smaller axons that might be expected in a regenerating population (Fig 49).

Teased Fibres

Examination of teased fibres from the saphenous nerve in affected animals showed fibres in various stages of degeneration, however, of more interest was the presence of fibres in which distal degeneration and distal regeneration could be identified. Fig. 50 shows a single fibre from one rat killed after 10 weeks dosing with 600mg/kg/day pyridoxine in which the nodes of Ranvier at two normal internodes are indicated: beyond these the succeeding internode shows early axonal degeneration with clear discontinuity of the myelin sheaths. Fig. 51 is of teased fibre from a rat after 4 weeks dosing with 600mg/kg/day showing a normal internode proximal to several short, regenerated internodes. These figures illustrate

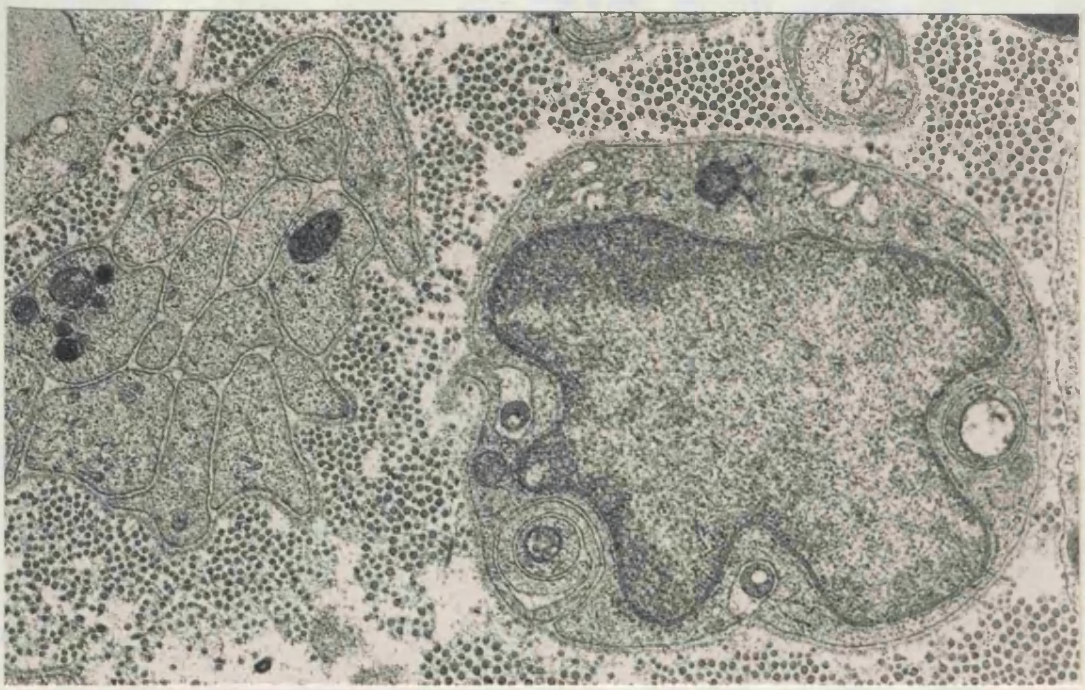

Fig. 48 Saphenous nerve 600mg/kg/day for 10 days. Electron micrograph showing denervated Schwann cell processes. On the left is a band of Bungner and on the right is a Schwann cell and processes of what was probably an unmyelinated fibre. x 26,400.

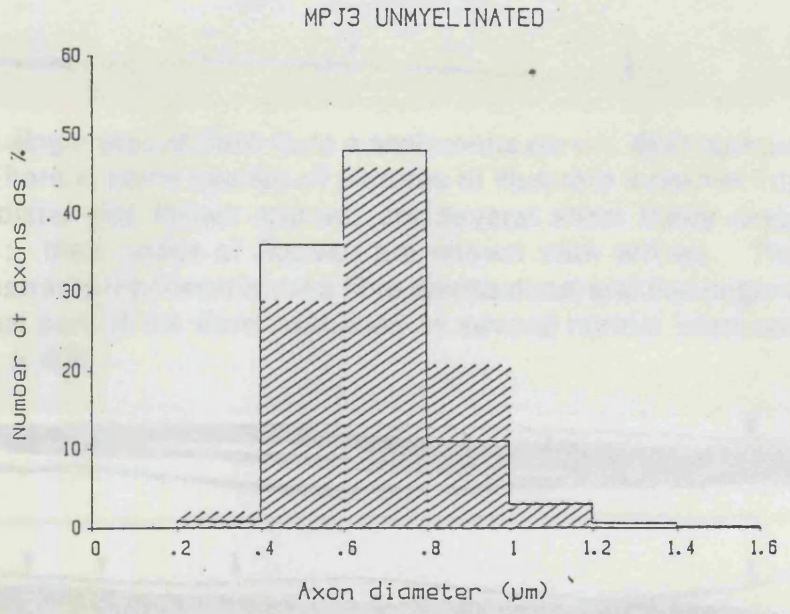

Fig. 49 Saphenous nerve. 600mg/kg/day for 27 days. Histogram showing the size distribution of unmyelinated axons in control (open) and experimental (hatched) nerves. There is close correspondence between the two histograms.

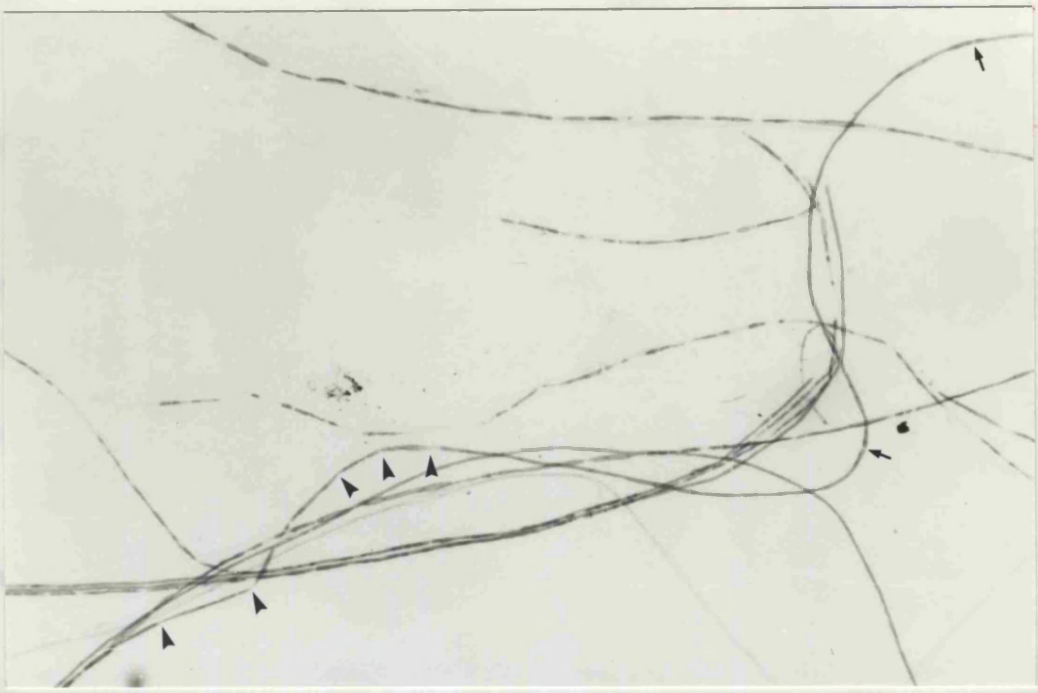

Fig. 50 Teased fibres from saphenous nerve; 600 mg/kg/day for 10 days. Two normal nodes of Ranvier are shown with arrows. At the distal end of this fibre (to the left) the myelin sheath is segmented, an early indication of axonal degeneration (arrowheads). Several other degenerating fibres are also seen. x 160.

Fig. 51 A single teased fibre from a saphenous nerve; 600mg/kg/day for 27 days. There is some overlap of pictures to illustrate a normal internode at whose distal end (lower picture) are several short thinly myelinated internodes ; their nodes of Ranvier are shown with arrows. This fibre possibly illustrates regeneration of a fibre whose distal end had degenerated. The proximal part of the fibre continued as several normal internodes (not illustrated). x 400.

Fig. 52 A single teased fibre from the same nerve as Fig. 51. Arrows mark three consecutive widened nodes of Ranvier. The arrowhead marks similar points along the tissue. The fibre showed some irregularity of its myelin sheath, possibly indicating axonal atrophy. x 160.

that a process of distal degeneration and regeneration occurs, at least in some fibres. Fig. 52 shows a fibre from a 4 week dosed animal with 600mg/kg/day in which three successive widened nodes are seen. The myelin appears irregular, there is also myelin folding possibly associated with axonal atrophy.

Intraneural Injection of Pyridoxine

Pyridoxine at different concentrations (20%, 10%, 1%, 0.1%, 0.01%) was injected into the sciatic nerve. Injected volumes were of approximately 20μl, so that quantities of pyridoxine given were $4x10^{-5}$, $2x10^{-5}$, $2x10^{-6}$, $2x10^{-7}$, $2x10^{-8}$g respectively. Control rats were given 20μl of distilled water. Six rats were killed at 4 days, 15 rats at 7 days and 3 rats at 14 days. Five controls were killed at the same intervals.

The level of bifurcation of the sciatic nerve into tibial and peroneal branches varies from one animal to another; in some rats injection was made into the single unbranched sciatic nerve, in others it was made into the larger, tibial branch. After immersion fixation (see methods) proximal and distal 0.5cm segments of nerve were taken approximately 1cm above and below the site of injection respectively.

In some cases it was difficult to identify the exact site of injection. In later experiments the site was marked by placing a suture in adjacent tissues. In many cases both ends of the proximal segment of nerve taken for histology were examined. Generally the upper level corresponded to the upper limit of proximal spread of pyridoxine, whilst the lower level lay in the

region of its maximal effect.

A few failures were due mainly to incorrect positioning of the needle; in these cases no damage was found within the nerve.

Clinical examination

At the time of killing all of the animals were examined. In those with successful injections, there was reduced grip of the injected limb and in a few the limb appeared to be partially paralysed. Control rats showed no physical abnormalities.

General histological findings after injection

The main effect at all concentrations of pyridoxine was axonal degeneration; there was no obvious relationship to dose. It was possible from the pattern of degeneration, which was usually massive, to identify the pathway that the injected pyridoxine had followed, showing its limited proximal movement; probably only about 1cm, and sometimes non-uniform lateral spread. When the injection was made into the tibial nerve it was possible to observe in proximal sections that only that fascicle was affected, there being no lateral spread through the septum of perineurium separating the two fascicles (Fig 53a,b).

In control nerves there was occasional evidence of needle track damage affecting a few myelinated fibres.

<u>4 days</u>

At the proximal end of the nerve most of the fibres showed axonal degeneration with a particular finding that in a great proportion of fibres the myelin sheath collapsed and the degenerated fibres were elongated or "cigar

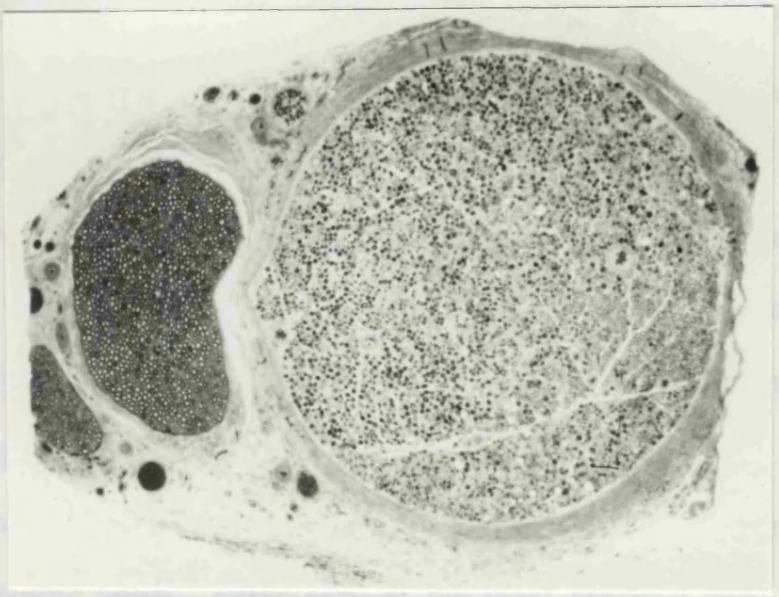

Fig. 53a 1μm resin section showing tibial nerve injected with 0.1% pyridoxine, 7 days survival. The smaller peroneal branch is normal compared with the tibial which shows marked oedema separating myelinated fibres. x 80.

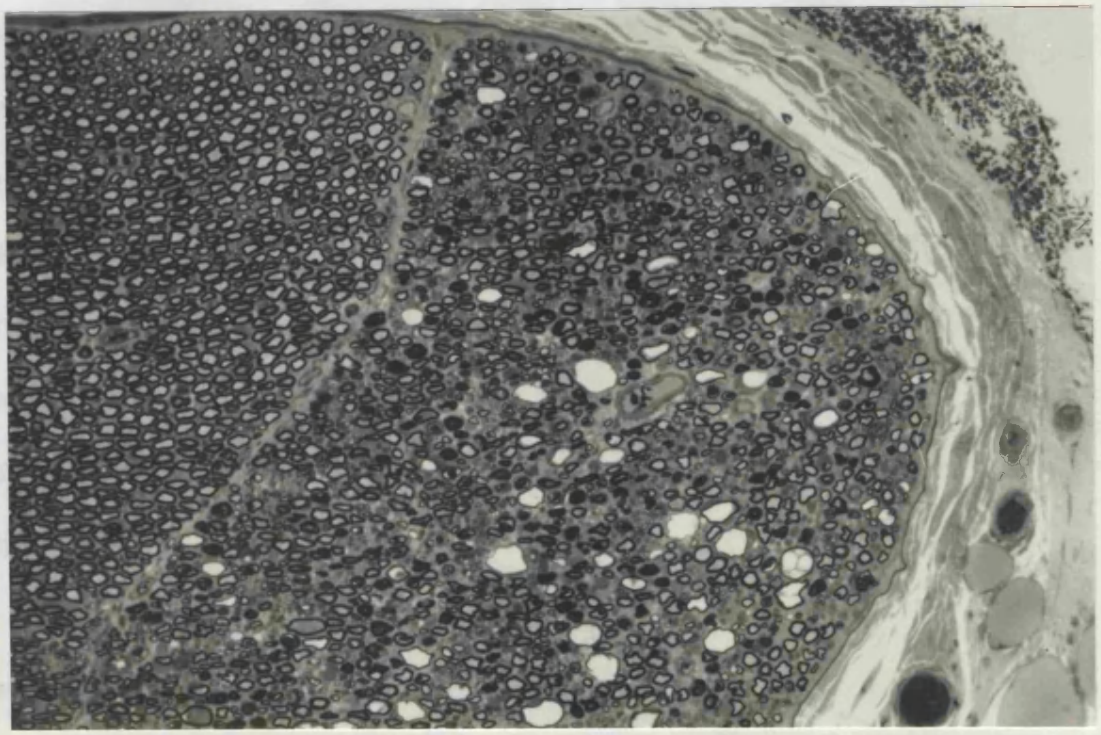

Fig. 53b 1μm resin section showing the tibial (right) and peroneal (left) branches divided by a septum, 7 days after injection of 0.1% pyridoxine in the tibial nerve. Degenerating fibres are seen restricted to the tibial branch. There has been no lateral spread to the peroneal nerve through the septa. x 188.

shaped" (Fig. 54). The axon in many of these fibres was no longer recognizable, or showed dense staining both on light and electron microscopy. Apart from the unusual shape of the degenerating fibres, they showed no differences from the non-specific axonal degeneration.

Unmyelinated axons appeared to be very susceptible. In some areas where there was little myelinated fibre degeneration the unmyelinated fibres were severely damaged, swollen and empty axons were commonly seen in the surviving fibres (Fig. 55).

Regeneration was a major feature in these nerves, both in myelinated and unmyelinated fibres. Particularly at the most proximal level of the injected nerve, many degenerated fibres had regenerating axons within their basement membranes (Fig 56). Regenerating axon sprouts could also be identified in otherwise normal-looking myelinated fibres (Fig 57). Myelination of these axons was very rare at this time. Growth cones, identified by the presence in them of large amounts of smooth membranous structures, were seen within the basement membrane of both degenerating (Fig 58) and normal-appearing myelinated fibres and occasionally in extratubal sites; they sometimes reached a considerable size. They were seen lying freely in the endoneurial space or enclosed by macrophage and probably fibroblast cytoplasm (Fig 59).

Regeneration of unmyelinated axons was also conspicuous, although it was sometimes difficult to differentiate between axons and Schwann cell processes. Neither was it always clear whether the regenerating axons were of myelinated or unmyelinated fibre origin. At this time, myelination of axon

Fig. 54 Low power electron micrograph from proximal level of sciatic nerve after 1% pyridoxine injection, 4 days survival. Several degenerated axons are seen, three of these are "cigar shaped" with collapsed myelin sheaths. Another degenerated myelinated fibre shows denser staining of its axon. One myelinated fibre appears normal. x 3,800.

Fig. 55 Electron micrograph from proximal level of sciatic nerve injected with 1% pyridoxine, 4 days survival. Area of nerve with little myelinated fibre degeneration but severe unmyelinated fibre degeneration. A single swollen unmyelinated axon (asterisk) is seen; a second pale process (arrow) is difficult to identify. x 10,000.

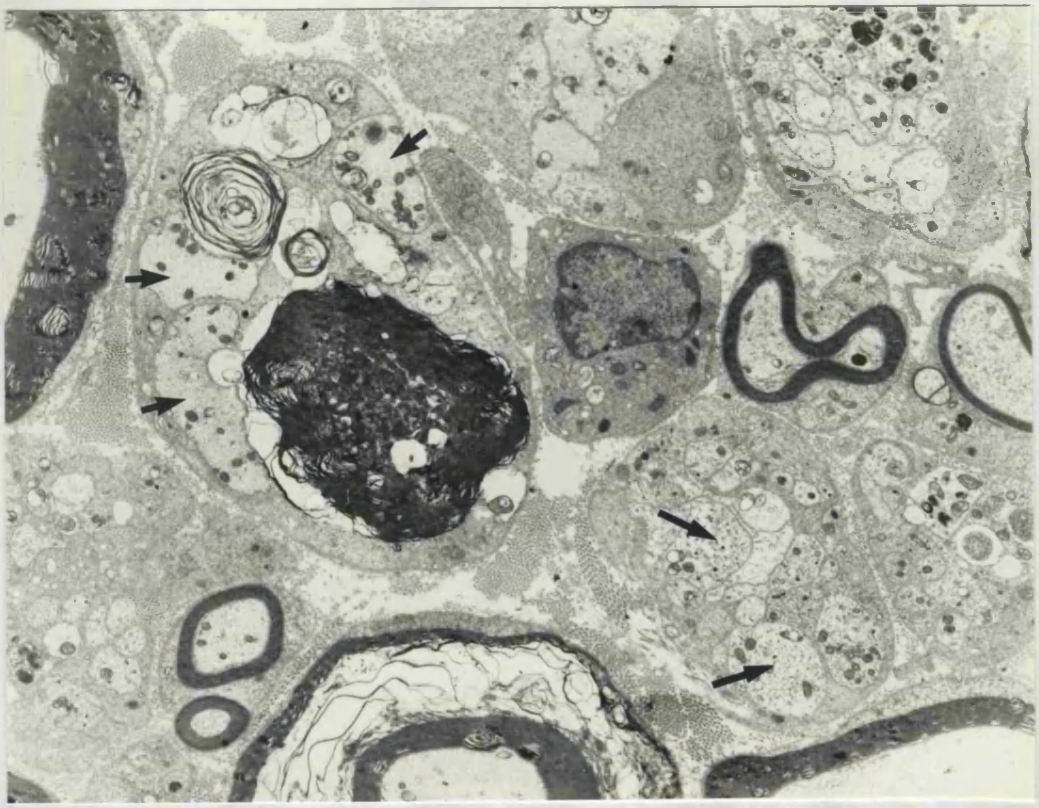

Fig. 56 Electron micrograph from proximal level of sciatic nerve injected with 0.1% pyridoxine, 4 days survival. Regenerating sprouts (small arrows) inside the basement membrane of a degenerated myelinated fibre. Several structures probably unmyelinated fibres, contain groups of axons (large arrows) with no intervening Schwann cell cytoplasm. x 4,950.

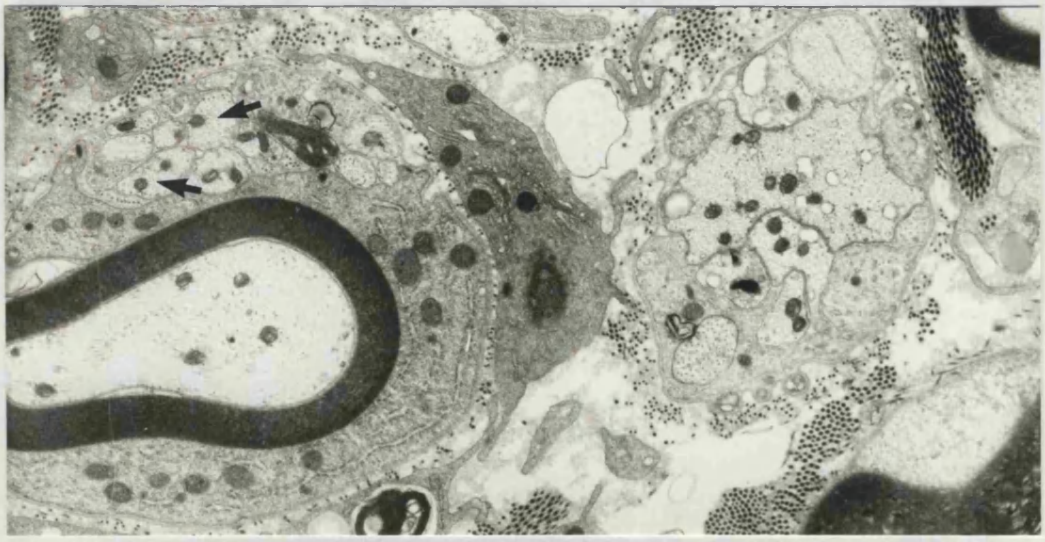

Fig. 57 Electron micrograph from proximal level of sciatic nerve injected with 0.1% pyridoxine, 4 days survival. Many regenerating sprouts (arrows) are seen within the basement membrane of an otherwise normal myelinated fibre. Several axonal sprouts are seen in an adjacent fibre, probably originally an unmyelinated fibre on the right. x 10,000.

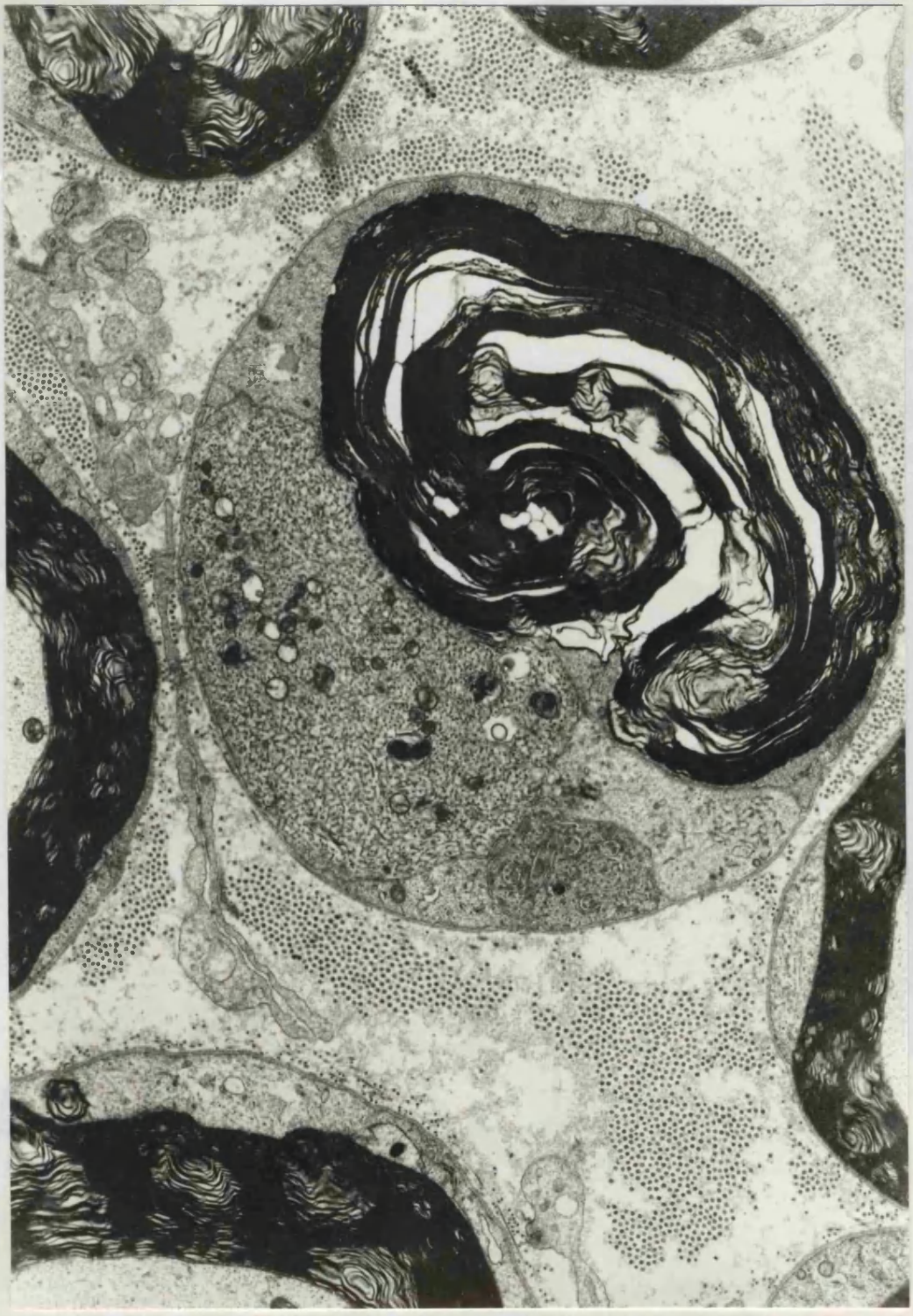

Fig. 58 Electron micrograph of proximal level of sciatic nerve injected with 0.1% pyridoxine, 4 days survival. There is a large growth cone inside the basement membrane of a degenerating myelinated fibre. The growth cone is recognizable by the presence of membranous profiles. x 10,000.

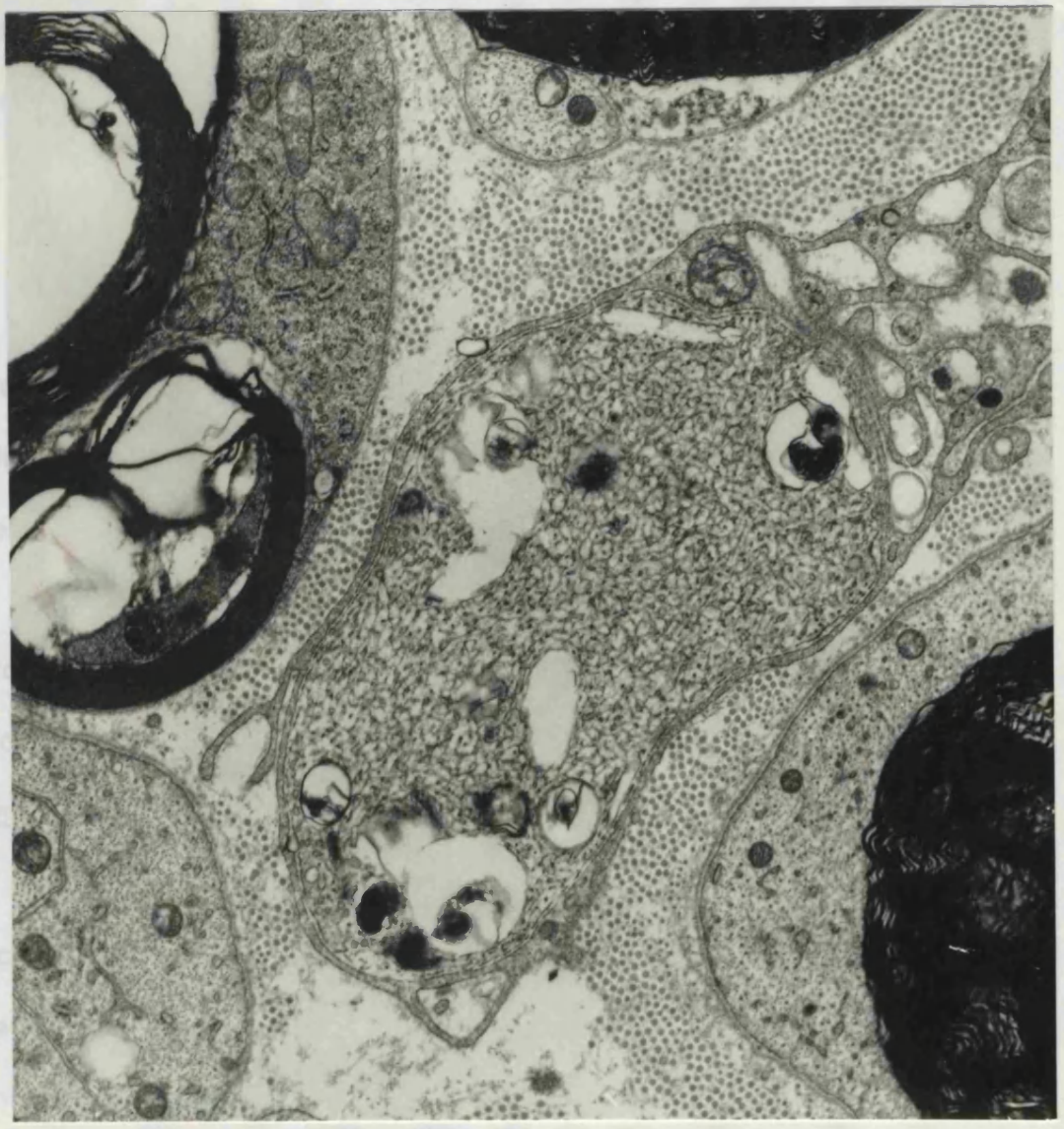

Fig. 59 Electron micrograph of proximal level of sciatic nerve injected with 0.1% pyridoxine, 4 days survival. A growth cone in an extratubal site, here enclosed by fibroblast processes. x 19,000.

sprouts had generally not begun, to aid identification of myelinated fibres. Regenerating unmyelinated axons were of variable size but often tended to be larger than normal unmyelinated axons (Fig 60). The axons appeared to contain fewer microtubules than normal. In some cases the regenerating axons were closely packed with no intervening Schwann cell cytoplasm (Fig 61).

Most Schwann cells were hypertrophic, having abundant Schwann cell cytoplasm with prominent Golgi bodies and RER (Fig 62). The nuclei were increased in size, as were the nucleoli. Occasional mitoses were seen in degenerating fibres, both myelinated and unmyelinated fibres, and in otherwise normal-looking myelinated fibres.

In the nerve distal to the injection there was nerve fibre degeneration corresponding to the regions of the nerve affected by the injected pyridoxine.

7 days

At 7 days the pattern of nerve damage was similar, although in nerves injected with the two lowest doses myelin vacuolation was seen in otherwise normal-looking myelinated fibres (Fig 63); the vacuoles formed within the outermost lamellae. Vacuolated fibres were seen only at the limit of the injection where presumably the pyridoxine concentration was at its lowest. Electron microscopy showed the myelin splitting to occur at the major dense line (Fig. 64), and not at the intraperiod line, the usual site of myelin splitting when it occurs in a variety of situations (see Discussion).

Another feature of the proximal part of nerves injected with the two

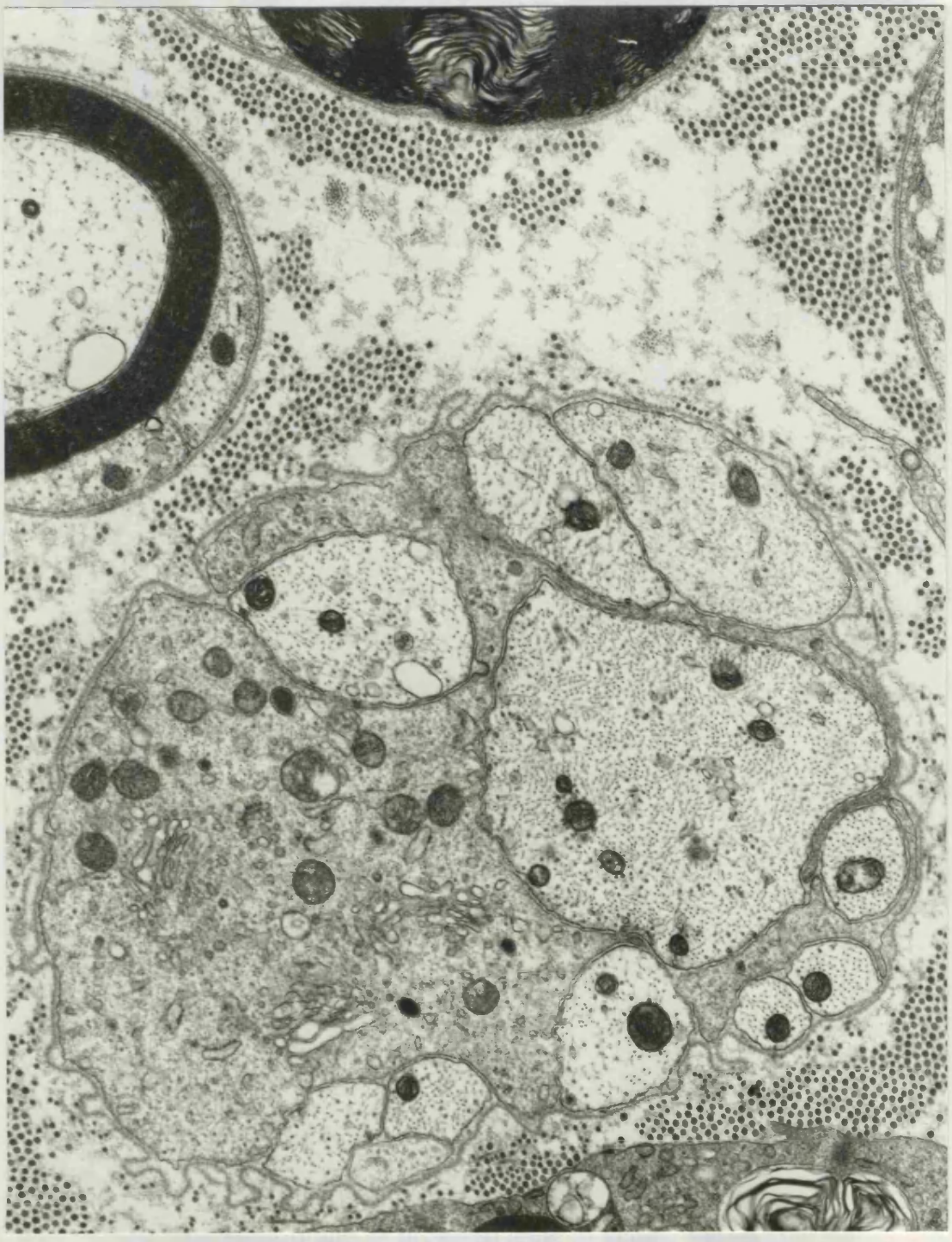

Fig. 60 Electron micrograph of proximal level of sciatic nerve injected with 0.1% pyridoxine, 4 days survival. Regenerating axons in what was probably an unmyelinated fibre. They tend to be larger than normal, the larger reaching a diameter of about 3.4μm x 19,000.

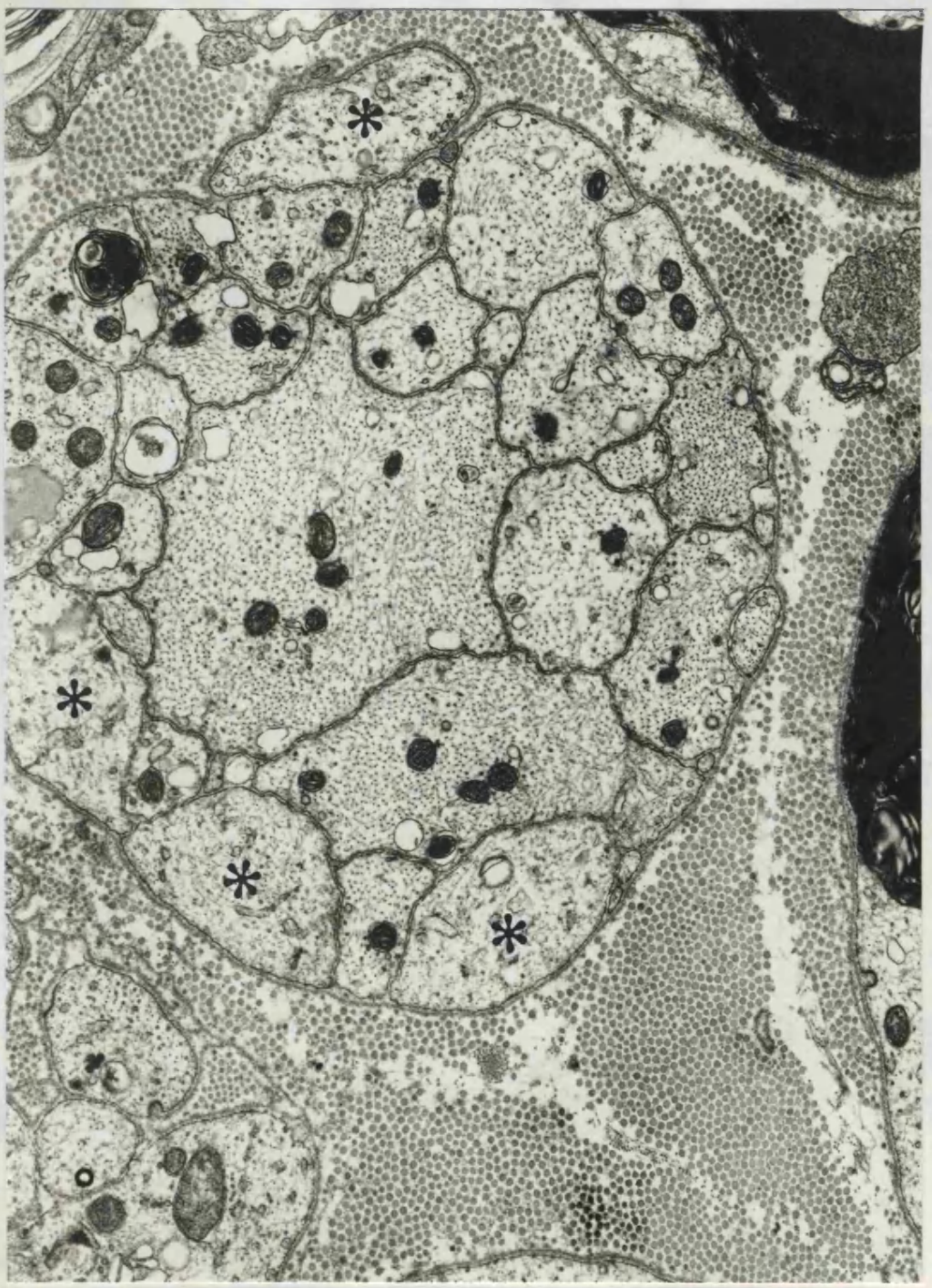

Fig. 61 Electron micrograph of proximal level of sciatic nerve injected with 0.1% pyridoxine, 4 days survival. Closely packed regenerating axons are surrounded by Schwann cell processes (asterisks). The largest axon is about 3.5μm at its maximum diameter. Differentiation of Schwann cell processes and axons can be difficult. x 19,000.

Fig. 62 Electron micrograph of proximal level sciatic nerve injected with 0.1% pyridoxine, 4 days survival . Hypertrophic Schwann cell with abundant cytoplasm and numerous Golgi profiles. The nucleus appears larger than normal. The myelinated axon contains an increased density of neurofilaments. x 10,000.

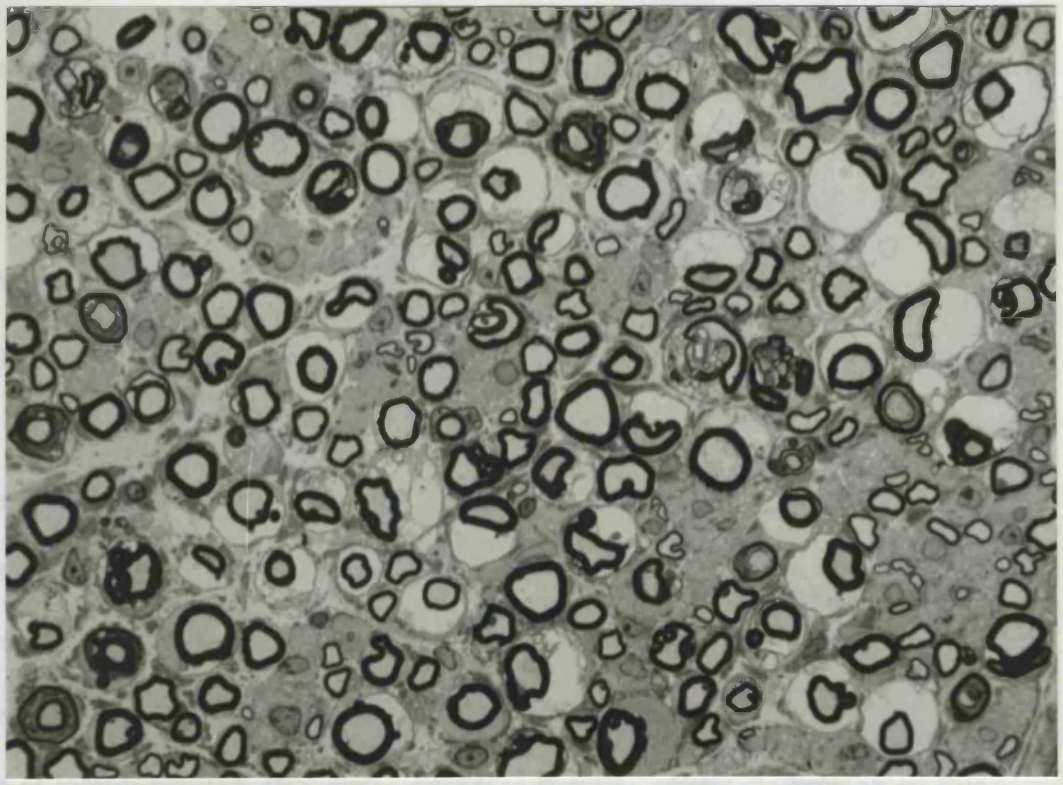

Fig. 63 1μm resin section from the proximal level of a sciatic nerve injected with 0.01% pyridoxine, 7 days survival, showing numerous vacuoles in otherwise normal myelinated fibres. These are seen by EM to be situated within the outermost myelin lamellae. x 754.

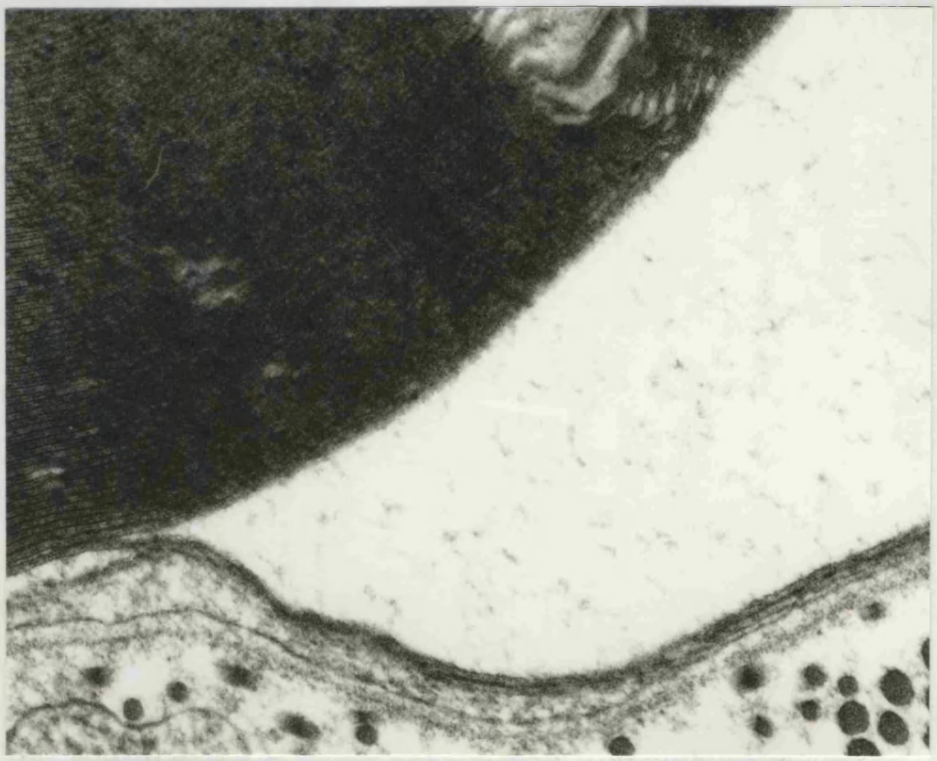

Fig. 64 Electron micrograph of sciatic nerve injected with 0.01% pyridoxine, 7 days survival. The vacuole is formed from myelin splitting at the major dense line. x 64,000.

lowest pyridoxine concentrations was an increase in axonal size, with a corresponding appearance of inappropriately thin myelin sheaths (Fig 65a). This was not associated with fibre degeneration. The mean axon size was 5.05 μm $\pm$ 2.2μm (n = 400), with a maximum axon size of 13μm compared with the normal maximum of 10 μm.

Electron microscopy showed these axons generally to have a normal density of organelles (Fig 65b). Occasional myelinated axons were seen to contain an increased density of neurofilaments. The fibre illustrated (Fig 66) is interesting in that it also shows a greatly expanded structure which is interpreted as being a degenerated axonal sprout. A smaller axon sprout of normal appearance is also present within the basement membrane of this fibre.

Degenerating fibres were still conspicuous but very few "cigar-shaped" fibres were seen at this slightly later stage.

Regenerating axons were still seen, often within the basement membrane of degenerating or otherwise normal-looking myelinated fibres (Fig 67a,b), and some of these had begun to myelinate (Fig 68). Growth cones were seen less frequently than at 4 days. Schwann cells still looked very active and mitoses were frequently seen associated with degenerating fibres and occasionally in normal-looking myelinated fibres (Fig 69).

The effect of intraneural pyridoxine on nerve regeneration following crush injury

It was shown in the previous experiments with intraneural injection

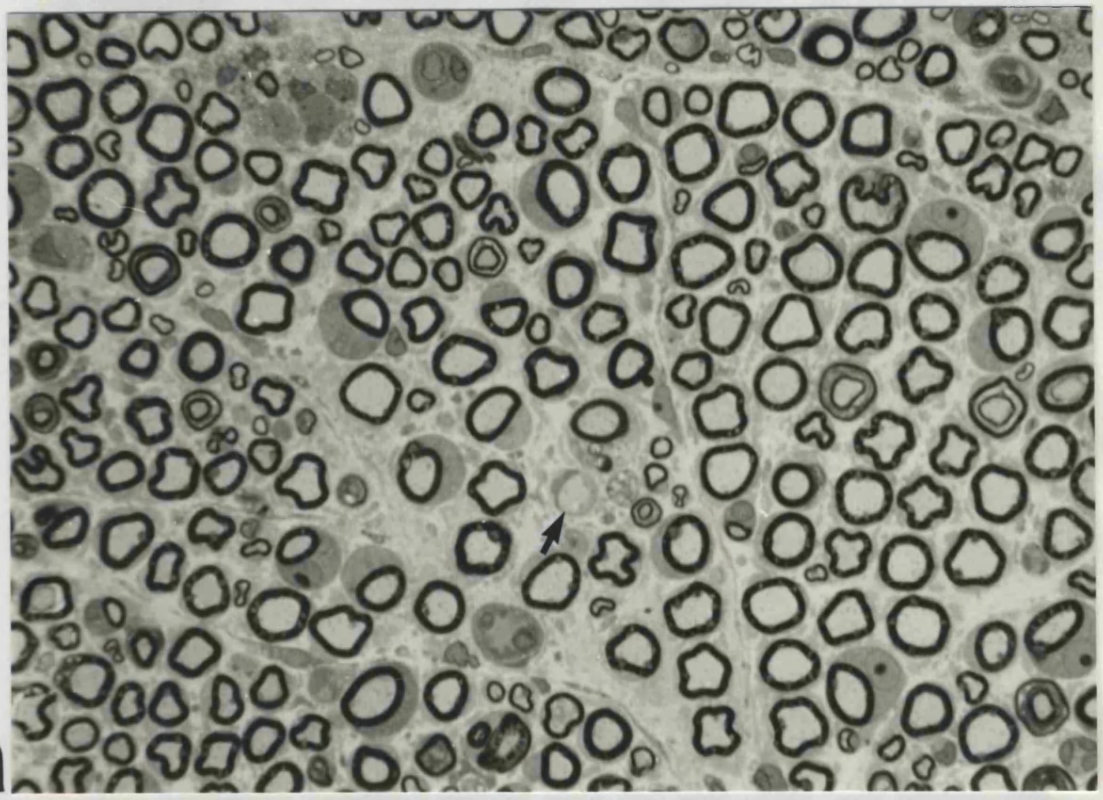

Fig. 65a 1μm resin section of proximal level nerve injected with 0.1% pyridoxine, 7 days survival. The majority of myelinated fibres have swollen axons and what appear to be inappropriately thin myelin sheaths. Hypertrophic Schwann cells are seen with large and prominent nucleoli. The arrow points to a large axon without a myelin sheath. x 640.

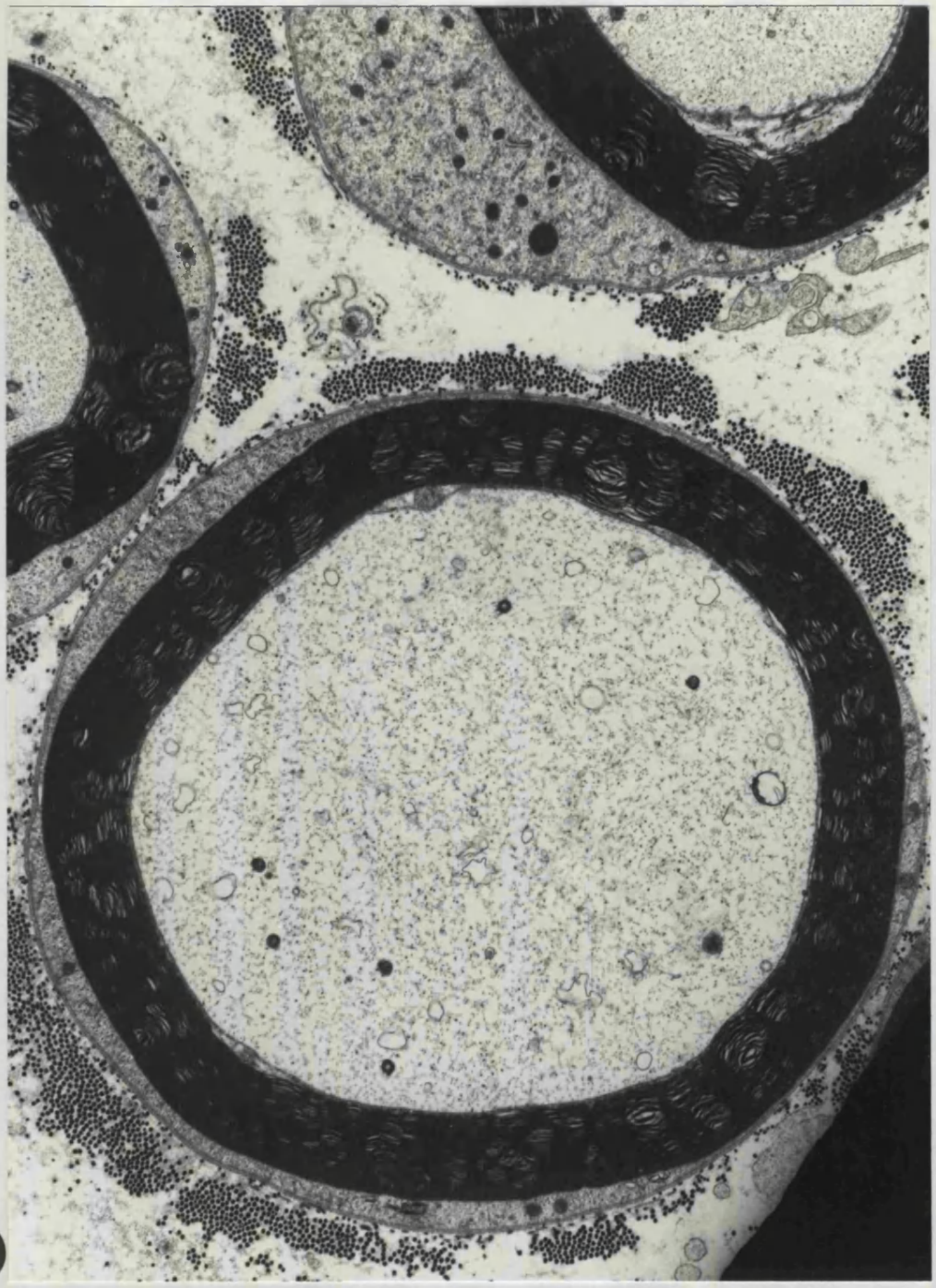

Fig. 65b Electron micrograph from proximal level of sciatic nerve injected with 0.1% pyridoxine, 7 days survival. Swollen axon (13μm) with a normal density of neurofilaments and microtubules but with increased number of SER profiles. The myelin sheath is thin. x 10,000.

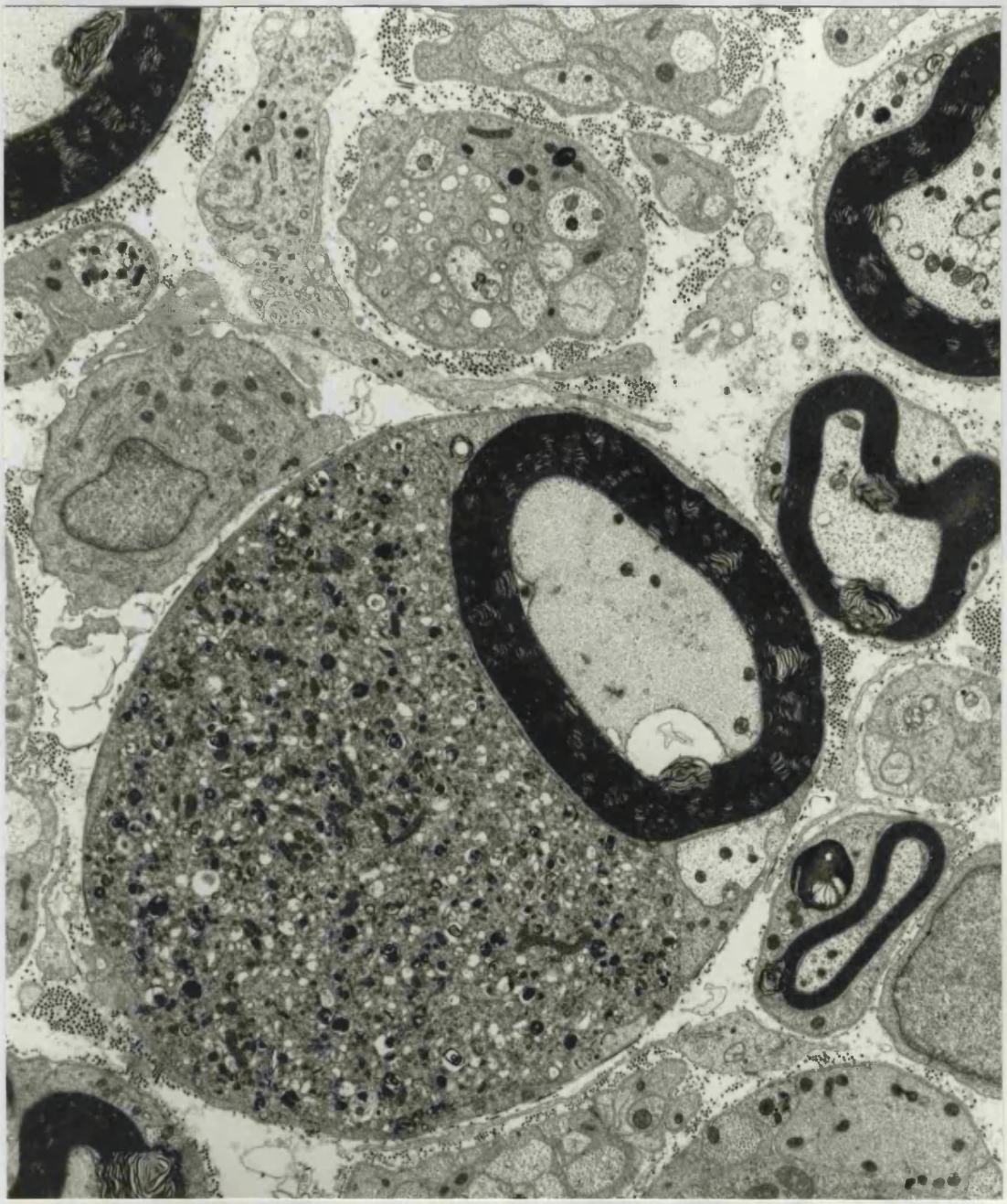

Fig. 66 Electron micrograph from proximal level of sciatic nerve injected with 0.1% pyridoxine, 7 days survival. Myelinated fibre with increased amount of axonal neurofilaments (compare with two adjacent myelinated axons). A greatly swollen process within the basement membrane of this fibre is probably a degenerating axonal sprout filled with mitochondria, dense bodies and vesicular profiles. Within the basement membrane is a small axonal sprout of normal appearance. x 9,100.

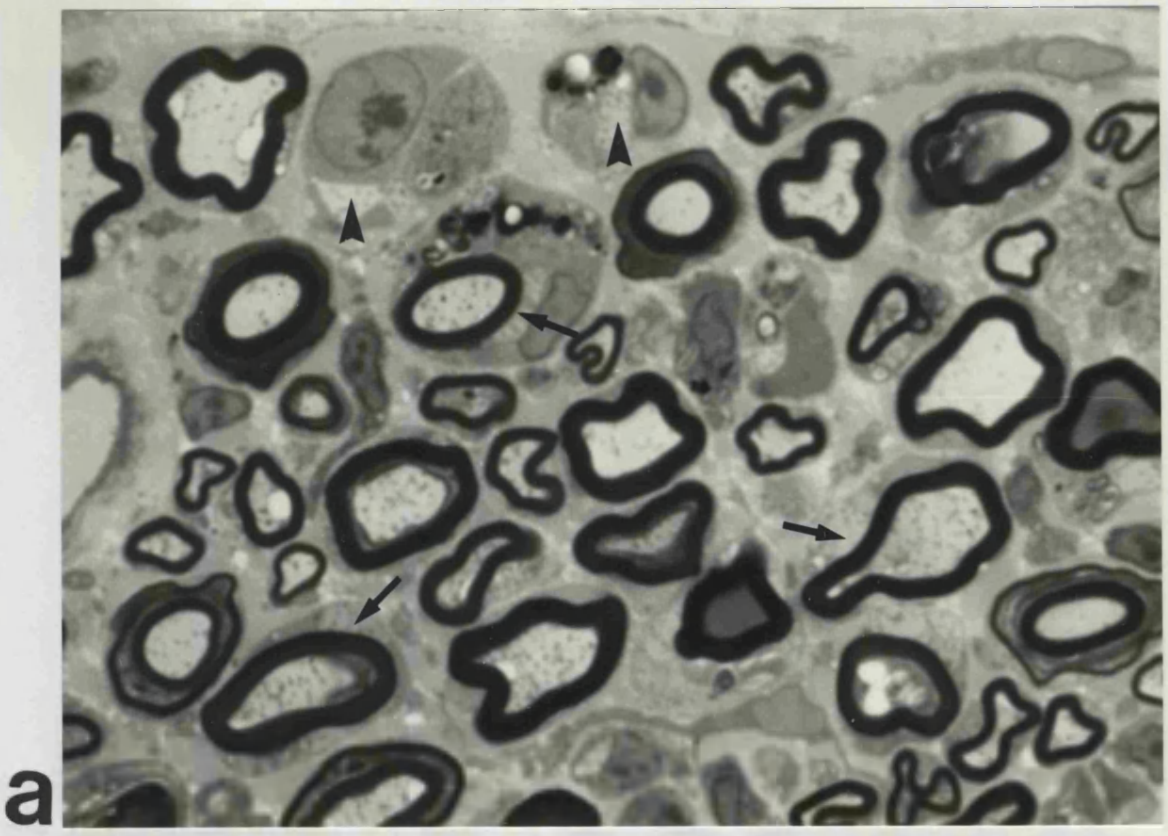

Fig. 67a 1μm resin section from sciatic nerve injected with 1% pyridoxine, 7 days survival. Several regenerating sprouts are seen within normal looking myelinated fibres (arrows). Large axonal sprouts are also present in what may have been myelinated fibres (arrowheads). Two myelinated fibres have very densely stained axons. x 754.

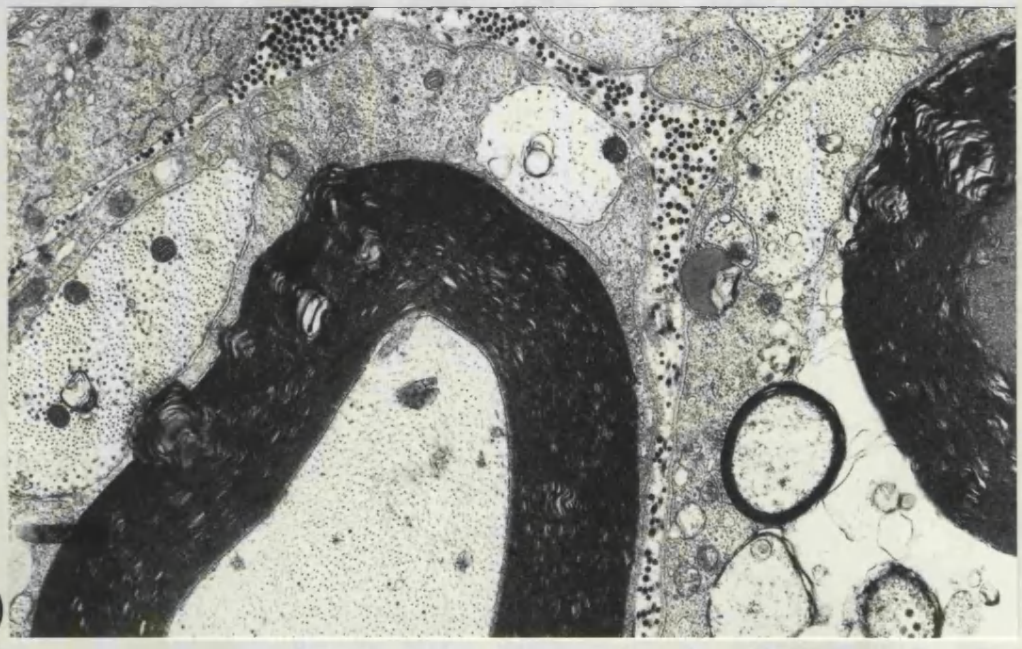

Fig. 67b Electron micrograph of sciatic nerve injected with 0.1% pyridoxine, 7 days survival. Two regenerating sprouts are seen in otherwise normal looking myelinated fibre. x 13,400.

Fig. 68 Electron micrograph from proximal level sciatic nerve injected with 20% pyridoxine, 7 days survival. Regenerating sprouts are beginning to myelinate. Note very thin myelin sheath compared to large axons. Several other axon sprouts are still unmyelinated. x 14,000.

Fig. 69 Electron micrograph from proximal sciatic nerve injected with 0.1% pyridoxine, 7 days survival. Schwann cell mitosis in an otherwise normal myelinated fibre. x 13,000.

of pyridoxine that although it caused nerve fibre degeneration there was evidence of abundant regeneration and a very active Schwann cell reaction. It was then decided to examine the effects of intraneural pyridoxine on regeneration following nerve crush. Regeneration would be compared with the effects of nerve crush only. 6 rats had their sciatic nerves crushed; 3 were killed at 7 days and 3 at 14 days. 8 rats had both crush and injection of 10% pyridoxine, 4 were killed at 7 days and 4 at 14 days. Clinical examination showed that all limbs became paralysed. Nerves were examined at a level just distal to the crush and at another level just proximal to the point of injection of pyridoxine. Although the level of crush at the point of injection was marked with sutures placed in adjacent tissues, it seemed that in some cases the nerves may have been displaced in relation to the landmarks.

At 7 days, in both crush only and crush and pyridoxine nerves, all fibres had degenerated. There was myelin debris and endoneurial oedema. Regenerating axons were seen in both groups and some had very thin myelin sheaths. Some clusters could be seen. In pyridoxine injection nerves the Schwann cell nuclei and nucleoli were conspicuous.

In order to compare regeneration between the two groups the 14 day survival animals were used; since the axons were larger and myelination was well advanced.

Fig. 70 A,B,C shows high power light micrographs of nerves after crush only (A) and crush and pyridoxine (B,C). This was the magnification used for measurement of axon diameter and myelin sheath thickness.

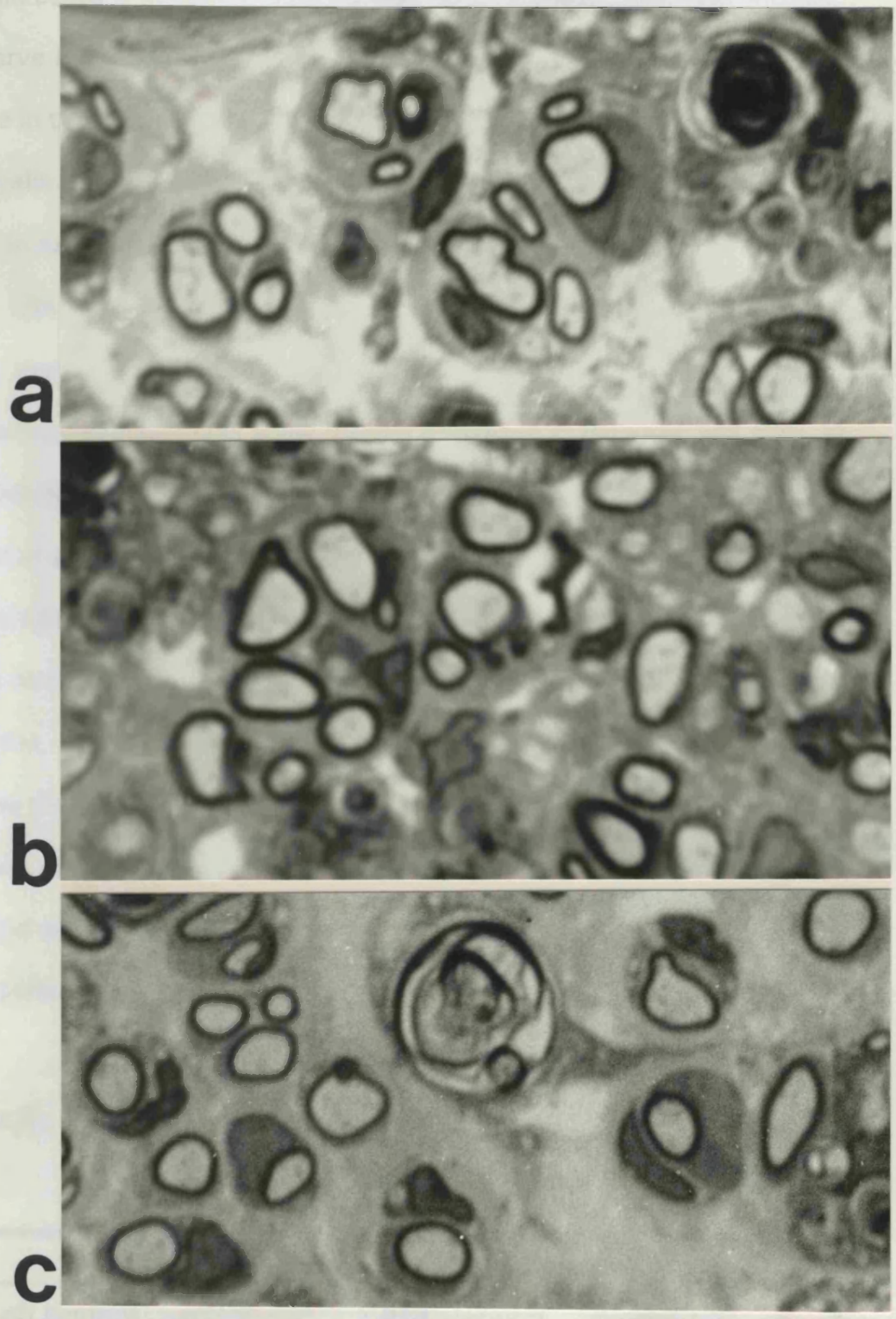

Fig. 70a,b,c 1μm resin sections from sciatic nerves crushed and injected with 1% pyridoxine (b and c). Survival 14 days. Regenerating myelinated fibres, some forming clusters and myelin debris are seen in all nerves. Fig. 70a shows a sciatic nerve after crush only, 14 days survival. In nerve (b), the myelin sheaths are seen to be thicker in some fibres than in the nerve only crushed (a). Nerve (c) showed no striking difference in relation to (a). x 2880.

Myelin debris is present in both nerves. Regenerating fibres form clusters. In nerve B, the myelin sheaths are seen in some fibres to be thicker than those in the crush only nerve A. In nerve C there was no striking difference in myelin sheath thickness, but some axons had reached a greater diameter than in nerve A.

An attempt was made to quantitate these findings although it became clear that there were many problems in interpreting the results. Firstly, some regenerating fibres show marked difference in their size and state of myelination between proximal and distal levels. It is important to compare levels at precisely the same distance from the point of crush. Disparities in the results may be due to difficulties in assessing this distance accurately. Fibre density measurements are affected by the presence of endoneurial oedema, which was more marked in some nerves than others. Table 8 shows the density of regenerating myelinated fibres from experiments done on two different occasions. Although the number of animals is small, the second experiment in particular indicated that pyridoxine injection was associated with an increased number of regenerating fibres.

Table 8 Numbers of regenerating myelinated axons expressed as (number of fibres/mm^2)

	1st experiment	2nd experiment
Crush controls (fibres/mm^2)	7,913	10,124
Crush + pyridoxine (fibres/mm^2)	8,533 9,441	17,740 16,568

The levels at which nerves are examined distal to the crush are also of great importance in showing regenerating axon size and myelin sheath thickness.

Fig. 71 shows the axon diameter distribution of the control nerve (crush only) and two experimental nerves (crush plus pyridoxine). One experimental nerve is very similar to the control, whilst the other shows that some axons have a greater diameter.

Fig. 72 (A,B,C) shows scatterplots of myelin sheath thickness plotted against fibre diameter and their regression lines.The spread around the regression line was more noticeable in a. In b and c there was a larger concentration around the regression line. The nerves examined are: Fig. 72A only crush and Figs. 72B and 72C crush plus pyridoxine. The nerves injected show that myelin sheath thickness varies from about .3μm to .9μm and the control from .2μm to .7μm. Their slopes and coefficient of correlation (r) are shown in Table 9.

Table 9

	Slope	r
Control	.34	.27
CRPy514	.37	.50
CRPy614	.44	.37

The final impression is that there is a slight difference in the animals injected with pyridoxine, in which numbers of regenerating fibres, axon diameters and myelin sheath thickness appear to be increased. The small number of

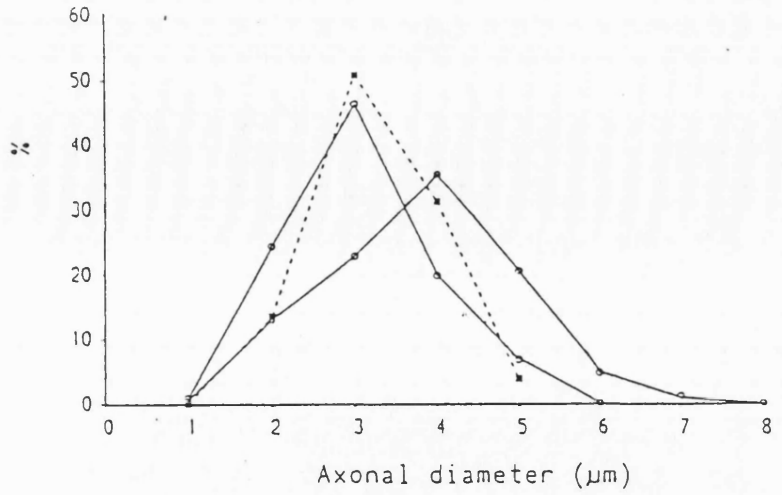

Fig. 71 Axon diameter distribution graph of a control nerve (crush only-dotted line), and two crushed nerves injected with 1% pyridoxine (continuous lines). One of the experimental nerves shows some axons with greater diameter than control.

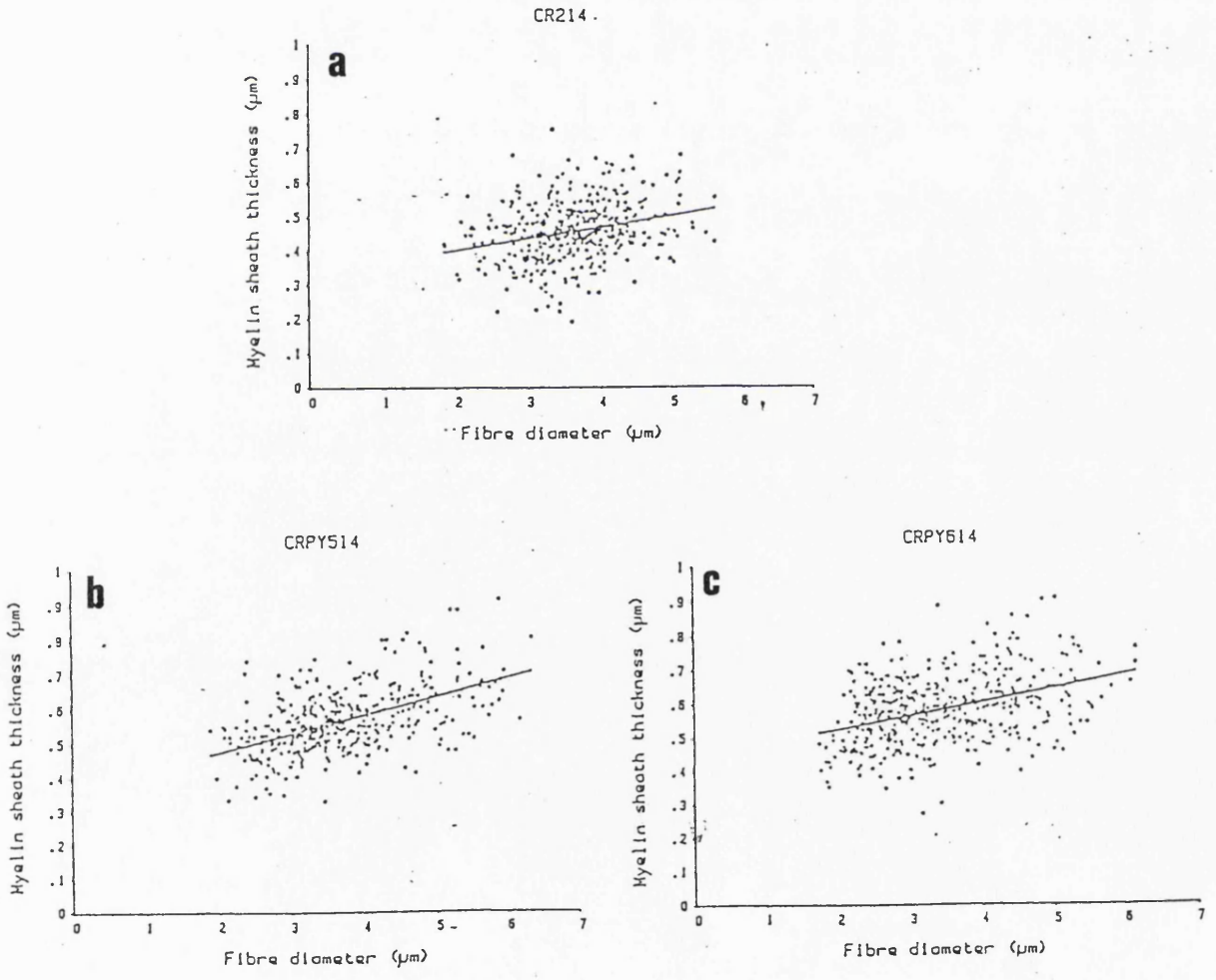

Fig. 72a,b,c Scatterplots of myelin sheath thickness plotted against fibre diameter (Fig. 72a - crush only, Fig. 72b and c - crush plus pyridoxine). Myelin sheath thickness in control nerve (Fig 72a - crush only) varies from .2µm to .7µm. Crushed nerves injected with pyridoxine (Fig. 72 b and c) show greater myelin sheath thickness varying from .3µm to .9µm.

animals examined and the problems with the levels of sciatic nerve examined (already referred to) do not allow further consideration about the beneficial effects of pyridoxine in enhancing regeneration. The finding of regenerating fibres in nerves of rats injected i.p. with pyridoxine might also suggest that it promotes nerve regeneration despite its damaging effect on the nerve cell body (see discussion).

CHAPTER 4. DISCUSSION

The doses used in this experimental study were greatly in excess of those normally used in man. However, a dose of 600mg/kg/day in a rat is almost equivalent to the exceptionally large doses used in two human cases (130g and 180g over a 3 day period) which caused permanent disability (Albin et al, 1987, Albin and Albers, 1990).

In this study there was an extremely variable response between individual animals to the same dose of pyridoxine, both in terms of clinical effects and pathology. For example, one animal dosed with 600 mg/kg/day for 10 days showed very severe DRG cell pathology and axonal degenerative changes, in contrast to others equally dosed, which showed no pathological changes. Increasing the number of doses of pyridoxine did not always have a cumulative effect. The percentage of degenerated myelinated axons was in some instances smaller in saphenous nerves of rats dosed for longer periods.

In pyridoxine toxicity studies, dose-dependent changes were described by Krinke (1980) in the dog, based on the degree of disability. In the study by Xu et al (1989) in the rat, much of the assessment for dose-dependence was made on a semi-quantitative basis and, for example severe degeneration was described in mixed nerves such as the sciatic nerve and posterior tibial nerve, which would have contained many unaffected motor fibres. It is possible that there was more variation than is apparent from the subjective semi-quantitative results shown.

It is interesting that individual variation was also found in experimental isoniazid neuropathy. Effectively, isoniazid causes pyridoxine deficiency (see literature review). Jacobs, Miller and Cavanagh (1979) described isoniazid neuropathy in rats, caused by an axonal lesion.
As in this pyridoxine study, there was also a marked variation between animals given equal doses.

There are genetic factors in isoniazid neuropathy, which in man predispose to variation and susceptibility to develop a neuropathy (Knight, Selin and Harris 1959). In human pyridoxine neurotoxicity, this variability is also noted but there is no evidence that it is genetically determined. To my knowledge genetic factors have not been reported before in rats to explain the variation in pathology found in this study. A possible explanation of the variability, is the route of administration used in this experiment, since on some occasions pyridoxine could have been injected intradermally instead of intra-peritoneally causing local swellings and differences in the rate of absorption. However, it is unlikely that this occurred to any great extent. An alternative suggestion is that the rate of excretion of pyridoxine is related to variable fluid intake.

In order to show whether the amount of pathology is related to blood levels of pyridoxine , an attempt should be made in future experiments to monitor pyridoxine levels.

Apart from differences in susceptibility within the same species there are also variable responses to pyridoxine between species. For example, mice, in this study and in the work of Xu, Sladky and Brown (1989) were

found to be very resistant to the toxic effects of pyridoxine. Larger animals such as rats, guinea-pigs and dogs are increasingly vulnerable, and from the species studied man appears to be the most sensitive. There are species differences in the rate of excretion. Rats excrete 80% of administered pyridoxine per day, in contrast to dogs who excrete 20% (Scudi, Unna and Antopol, 1940). This fact could explain why such high doses are necessary to produce toxic effects in the rat.

Pyridoxine neurotoxicity in man is associated with a purely sensory neuropathy, suggesting that DRG cells are specifically involved (Schaumburg et al, 1983; Albin et al, 1987). It is also well recognized that in experimental pyridoxine neurotoxicity, DRG cells are primarily affected (Antopol and Tarlov, 1942; Krinke et al, 1980; Windebank et al, 1985; Montpetit et al, 1988; Xu et al, 1989).

There was no evidence, in the present study, that motor cells were affected. Anterior horn cells appeared normal, and ventral roots were always conspicuously free of abnormality. Since 'motor' nerves contain a high proportion of sensory fibres it is not possible to obtain evidence of the absence of toxic effects in these nerves. Others had noted the absence of effects on motor fibres, well illustrated by the selective degeneration of the sensory endings of the muscle spindle, but with sparing of its intrafusal motor endings (Krinke et al, 1978).

The probable reason for the susceptibility of DRG cells is their location outside the blood nerve barrier. Although not all the blood vessels in dorsal root ganglia are fenestrated, tracer studies show that there is very

rapid leakage from these vessels (Jacobs, Macfarlane and Cavanagh, 1976). However many other areas lie outside the blood nerve barrier. Some of them were examined for evidence of neurotoxicity; these included the autonomic ganglia, where only very mild changes were found (such as nuclear eccentricity in a few cells), and ganglia in the myenteric plexus, in which there was no significant abnormality. Autonomic involvement has been described in human cases (Albin et al, 1987). In the present study, one of the more significant findings was a loss of unmyelinated axons in most of the nerves examined from susceptible animals. This has not been described in previous experimental studies of pyridoxine neurotoxicity. In view of the very mild changes in the autonomic ganglia, however, it is probable that most of the loss of unmyelinated fibres is due to effects upon DRG cells rather than autonomic ganglion cells.

Muscle spindles were not examined in the present study, although Krinke et al (1978) had demonstrated the selective vulnerability of their sensory, but not their motor nerve endings. Studies with the vascular tracer HRP have shown that although the capsule of the muscle spindle acts as a barrier to HRP, the polar regions of the muscle spindle, where the motor endings terminate, are open ended (Dow, Shinn and Ovalle, 1980) and HRP which leaks freely from the adjacent muscle capillaries, can penetrate into these regions. It might therefore have been expected, on the basis of vascular permeability, that motor nerve endings might be affected by circulating pyridoxine. The absence of changes to motor fibres suggests that circulating pyridoxine, in the concentrations reached following daily

intraperitoneal injection, has no direct effect upon axons.

Greater susceptibility of DRG cells compared to autonomic ganglion cells may be explained by the very large volume of axoplasm that DRG cell perikarya have to support, including their central extensions, perhaps rendering them more vulnerable to toxic effects. Jacobs (personal observation) comments that one DRG cell perikaryon may have to support at least one hundred times its own volume of axoplasm.

The distribution of neurotoxic effects has clearly been shown to be related to blood vessel permeability in the case of amiodarone and adriamycin toxicity (see review). In amiodarone neurotoxicity, drug-induced inclusions are a very convenient marker for the presence of the drug, and showed that autonomic ganglia were particularly affected, suggesting that in this case, factors other than the maintenance of large volumes of axoplasm are involved in determining susceptibility.

In other workers' descriptions of DRG cell changes induced by pyridoxine, neurofilaments seem to be the main organelle involved (Montpetit et al, 1988; Xu et al, 1989). In the present experiments, pyridoxine-susceptible rats showed severe, but often variable abnormalities in DRG cells. These included not only increased number of filaments (in both small and large cells) but also the presence of free ribosomes due to degranulation and dispersion of rough endoplasmic reticulum (RER), prominent Golgi complexes and increased numbers of mitochondria; very occasionally there was total loss of RER. In some rare neurons, neurofilaments were the main cytoplasmic component.

Increased numbers of filaments were also seen in some intraganglionic proximal axons sometimes forming a whorled pattern when seen ultrastructurally. These were similar to those described by Montpetit et al (1988) in dogs and by Xu et al (1989) in rats. The occasional swollen appearance of proximal axons in controls was also probably due to large numbers of filaments; their significance is not certain.

Another interesting finding was the almost complete dissolution of neurofilaments in some axons associated most of the times with accumulation of neurofilaments in DRG cells. The pyridoxine-induced neurofilament changes in DRG cells were studied by immunohistological methods with RT97 antibody and showed changes in the distribution of phosphorylated neurofilaments, with increased staining of some large cells and staining of many small cells which are not normally stained with this antibody.

Mechanisms whereby neurofilaments become abnormally distributed are not known, but two possibilities can be suggested. First, the 200 Kd neurofilament protein may become phosphorylated secondarily after being retained in the cell body for some unknown reason. Second, abnormal phosphorylation on the 200-Kd neurofilament subunit in perikarya may impair the movement of neurofilaments into the axon (perhaps by interfering with their loading into the axonal transport system), leading to accumulation of neurofilaments in cell bodies and very proximal axons.

It is possible that changes in the phosphorylation of perikaryal neurofilaments represent a non-specific neuronal reaction to injury as

described in the retina following optic nerve transection (Dräger and Hofbauer, 1984). Phosphorylated epitopes of neurofilaments appear in perikarya of motor neurons in rabbits intoxicated with aluminium salts (Troncoso et al, 1986), in perikarya containing neurofibrillary tangles in Alzheimer's disease (Sternberger, Sternberger and Ulrich, 1985), and in cell bodies of some motor neurons in amyotrophic lateral sclerosis. In addition, Lewy bodies contain epitopes of phosphorylated neurofilaments (Forno et al, 1986).

As far as other changes to DRG cells are concerned, the large empty vacuoles found in DRG cells by Krinke et al (1980) (dogs), Krinke, Naylor and Skorpil (1985), Montpetit et al (1988), Windebank et al, (1985) and Xu et al, (1989) in rats, were observed in the present study, but they were also seen in controls, although possibly to a lesser extent; again, their significance is not known.

The abnormal microtubule aggregates in close proximity to ribosomes and membranes of RER, described by Montpetit et al, (1988) in dogs were not seen in the present experiments.

Nuclear changes were often prominent in affected dorsal root ganglion cells. The nuclei tended to take a peripheral localization and the nuclear membrane an irregular contour. These nuclear changes, together with some of the cytoplasmic alterations involving dispersion of RER are not unlike those seen in chromatolysis and in some situations it is difficult to say if it is a primary or a secondary change (see later). In fact Antopol and Tarlov (1942) in the first studies of the effects of large doses of pyridoxine,

described the ganglion cell changes as chromatolytic, and Krinke, Taylor and Skorpil (1985) refer to DRG cells with features of the axon reaction. However the very severe abnormalities seen in some cells, and the death of others, are clear evidence of the direct toxic effect of pyridoxine rather than an axon reaction.

Difficulty in differentiating possible primary toxic effects on the neuronal cell body from an axonal reaction due to distal axonal damage has been described, for example, in triorthocresyl phosphate (TOCP) poisoning (Prineas, 1969a) and acrylamide intoxication (Sterman, 1982). TOCP is now recognised as acting primarily on the axon (Bouldin and Cavanagh, 1979a); the situation with acrylamide still seems somewhat controversial (Jones and Cavanagh, 1986), although it is very likely that this is also a primary axonopathy. Two possible mechanisms are suggested to explain the mechanism of dying back neuropathies as a result of those toxic neuropathy experiments. One is that there is a progressive compromise of neuron cell bodies, which then gradually fail to supply materials (cytoskeletal proteins and enzymes) that are necessary for the maintenance of the physical integrity of their axons. This hypothesis predicts that the degeneration first occurs in nerve terminals in those parts of the cell most remote from the perikaryon (Cavanagh, 1954). The second hypothesis is that toxic substances might act directly and multifocally on certain places between the cell body and the preterminals of the affected axon. The latter concept has been supported by several experiments showing that degeneration does not always take place at the axon terminals, but that it is distributed in a

multifocal fashion along the axon projecting from the neuron cell body (Spencer and Schaumburg, 1984).

In some of the pyridoxine-injected animals, satellite cells associated with both abnormal and sometimes apparently normal DRG cells seemed to be more numerous than normal. When associated with abnormal ganglia the cytoplasmic processes of satellite cells were more abundant than normal, forming numerous finger-like processes. Their cytoplasm and nuclei had a normal appearance. Increased numbers of satellite cell processes have been noted in other experimental situations, as in acrylamide-treated rats (Jones and Cavanagh, 1986), being also a marked feature in cisplatin toxicity (Tomiwa, Nolan and Cavanagh, 1986). This enhanced activity of satellite cells suggests an increased metabolic interaction with the neuron.

Occasional mitoses were also found in satellite cells. They have been described in developing DRG cells (Pannese, 1974) but are not normally seen in adult animals. This finding and the previously discussed proliferation of finger-like processes seen by electron microscopy, are most likely to represent a non-specific reaction to neuronal damage. The significance of the perikaryal changes will be discussed later.

With regard to the nerve fibres changes, myelinated fibre degeneration was found to be more severe at distal than at proximal levels of the saphenous nerve in all the affected animals studied, the larger fibres being the more affected. In earlier studies, a dying back type of neuropathy was suggested by Krinke (1978) but this was based only on the examination of rat plantar muscle spindles and loss of large myelinated fibres in the tibial

nerve. In a later paper (Krinke et al, 1980) no evidence of a dying back pattern was found in nerves of dogs dosed with pyridoxine.

When relatively small doses of pyridoxine were given to rats Windebank et al (1985) no proximo-distal gradient of fibre degeneration was found, although, as pointed out in the literature review, the method of assessment, using teased fibres, was not ideal. Xu et al (1989) made a semi-quantitative study of nerve fibre degeneration caused by pyridoxine. Few details are given of the methods employed for quantitation, although it is clear that this was done at light microscope level. Degenerating fibres often show marked swelling or shrinkage whilst the myelin sheaths remains intact, and this can give misleading results of measurement of fibre size. Early stages of degeneration may not be recognised by light microscopy. No proximo-distal gradient of fibre degeneration was found. However, the peripheral nerves studied by Xu et al (1989) included mixed nerves (sciatic and tibial nerves) and the sural, a predominantly sensory nerve, but which in the rat also contains motor fibres (Peyronnard and Charron, 1982), so that the proportions of degenerated fibres are difficult to interpret.

Montpetit et al (1988) (using dogs) were the only group who described having studied different levels of several peripheral nerves, including the saphenous, but without giving detailed explanations of the pathology. Their findings gave the impression that the nerves were affected throughout their entire length, with no proximo-distal gradient.

In the present study, using an entirely sensory nerve, there was a clear difference in the percentage of degenerated myelinated fibres between

proximal and distal levels of the nerves examined, providing evidence of a dying back type of neuropathy.

Although not studied quantitatively, the pattern of fibre degeneration within the dorsal columns of the spinal cord showed that the gracile tract was more affected than the cuneate, and more severely at cervical than at lumbar level, confirming a proximo-distal distribution of damage, also consistent with a dying back type of neuropathy. Xu et al (1989) found moderate axonal degeneration in the gracile, but none in the cuneate tracts, although they report no difference in severity between cervical and lumbar levels. Dorsal column degeneration was noted by Antopol and Tarlov (1942), Phillips et al (1978) and Krinke et al (1980) but with no indication of the fascicles or levels affected. Montpetit et al (1988) describe degeneration in the gracile and medial cuneate fascicles, without reference to levels.

The spinal cord and peripheral nerve findings in the present experiment show that pyridoxine at high doses causes distal axonal degeneration of centrally and peripherally directed sensory fibres.

Recently, Miura et al,(1993), described a progressive degeneration of motor nerve terminals in the gracile axonal dystrophy (GAD) mouse with hereditary sensory axonopathy. Previous studies (Kikuchi et al, 1990) showed that in the same animal there was also axonal degeneration of both the central and distal ends of primary sensory neurons. This mutant may serve as an experimental model for hereditary forms of sensory and motor axonal neuropathies in man. Pyridoxine induced neurotoxicity also produces

a sensory dying back neuropathy, providing a useful model for the study of hereditary sensory neuropathies like Friedreich's ataxia.

Degeneration of myelinated fibres in peripheral nerves was also accompanied by loss of unmyelinated axons, which in some of the nerves also showed a distal involvement. There was however a wide variation in the number of unmyelinated axons. This may be explained by the relatively small area studied in each nerve, the tendency of unmyelinated axons to assemble in clusters, mainly in small nerves like the saphenous, and also by the possible inclusion of regenerated unmyelinated axons in the counts (see later). Degeneration of unmyelinated axons has not been reported in previous studies of experimental pyridoxine neurotoxicity, although in human cases (Albin et al, 1987) there is mention of autonomic involvement which may have been related to loss of unmyelinated axons.

An important aspect of the present work was the ultrastructural studies on the peripheral nerve fibres showing changes affecting the numbers and distribution of neurofilaments and microtubules. These changes were seen in myelinated fibres which had appeared normal by light microscopy. (In one nerve the changes were visible by light microscopy). These alterations of axonal organelles were seen in animals with very little pathology in their DRG cells. Neurofilaments were reduced in numbers, and there was often a roughly peripheral rim of axoplasm with virtually no organelles. In these axons, there were central clusters of microtubules, but no quantitative evidence of loss of these organelles. Both small and larger myelinated fibres showed this filament loss and central clustering of

microtubules which seemed to be present in proximal and distal levels of the saphenous nerve. The different levels were not studied quantitatively to discover whether there was a proximo-distal gradient of these changes. The loss of neurofilaments contrasted with the normal or sometimes increased numbers of neurofilaments in very proximal, intraganglionic fibres. This loss of filaments and clustering of microtubules has not been described in previous studies of pyridoxine toxicity. The only other situation with a similar pattern of organelle changes is seen in the small axons of optic nerves of IDPN (ß,ß'-iminodipropionitrile) treated guinea pigs (Parhad, Clark and Griffin, 1987). IDPN produces a proximal accumulation and a distal depletion of neurofilaments, due either to alterations of properties of neurofilaments (Ochs and Brimijoin, 1992) or effects on axonal transport (Griffin et al, 1985).

Neurofilaments play an important role in maintaining axonal calibre (Hoffman and Griffin, 1993). However in the present study, in those fibres with reduced numbers of neurofilaments, the axon size was not obviously reduced i.e. the ratio of axon size to fibre size - the 'g' ratio, appeared normal. Other, atrophic fibres with low values of 'g', were seen, and it was noted that they usually showed a normal distribution of axonal organelles. It is suggested that an axon which shows loss of filaments may eventually adapt to a size determined by the numbers of neurofilaments present thus becoming an atrophic axon. In the present study neurofilament loss and microtubule clustering was a very early change, and it is inferred that these abnormalities may eventually lead first to axonal atrophy and then to fibre

degeneration.

An unexpected finding in this experiment was the presence of myelinated and unmyelinated fibre regeneration. In spite of continuing daily dosing, regenerated myelinated fibres were seen, in affected animals, after 27 days, and were quite numerous at 44 days. The number of regenerating fibres was greater at proximal than at distal levels of the saphenous nerve.

In some affected animals, larger numbers of unmyelinated axons were found proximally than distally. Problems of counting unmyelinated axons have been pointed out. Measurement of the diameter of these axons showed a unimodal peak at about 1 μm, and not the bimodal distribution found in human neuropathies and in ageing nerves (Ochoa and Mair, 1969b; Ochoa, 1970) where the second smaller peak was thought to be due to regenerating axons. It cannot be stated with certainty, therefore, that there was regeneration of unmyelinated axons. The finding of regeneration in these animals suggests that some of the DRG cell changes could indeed have been chromatolytic in nature.

In toxic neuropathies regeneration whilst exposure to the toxic substance is maintained, is not usually a notable feature. However, there are examples, of which two can be mentioned. In isoniazid neuropathy, regeneration is a characteristic feature during dosing (Jacobs, Miller and Cavanagh, 1979). This was not an unexpected finding since isoniazid produces its toxic effect directly and multifocally to the axon, with preservation of neuronal cells. In their study Jacobs, Miller and Cavanagh (1979) described degeneration of some motor fibres throughout most of

their length but invariably with preservation of the most proximal parts of the nerve, and prominent regeneration. The association of regeneration of nerve fibres and sparing of the more proximal regions of the nerve, supports the idea that isoniazid produces no direct toxic effect on the nerve cell body.

Another example of regeneration during dosing is experimental cuprizone toxicity. Apart from the myelin vacuolation and subsequent demyelination in the central nervous system of mice, there is peripheral axonal degeneration (Love, 1988). Despite continuous administration, there is also, after about two weeks of dosing, evidence of axonal regeneration. Whether cuprizone acts on the nerve cell bodies or directly on the axon is not known.

After axotomy, the amount of neurofilament proteins transported by regenerating axons is reduced (Hoffman and Lasek,1980), a change that coincides temporally with reductions in axonal calibre (Hoffman et al, 1985). These changes in calibre appear initially in the most proximal regions of the axon and progress in a proximal-to-distal direction at the rate of neurofilament transport (Hoffman et al, 1985). Moreover when the delivery of neurofilament proteins returns to preaxotomy levels, axonal calibres return to normal. Rosenfeld et al(1987), showed that phosphorylated neurofilament proteins appear in perikarya of axotomized neurons, suggesting that axonal injury is associated with changes in the processing of neurofilaments within neurons. In addition, the presence of abnormal neurofilament immunoreactivity in perikarya initially appears similar following either reversible or irreversible lesions.

Regeneration of myelinated fibres in pyridoxine intoxicated animals during dosing suggests that some protective response must take place in the sensory neurons. For example it is known that neurons in the central nervous system express heat shock proteins after ischaemia, status epilepticus and hyperthermia (Nowak, Bond and Schlesinger, 1990). There is also evidence that neurons in culture are protected from glutamate toxicity by heat shock proteins (Rordorf, Koroshetz and Bonventre, 1991). Methods to demonstrate heat shock proteins could be applied in pyridoxine toxicity to observe if a similar protective response is present. Other protective mechanisms could be investigated.

Intraneural injection of pyridoxine was investigated to see what was its direct effect upon axons. At all concentrations used, the injected pyridoxine caused severe axonal degeneration. There were some technical difficulties in obtaining sections at appropriate levels of the nerve injected. When the injection was made into the tibial branch of the sciatic nerve just distal to its separation from the sciatic nerve, pyridoxine, which was directed proximally, caused severe degeneration of the tibial fascicle. However, there was no evidence of fibre degeneration in the adjacent peroneal fascicle, separated from the tibial by a septum of perineurium. This shows that pyridoxine does not readily cross the barrier imposed by the perineurium.

No specific features were noticed in the process of axonal degeneration. The unmyelinated axons appeared to be more susceptible than myelinated fibres, since, in areas where myelinated fibres were unaffected,

the unmyelinated axons were sometimes degenerating. This can possibly be explained by the easier access of pyridoxine to the axon of an unmyelinated fibre. In a myelinated fibre, the structure of the nodal region would perhaps impede the access of a substance in the endoneurial compartment, except directly at the node of Ranvier.

Intraneural injection of pyridoxine has not previously been performed. Whilst causing widespread axonal degeneration it paradoxically seemed to elicit a greater regenerative response than normal. At proximal levels of the extent of spread of pyridoxine, prolific regenerating axonal sprouts were seen within the basement membrane of degenerating fibres and also in normal looking myelinated fibres. Regenerating unmyelinated axons tended to be larger than normal and there was conspicuous Schwann cell proliferation. The presence of regenerated axons within the basement membrane of apparently normal myelinated fibres can be explained on the basis of retrogradely directed growth of some regenerated sprouts, or to sprouting from nodes of Ranvier proximal to nerve damage. These patterns of axonal regeneration were clearly shown in silver preparations by Ramon Y Cajal (1928) and in the study by Friede and Bischhausen (1980) following nerve section. However, in the pyridoxine injected nerves, large and/or multiple axons were seen, suggesting a more florid regenerative response than normal.

Peripheral nerve regeneration is an invariable consequence of crush or transection. Reactive axonal sprouts grow across the site of injury and enter the Schwann cell processes (contained within the original basement

membranes) which form the bands of Bungner, and continue to grow towards the periphery to re-innervate appropriate target organs. It is apparent that this process is dependent on an intrinsic neuronal response to injury, and an interaction between the Schwann cells and the macrophages recruited in the endoneurium and possible secretion of nerve growth factor by the Schwann cell (Hall, 1989). It was felt that the enhanced regenerative response might be due to increased expression of NGF and NGF receptor in the Schwann cells.

An attempt should be made in the future to immunostain some nerves regenerating after intraneural injection of pyridoxine, with nerve growth factor receptor antibody, in order to be able to show and possibly measure the expression of NGF. Herdegen et al (1993), studied expression of the transcription factor c-JUN and the neuropeptides galanin and calcitonin gene related peptide in axotomized neurons following sciatic nerve transection. The c-JUN protein belongs to the group of transcription factors encoded by immediate early genes. These proteins are induced in neurons by various stimuli and mediate via a stimulus-transcription cascade the reactive alterations of protein synthesis (Curran, Fos and Jun, 1991). Recent data have shown that expression of c-JUN in neurons following transection of their axons belongs to the earliest genetic events following nerve transection (Herdegen et al, 1991). The persistent expression of c-JUN is supposed to play a role in the initiation and progress of axonal regeneration. Expression of neuropeptides galanin and calcitonin gene related peptide started within five hours following the onset of c-JUN expression (Herdegen et al,1993).

These immunocytochemical studies can be adapted in the future to study regeneration in pyridoxine neurotoxicity.

Besides this increased regenerative response, there was the expected Schwann cell proliferation, and mitoses were seen frequently. Hypertrophy of Schwann cell cytoplasm was noted. A phase of hypertrophy of the Schwann cell is known to anticipate its division (Ramon Y Cajal, 1928), although the pyridoxine-exposed Schwann cells were often markedly hypertrophic, possibly suggesting a direct, though probably short-lived, effect of the vitamin. Schwann cell cytoplasmic changes were seen in other experimental toxic neuropathies, for example in nerves of rats given 2,5-hexanedione (Powell et al, 1978).

Another interesting finding was the presence of myelin vacuolation which was seen at the more distant levels from the site of the injection where most probably the concentration of pyridoxine was lower. Intra-myelin vacuolation occurred in the nerves which received the lowest dose of intraneural pyridoxine, and this was the only abnormality in this experiment which could be related to the dose and concentration of pyridoxine injected. Other substances are known to produce vacuolation of peripheral myelin; these include hexachlorophene (Towfighi et al, 1973) (also causing central nervous system myelin vacuolation) and cuprizone (Love, 1988) which produces a distal peripheral axonopathy but also some myelin vacuolation. Intramyelinic vacuoles in the CNS are known to be caused by triethyl tin (Jacobs et al, 1977), isoniazid (Blakemore, 1980) and cycloleucine (Lee, Surtees and Duchen, 1992). The vacuolation is caused by

accumulation of fluid between the lamellae of the myelin sheath. In all of these cases the separation of myelin lamellae occurs at the intraperiod line, but in pyridoxine-induced vacuolation, splitting was at the major dense line. The cause of myelin vacuolation by whatever agent is not understood, however, it does suggest a direct effect on the myelin-forming cell - in the case of pyridoxine, the Schwann cell.

In view of the apparently enhanced regenerating response produced by intraneural pyridoxine, it was decided to study its effects on nerves regenerating after a crush lesion. The animals used in this experiment were killed 14 days after crush and contemporaneous pyridoxine injection. By this time most of the regenerating fibres were myelinated and were large enough for morphometric studies. There were several problems with this experiment particularly in relation to the levels of nerve examined, so that regeneration with and without pyridoxine could be compared. The final impression was that in pyridoxine- injected nerves there were increased numbers of regenerating fibres and that myelination was somewhat more advanced. It is likely that the effects of pyridoxine are quite transient.

The only study of the possible effects of pyridoxine (combined with thiamine and cyanocobalamin) on nerve regeneration appears to be that of Becker, Kienecker and Dick (1990). A cold-induced lesion was made in the saphenous nerve of rabbits. The effects of daily intramuscular injections of the vitamin mixture (commonly used in medical practice in a wide variety of conditions) on regeneration was studied. Unfortunately, the findings are difficult to interpret because of inadequate information. The number of

regenerated myelinated axons in the experimental group was described as significantly higher than the control group. However, they also found that the number of **degenerated** fibres was lower in the treated nerves than in the controls, which leaves one in doubt as to the effectiveness of the cold lesion in causing total fibre degeneration.

Further studies might be worthwhile to investigate the effect of low levels of pyridoxine on regeneration, although currently the main problem with pyridoxine in a therapeutic setting appears to be recognition of a safe dose (Bernstein, 1990). Clinical studies in patients with diabetic neuropathy and carpal syndrome, given doses of 150 or 100mg/day, some for as long as 5 years, have shown no evidence either of deterioration or of improvement of their neuropathies, although the need for a long-term study is acknowledged.

CHAPTER 5. CONCLUSIONS

Many factors have a bearing on the expression of pyridoxine neurotoxicity, such that variable responses of individual animals were seen in the present study, precluding the construction of a dose response curve.

Nevertheless, within the doses and time scales of these experiments, pyridoxine did cause degeneration of DRG cells, albeit in small numbers. In this sense the pathology can be described as a neuronopathy. The majority of the DRG cells, however, are affected sublethally, and some may remain unaffected. Accumulation of phosphorylated neurofilaments was the most significant finding in these cells. This suggests that interference with axoplasmic flow is a major effect of the pyridoxine and is associated with the axonal changes which ultimately lead to a "dying back" pattern of axonal degeneration of both centrally and peripherally directed sensory fibres. Whilst suspected as a pathological process by Krinke (1978) the "dying back" distribution of fibre degeneration had not been demonstrated previously.

According to the view of Spencer and Schaumburg (1978) distal axonopathies are due to local, neurotoxic effects upon the axon, a mechanism confirmed in the case of hexacarbon, CS_2, organophosphorous and isoniazid neuropathies. Pyridoxine, however, appears to act directly on the posterior root ganglion cells and thus interferes with axoplasmic flow and causes a "dying-back" neuropathy. This mechanism is in agreement with Cavanagh's concept of neurotoxic substances acting on the perikaryon

leading to distal axonal degeneration.

The presence of chromatolysis, as with the dispersion of rough endoplasmic reticulum in pyridoxine toxicity, has been regarded as evidence of the toxin causing damage locally to the axon. Thus the unaffected cell body would be capable of axonal regeneration and the chromatolysis is due to the axon reaction. By this argument, the presence of chromatolysis would seem to exclude the possibility of a primary effect upon the neuron. However, in the present study, it seems likely that the chromatolysis-like changes are due to a direct effect of the pyridoxine on the neuron.

Whilst DRG vascular permeability must be of importance in allowing the ready access of pyridoxine to the DRG cells, it is probably the metabolic demands of these cells that dictate the pattern of this neuropathy, since there is little evidence of affects on the other regions studied which are without a blood nerve barrier.

Local injection of pyridoxine into nerve caused massive fibre degeneration even with the smallest doses used. Paradoxically, there was evidence of enhanced regeneration possibly related to short term effects of pyridoxine upon Schwann cells. This finding also emphasises the direct effect of systemically administered pyridoxine on the dorsal root ganglion cells.

Although this study has established the "dying-back" nature of the neuropathy, the major action of the toxin on the dorsal root ganglion cells, and the effect on axonal transport, the biochemical mechanisms by which pyridoxine causes a neuropathy remain to be elucidated.

CHAPTER 6. REFERENCES

Abercrombie M, Johnson ML (1946) Quantitative histology of Wallerian degeneration. I. Nuclear population in rabbit sciatic nerve. *Journal of Anatomy*, **80**, 37-50.

Aguayo AJ, Bray GM (1975) Pathology and pathophysiology of unmyelinated nerve fibres. In: *Peripheral Neuropathy* (Eds. Dyck PJ, Thomas PK, Lambert EA) WB Saunders, Philadelphia, 363-390

Aguayo AJ, David S, Richardson PM, Bray GM (1982) Axonal elongation in peripheral and central nervous system transplants. In: *Advances in Cellular Neurobiology* (Eds. Fedoroff S, Hertz L) Vol. 3, Academic Press, New York, 215-234.

Aitken JT, Sharman M, Young JZ (1947) Maturation of regenerating nerve fibres with various peripheral connections. *Journal of Anatomy*, **81**, 1-22.

Albin RL, Albers JW (1990) Long-term follow-up of pyridoxine-induced acute sensory neuropathy-neuronopathy. *Neurology*, **40**, 1319.

Albin RL, Albers JW, Greenberg HS, Townsend JB, Lynn R B, Burke JM, Alessi AG (1987) Acute sensory neuropathy - neuronopathy from pyridoxine overdose. *Neurology*, **37**, 1729-1732.

Andres KH (1961) Untersuchungen über den Feinbau von Spinalganglien. *Zeitschrift für Zellforschung und mikroskopische Anatomie*, **55**, 1-48.

Antopol W, Tarlov IM (1942) Experimental study of the effects produced by large doses of vitamin B_6. *Journal of Neuropathology and Experimental Neurology*, **1**, 330-336.

Asbury AK, Gale MK, Cox SC, Baringer JR, Berg BO (1972) Giant axonal neuropathy - a unique case with segmental neurofilamentous masses. *Acta Neuropathologica*, **20**, 237-247.

Bauernfeind JC, Miller ON (1976) Pyridoxine: nutritional and pharmaceutical usage, stability, bioavailability, antagonists and safety. In: *Human vitamin*

B_6 requirements. Washington DC: National Academy of Sciences USA, 78-100.

Becker KW, Kienecker EW, Dick P (1990) A contribution to the scientific assessment of degenerative and regenerative processes in peripheral nerve fibres following axonotmesis under the systemic administration of vitamins B_1, B_6 and B_{12} - light and electron microscopy findings in the saphenous nerve of the rabbit. *Neurochirurgia*, **33**, 113-121.

Beesley R A, Daniel P M (1956) A simple method for preparing serial blocks of tissue. *Journal of Clinical Pathology*, **9**, 267-268.

Berger A, Schaumburg H H (1984) More on neuropathy from pyridoxine abuse. *New England Journal of Medicine*, **311**, 986-987).

Bernstein AL (1990) Pyridoxine in clinical neurology. *Annals of the New York Academy of Sciences*, **585**, 250-260.

Berthold CH (1978) Morphology of normal peripheral axons. In: *Physiology and Pathology of Axons* (Ed. Waxman S G), Raven Press, New York, 3-63.

Beuche W, Friede RL (1984) The role of non-resident cells in Wallerian degeneration. *Journal of Neurocytology*, **13**, 767-796.

Beuche W, Friede RL (1985) A new approach toward analyzing peripheral nerve fibre populations. II. Foreshortening of regenerated internode corresponds to reduced sheath thickness. *Journal of Neuropathology and Experimental Neurology*, **44**, 73-84.

Biehl JP, Vilter RW (1954). Effects of isoniazid on vitamin B_6 metabolism, its possible significance in producing isoniazid neuritis. *Proceedings of the Society of Experimental Biology* (N.Y.), **85**, 389-392.

Bigotte L, Arvidson B, Olsson Y (1982) Cytofluorescence localization of adriamycin in the nervous system. II Distribution of the drug in somatic and autonomic peripheral nervous systems of normal adult mice after intravenous injection. *Acta Neuropathologica*, **57**, 130-136.

Black AL, Guirard BM, Snell EE (1978) The behaviour of muscle

phosphorylase as a reservoir for vitamin B_6 in the rat. *Journal of Nutrition*, **108**, 670-677.

Black MM, Lasek RJ (1980) Slow components of axonal transport. Two cytoskeletal networks. *Journal of Cell Biology*, **86**, 616-623.

Blakemore WF (1980) Isoniazid. In: *Experimental and Clinical Neurotoxicology*. (Eds. Spencer PS, Schaumburg HH). Williams and Wilkins, Baltimore, 476-489.

Bouldin TW, Cavanagh JB (1979a) Organophosphorous neuropathy I. A teased-fiber study of the spatio-temporal spread of axonal degeneration. *American Journal of Pathology*, **94**, 241-252.

Bouldin TW, Cavanagh JB (1979b) Organophosphorous neuropathy II. A fine-structural study of the early stages of axonal degeneration, *American Journal of Pathology*, **94**, 253-262.

Bradbury MWB, Crowder J (1976) Compartments and barriers in the sciatic nerve of the rabbit. *Brain Research*, **103**, 515-526.

Bradley WG, Asbury AK (1970) Duration of synthesis phase in neurilemmal cells in mouse sciatic nerve during degeneration. *Experimental Neurology*, **26**, 275-282.

Bush MS, Reid AR, Allt G (1993) Blood-nerve barrier: ultrastructural and endothelial surface charge alterations following nerve crush. *Neuropathology and Applied Neurobiology*, **19**, 31-40.

Carden MJ, Trojanowsky JQ, Schlaepfer WW, Lee VM-Y (1987) Two stage expression of neurofilament polypeptides during rat neurogenesis with early establishment of adult phosphorylation patterns. *Journal of Neuroscience*, **7**, 3489-3504.

Cavanagh JB (1954) The toxic effects of tri-ortho-cresyl phosphate on the nervous system. An experimental study in hens. *Journal of Neurology, Neurosurgery and Psychiatry*, **17**, 163-172.

Cavanagh JB (1967) On the pattern of change in peripheral nerves produced by isoniazid intoxication in rats. *Journal of Neurology, Neurosurgery and Psychiatry*, **30**, 26-33.

Clemence A, Mirsky R, Jessen KR (1989) Non-myelin forming schwann cells proliferate rapidly during Wallerian degeneration in the rat sciatic nerve. *Journal of Neurocytology*, **18**, 185-192.

Coburn SE, Townsend DW (1989) Modelling vitamin B_6 metabolism in rodents (review). *In-Vivo*, **3**, 215-223.

Compton MM, Cidlowski JA (1986) Vitamin B_6 and glucocorticoid action. *Endocrinological Review*,**7**, 140-148.

Costa-Jussà FR, Jacobs JM (1985) The pathology of amiodarone neurotoxicity. I Experimental studies with reference to changes in other tissues. *Brain*, **108**, 735-752.

Dalton K, Dalton MJT (1987) Characteristics of pyridoxine overdose neuropathy syndrome. *Acta Neurologica Scandinavica*, **76**, 8-11.

Doinikow B (1913) Histologische und histopathologische Untersuchungen am peripheren Nervensystem mittels Vitallen Farbung. *Folio Neurobiologica*, **7**, 731-749.

Dow, PR, Shinn SL, Ovalle WK (1980) Ultrastructural study of a blood-muscle spindle barrier after systemic administration of horseradish peroxidase. *American Journal of Anatomy*, **157**, 375-388.

Dräger UC, Hofbauer A (1984) Antibodies to heavy neurofilament subunit detect a subpopulation of damaged ganglion cells in retina. *Nature*, **309**, 624-628.

Droz B, Rambourg A, Koenig HL (1975) The smooth endoplasmic reticulum: structure and role in the renewal of axon membrane and synaptic vesicles by fast axonal transport. *Brain Research*, **93**, 1-13.

Duce IR, Keen P (1976) A light and electron microscope study of changes

occurring at the cut ends following section of the dorsal root of rat spinal nerves. *Cell Tissue Research*, **170**, 491-505.

Dyck PJ, Hopkins AP (1972) Electron microscopic observation on degeneration and regeneration of unmyelinated fibres. *Brain*, **95**, 223-234.

Ehrlich P (1885) *Das Sauerstoff-Bedurfnis des Organismus*. Hirschwald, Berlin.

Ellisman MH, Lindsey JD (1983) The axoplasmic reticulum within myelinated axons is not transported rapidly. *Journal of Neurocytology*, **12**, 393-411.

d'Eshougues JR, Gille C, Smadja A (1961) Intolerance a la chloroquine et deficit en pyridoxine en trois cas de maladie lupique. *Presse Medicale*, **69**,2524.

Ferri G L, Zareh S, Amadori A, Bastone A, Sbraccia M, Dahl D, Frontali N (1988) 2,5-Hexanedione-induced accumulations of neurofilament-immunoreactive material throughout the rat autonomic nervous system. *Brain Research*, **444**, 383-388.

Frater-Schröder M, Alder S, Zbinden G. (1976) Neurotoxic effects of pyridoxine and analogs in rats. In: *The Prediction of Chronic Toxicity from Short Term Studies* (Eds. Duncan WAM, Leonard BJ, Brunaud M) Excerpta Medica, American Elsevier Publishing Company, Inc. New York 277-284.

Fujimoto S (1966) Effect of pyridoxal phosphate on toxicity and antitumor activity of mitomycin-C and 4-deoxypyridine hydrochloride in rats: Preliminary observations. *Cancer Chemotherapy Reports*, **50**, 313-318.

Frater-Schröder M, Mahrer-Busato M. (1975) A model reaction demonstrating alkylating properties of pyridoxal, involving an o-quinone methide intermediate. *Bioorganic Chemistry*, **4**, 332-341.

Friede RL, Beuche WA (1985) A new approach toward analyzing peripheral nerve populations. I. Variance in sheath thickness corresponds to different geometric proportion of the internodes. *Journal of Neuropathology and Experimental Neurology*, **44**, 60-72.

Friede RL, Bischhausen R (1980) The fine structure of stumps of transected nerve fibers in subserial sections. *Journal of Neurological Sciences*, **44**, 181-203.

Friede RL, Miyagishi T, Hu KH (1971) Axon caliber, neurofilaments, microtubules, sheath thickness and cholesterol in cat optic nerve fibers. *Anatomical Record*, **108**, 365-373.

Friede RL, Samorajski T (1967) Relation between the number of myelin lamellae and axon circumference of fibers of vagus and sciatic nerves of mice. *Journal of Comparative Neurology*, **130**, 223-231.

Friede RL, Samorajski T (1970) Axon caliber related to neurofilaments and microtubules in sciatic nerve fibers of rats and mice. *Anatomical Record*, **167**, 379-387.

Food Chemicals Codex, Second Edition, 1972, National Academy of Sciences, Washington, DC, 689.

Forno LS, Sternberger LA, Sternberger NH, Streffing AM, Swanson K, Eng LF (1986). Reaction of Lewy bodies with antibodies to phosphorylated and non-phosphorylated neurofilaments. *Neuroscience Letters*, **64**, 253-258.

Gammon GD, Bunge FW, King G (1953) Neural toxicity in tuberculous patients treated with isoniazid. *Archives of Neurology and Psychiatry* (Chicago) **70**, 64-69.

Goldstein ME, Sternberger NH, Sternberger LA (1987) Phosphorylation protects neurofilaments against proteolysis. *Journal of Neuroimmunology*, **14**, 149-160.

Gowers WR (1986) A manual of diseases of the nervous system. **Vol I**, *Diseases of the spinal cord and nerves*. J and A Churchill, London.

Greenfield JG (1954) *The Spinocerebellar Degenerations*, Blackwell, Oxford, 14-15.

Gregg RW, Mole POJM, Montpetit VJ, Mikael NZ, Redmond D, Gadia M,

Stewart DJ (1992) Cisplatin neurotoxicity: the relationship between dosage, tissue and platinum concentration in neurologic tissues and morphologic evidence of toxicity. *Journal of Clinical Oncology*, **10**, 795-803.

Griffin J, Cork LC, Toncoso JC, Price DL (1982) Experimental neurotoxic disorders of motor neurons: neurofibrillary pathology. *Advances in Neurology*, **36**, 389-403.

Griffin JW, Hoffman PN (1993) Degeneration and regeneration in the peripheral nervous system. In: *Peripheral Neuropathy*, (Eds. Dyck PJ, Thomas PK, Griffin JW, Low PA, Poduslo JF), WB Saunders, Philadelphia, 361-376.

Griffin JW, Watson F (1988) Axonal transport in neurological disease. *Annals of Neurology*, **23**, 3-13.

Gunn ADG (1985), Vitamin B_6 and the premenstrual syndrome. In: *International Journal for Vitamin and Nutrition Research*, (Eds. Hanck A, Hornig D), suppl. **27**, 213-224.

Gutmann E, Sanders FR (1983) Recovery of fibre numbers and diameter in the regeneration of peripheral nerves. *Journal of Physiology* (London), **101**, 489-518.

Gyorgy P (1934) Vitamin B_2 and the pellagra-like dermatitis in rats. Nature, **133**, 498-499.

Gyorgy P (1935) Investigations on the vitamin B_2 complex: The differentiation of lactoflavin and the "rat antipellagra factor". *Biochemistry Journal*, **29**, 741-775.

Haftek J, Thomas PK (1968) Electron microscope observations on the effects of localized crush injuries on the connective tissues of peripheral nerve. *Journal of Anatomy*, **103**, 233-243.

Hall SM (1986) The effect of inhibiting Schwann cell mitosis on the reinnervation of acellular allografts in the peripheral nervous system. *Neuropathology and Applied Neurobiology*, **12**, 401-414.

Hall SM (1989) Regeneration in the peripheral nervous system. *Neuropathology and Applied Neurobiology*, **15**, 513-529.

Hanrahan JP, Gordon MA (1989) Mushroom poisoning. *Journal of the American Medical Association*, **251**, 1057-1061.

Hatai S (1902) Number and size of the spinal ganglion cells and dorsal root fibres in the white rat at different ages. *Journal of Comparative Neurology*, **12**, 107-124.

Henderson LM (1985) Intestinal absorption of B_6 vitamers. In: *Vitamin B_6: its role in health and disease*, (Eds, Reynolds RD, Leklem JE), Alan R Liss, New York, 25-33.

Henderson LM, Hulse JD (1978) Vitamin B_6 relationship in tryptophan metabolism. In: National Research Council. *Human vitamin B_6 requirements*. Washington DC: National Academy of Sciences, 21-36.

Hendry IA, Stoeckel K, Thoenen H, Iversen LL (1974) The retrograde axonal transport of nerve growth factor. *Brain Research*, **68**, 103-121.

Herdegen T, Fiallos-Estrada CE, Bravo R, Zimmermann M (1993) Colocalisation and covariation of c-JUN transcription factor with galanin in primary afferent neurons and with CGRP in spinal motoneurons following transection of rat sciatic nerve. *Molecular Brain Research*, **17**, 147-154.

Herdegen T, Kummer W, Fiallos-Estrada CE, Bravo R (1991) Expression of c-JUN, JUN B and JUN D proteins in rat nervous system following transection of vagus nerve and cervical sympathetic trunk. *Neuroscience*, **45**, 413-422.

Hildebrand C, Mustafa GY, Bowe C, Kocsis D (1987) Nodal spacing along regenerated axons following a crush lesion of the developing rat sciatic nerve. *Developmental Brain Research*, **32**, 147-154.

Hines JD, Cowan DH (1970) Studies on the pathogenesis of alcohol induced sideroblastic bone-marrow abnormalities. *New England Journal of Medicine*, **283**, 441-446.

Hodges R E (1982) Megavitamin therapy. *Primary Care*, **9**, 605-619.

Hoffman PN, Griffin JW (1993) The control of axonal caliber. In: *Peripheral Neuropathy*, (Eds. Dyck PJ, Thomas PK, Griffin JW, Low PA, Poduslo JF), WB Saunders, Philadelphia, 389-402.

Hoffman PN, Lasek R (1975) The slow component of axonal transport. Identification of major structural polypeptides of the axon and their generality among mammalian neurons. *Journal of Cell Biology*, **66**, 351-366.

Hoffman PN, Lasek RJ (1980) Axonal transport of the cytoskeleton in regenerating motor neurons: constancy and change. *Brain Research*, **202**, 317-333.

Hoffman PN, Thompson GW, Griffin JW, Price DL (1985) Changes in neurofilament transport coincide temporally with alterations in the caliber of axons in regenerating motor fibres. *Journal of Cell Biology*, **101**, 1332-1340.

Holtzman E (1971) Cytochemical studies of protein transport in the nervous system. *Philosophical transactions of the Royal Society of London* B, **261**, 407-21.

Hughes HB, Biehl JP, Jones AP, Schmidt LH (1954) Metabolism of isoniazid in man as related to the occurrence of peripheral neuritis. *American Review of Tubercular Pulmonary Disease*, **70**, 266-273.

Ink SL, Henderson LM (1984) Vitamin B6 metabolism. *Annals Review Nutrition*, **4**, 455-470.

Jacobs JM (1977) Penetration of systemically injected horseradish peroxidase into ganglia and nerves of the autonomic nervous system. *Journal of Neurocytology*, **6**, 607-618.

Jacobs JM (1980) Vascular permeability and neural injury. In: *Experimental and Clinical Neurotoxicology*, (Eds Spencer PS, Schaumburg HH) Williams and Wilkins, Baltimore, 102-117.

Jacobs JM, Carmichael N, Cavanagh JB (1975) Ultrastructural changes in the dorsal root and trigeminal ganglia of rats poisoned with methyl mercury. *Neuropathology and Applied Neurobiology*, **1**, 1-19.

Jacobs JM, Cremer JE, Cavanagh JB (1977) Acute effects of triethyltin on the rat myelin sheath. *Neuropathology and Applied Neurobiology*, **3**, 169-181.

Jacobs JM, Le Quesne PM (1992) Toxic disorders In: *Greenfield's Neuropathology* (Eds: Adams JH, Duchen LW) Edward Arnold, London, 881-987.

Jacobs JM, Love S (1985) Qualitative and quantitative morphology of human sural nerves at different ages. *Brain*, **108**, 897-204.

Jacobs JM, Macfarlane RM, Cavanagh JB (1976) Vascular leakage in the dorsal root ganglia of the rat studied with horseradish peroxidase. *Journal of the Neurological Sciences*, **29**, 95-107.

Jacobs JM, Miller RH, Cavanagh JB (1979) The distribution of degenerative changes in INH neuropathy. Further evidence for focal axonal lesions. *Acta Neuropathologica*, **48**, 1-9.

Jacobs JM, Miller RH, Whittle A, Cavanagh JB (1979) Studies on the early changes in acute isoniazid neuropathy in the rat. *Acta Neuropathologica*, **47**, 85-92.

Jessell TM, Dodd J (1986) Neurotransmitters and differentiation antigens in subsets of sensory neurons projecting to the spinal dorsal horn. In: *Neuropeptides in Neurologic and Psychiatric Disease*. (Eds. Martin JB, Barchas JD), Raven Press, New York, 111-133.

Jones HB, Cavanagh JB (1986) The axon reaction in spinal ganglion neurons of acrylamide in treated rats. *Acta Neuropathologica* **71**, 55-63.

Jones WA, Jones GP (1953) Peripheral neuropathy due to isoniazid. *Lancet*, **1**, 1073-4.

Julien JP, Mashynski WE (1983) The distribution of phosphorylation sites among identified proteolytic fragments of mammalian neurofilaments. *Journal of Biological Chemistry*, **258**, 4019-4025.

Kabir H, Leklem JE, Miller LT (1983) Measurements of glycosylated vitamin B_6 in foods. *Journal of Food Sciences*, **48**, 1422-1425.

Karnes J, Robb R, O'Brien PC, Lambert EH, Dyck PJ (1977) Computerized image analysis recognition for morphometry of nerve attribute of shape of sampled transverse sections of myelinated fibres which best estimates their average diameter. *Journal of the Neurological Sciences*, **34**, 43-51.

Karnovsky NJ (1965) A formaldehyde-glutaraldehyde fixative of high osmolarity for use in electron microscopy. *Journal of Cell Biology*, **27**, 137A.

Kikuchi T, Mukoyama M, Yamazaki K, Moriya H (1990) Axonal degeneration of ascending sensory neurons in gracile axonal dystrophy mutant mouse. Acta Neuropathologica (Berlin), **80**, 145-151.

Kiernan JA (1979) Hypotheses concerned with axonal regeneration in the mammalian nervous tissue. *Biology Review*,**54**, 155-197.

Klosterman HJ (1974) Vitamin B_6 antagonists of natural origin. *Journal of Agriculture and Food Chemistry*, **22**, 13-16.

Knight RA, Selin MJ, Harris HW (1959) Genetic factors influencing isoniazid blood levels in humans. *Trans-American Conference on Tuberculosis Chemotherapy*, **18**, 52.

Korner WF, Vollm J (1975) New aspects of the tolerance of retinol in humans. *International Journal of Vitamins and Nutrition Research*, **45**, 363-379.

Krinke G, Heid J, Bittiger H, Hess R (1978) Sensory denervation of the plantar lumbrical muscle spindles in pyridoxine neuropathy. *Acta Neuropathologica*, **43**, 213-6.

Krinke G, Naylor DC, Skorpil V (1985) Pyridoxine megavitaminosis: an analysis of the early changes induced with massive doses of vitamin B_6 in rat primary sensory neurons. *Journal of Neuropathology and Experimental Neurology*, **44**, 117-129.

Krinke G, Schaumburg HH, Spencer PS, Surtees J, Thomann P, Hess R (1980) Pyridoxine megavitaminosis produces degeneration of peripheral sensory neurons (sensory neuronopathy) in the dog. *Neurotoxicology*, **2**, 13-24.

Lasek RJ (1982) Translation of the neuronal cytoskeleton and axonal locomotion. *Philosophical Transactions of the Royal Society of London* B, **229**, 313-327.

Lasek RJ, Oblinger MM, Drake PF (1983) Molecular biology of neuronal geometry: Expression of neurofilament genes influences axonal diameter. *Cold Spring Harbor Symposia of Quantitative Biology*, **48**, 731-744.

Lawson SN (1979) The postnatal development of large light and small dark neurons in mouse dorsal root ganglia: a statistical analysis of cell numbers and size. *Journal of Neurocytology*, **8**, 275-94.

Lawson SN, Harper AA, Harper EI, Garson JA, Anderton BH (1984) A monoclonal antibody against neurofilament protein specifically labels a subpopulation of rat sensory neurones. *Journal of Comparative Neurology*, **228**, 263-72.

Le Quesne PM (1975) Neuropathy due to drugs. In: *Peripheral Neuropathy* (Eds. Dyck PJ, Thomas PK, Lambert EH) WB Saunders, Philadelphia, 1263-1280.

Lee C-C, Surtees R, Duchen LW (1992) Distal motor axonopathy and central nervous system myelin vacuolation caused by cycloleucine, an inhibitor of methionine adenosyltransferase. *Brain*, **115**, 935-955.

Lee VM-Y, Otvos L, Carden MJ, Hollosi M, Dietzcshold B, Lazzarini RA (1988) Identification of the major multiphosphorylation site in mammalian neurofilaments. *Proceedings of the National Academy of Sciences U.S.A*, **85**, 1998-2002.

Leklem JE (1988) Vitamin B_6 metabolism and function in humans. In: *Clinical and Physiological Applications of vitamin B_6* (Ed. Leklem JE) Alan Liss, Inc, New York, 3-28.

Leklem JE, Shultz TD (1983) Increased plasma pyridoxal 5'-phosphate and vitamin B_6 in male adolescents after a 4500 meter run. *American Journal of Clinical Nutrition*, **38**, 541-548.

Lepkovsky S, Jukes T, Krause M (1936) The multiple nature of the third factor of the vitamin B complex. *Journal of Biological Chemistry*, **115**, 557-566.

Lewandowsky M (1900) Zur Lehre von der Cerebrospinalflussigheit. *Zeitschrift Klinische Medizin*, **40**, 480-494.

Lieberman AR (1976) Sensory ganglia. In: *The peripheral Nerve*, (Ed. Landon DN), Chapman and Hall, London, 188-278.

Lindenbaum MN, Carbonetto S, Grosveld F, Flavell D, Mushinski WE (1988) Transcriptional and post-transcriptional effects of nerve growth factor on expression of the three neurofilament subunits in PC-12 cells. *Journal of Biological Chemistry*, **263**, 5662-5667.

Lindholm D, Heumann R, Meyer M, Thoenen H (1987) Interleukin-1 regulates synthesis of nerve growth factor in non-neuronal cells of rat sciatic nerve. *Nature*, (London) **330**, 658-659.

Litersky JM, Johnson GV (1992) Phosphorylation by cAMP-dependent protein kinase inhibits the degradation of tau by calpain. *Journal of Biological Chemistry*,**267**, 1563-1568.

Litwack G, Miller-Diener A, DiSorbo DM, Schmidt TJ (1985) Vitamin B_6 and the glucocorticoid receptor. In: *Vitamin B_6 its role in health and disease*, (Eds. Reynolds RD, Leklem JE) Alan R Liss, New York, 177-191.

Love S (1988) Cuprizone neurotoxicity in the rat: morphologic observations. *Journal of the Neurological Sciences*, **84**, 223-237.

Lumeng L, Brashear RE, Li TK (1974) Pyridoxal 5'-phosphate in plasma: source, protein binding and cellular transport. *Journal of Laboratory and Clinical Medicine*, **84**, 334-343.

Lumeng L, Cleary RE, Li TK (1974) Effect of oral contraceptives on the plasma concentration of pyridoxal phosphate. *American Journal of Clinical Nutrition*, **27**, 326-333.

Maeda N, Kon K, Sekiya M, Shiga T (1980) Functional restoration of ACD-blood by pyridoxal 5'-phosphate. *British Journal of Haematology*, **45**, 467-480.

Maia M, Pires MM, Guimarães A (1988) Giant axonal disease. Report of three cases and review of the literature. *Neuropediatrics*, **19**, 10-15.

Marsland TA, Glees P, Erikson LB (1954) Modification of the Glees silver impregnation for paraffin sections. *Journal of Neurology, Neurosurgery and Psychiatry*, **13**, 587-591.

Mata M, Kupina N, Fink DJ (1992) Phosphorylation-dependent neurofilament epitopes are reduced at the node of Ranvier. *Journal of Neurocytology*, **21**, 199-210.

McCormick DB, Gregory ME, Snell EE (1961) Pyridoxal phosphokinases. 1-Assay, distribution, purification and properties. *Journal of Biological Chemistry*, **236**, 2076-2084.

McCormick DB, Snell EE (1959) Pyridoxal kinase of human brain and its inhibition by hydrazine derivatives. *Proceedings of the National Academy of Sciences USA*, **45**, 1371-1379.

Merril AH Jr, Henderson JM, Wang E, Codner MA, Hollins B, Millikan WJ (1986) Activities of the hepatic enzymes of vitamin B_6 metabolism for patients with cirrhosis.*American Journal of Clinical Nutrition*, **44**, 461-467.

Merril AH Jr, Henderson JM, Wang E, McDonald BW, Millikan WJ (1984) Metabolism of vitamin B6 by human liver. *Journal of Nutrition,* **114**, 1664-1674.

Middleton HM (1982) Characterization of pyridoxal 5'-phosphate disappearance from in vivo perfused segments of rat jejunum. *Journal of Nutrition*, **112**, 269-275.

Miura H, Oda K, Endo C, Yamazaki K, Shibasaki H, Kikuchi T (1993) Progressive degeneration of motor nerve terminals in GAD mutant mouse with hereditary sensory axonopathy. *Neuropatholoy and Applied Neurobiology*, **19**, 41-51.

Monaco S, Autilio-Gambetti L, Lasek RS, Katz MJ, Gambetti P (1989) Experimental increase of neurofilament transport rate: decreases in neurofilament number and in axon diameter. *Journal of Neuropathology and Experimental Neurology*, **48**, 23-32.

Montpetit VJA, Clapin DF, Tryphonas L, Dancea S (1988) Alteration of neuronal cytoskeletal organization in dorsal root ganglia associated with pyridoxine neurotoxicity. *Acta Neuropathologica*, **76**, 71-81).

Nixon RA (1993) The regulation of neurofilament protein dynamics by phosphorylation: Clues to neurofibrillary pathobiology. *Brain Pathology*, **3**, 29-38.

Nixon RA, Brown BA, Marotta CA (1982) Posttranslational modifications of a neurofilament protein during axoplasmic transport. Implications for regional specialization of CNS axons. *Journal of Cell Biology*, **94**, 150-158.

Nixon RA, Lewis SE, Dahl D, Marotta CA, Drager UC (1989) Post-translational modifications of the three neurofilament subunits in mouse retinal ganglion cells: Neuronal sites and time course in relation to subunit polymerization and axonal transport. *Molecular Brain Research*, **5**, 93-108.

Nixon RA, Paskevich P, Sihag RK, Wheelock T (1991) Morphologic correlates of neurofilament carboxyl terminal phosphorylation. *Journal of Cell Biology*, **115**, 365 (abstract).

Nowak TSJ, Bond V, Schlesinger MJ (1990) Heat shock RNA levels in brain and other tissues after hyperthermia and transient ischemia. *Journal of Neurochemistry*, **54**, 451-458.

Oblinger MM (1988) Biochemical composition and dynamics of the axonal cytoskeleton in the corticospinal system of the adult hamster. *Metabolism of Brain Disorders*, **3**, 49-65.

Ochoa J (1970) Isoniazid neuropathy in man: quantitative electron microscopy study. *Brain*, **93**, 831-850.

Ochoa J (1976) The unmyelinated nerve fibre. In: *The Peripheral Nerve*, (Ed. Landon DN), Chapman and Hall, London, 106-158.

Ochoa J, Mair WGP (1969a) The normal sural nerve in man. I. Ultrastructure and numbers of fibres and cells. *Acta Neuropathologica*, **13** 197-216.

Ochoa J, Mair WGP (1969b) The normal sural nerve in man. II. Changes in the axons and Schwann cells due to ageing. *Acta Neuropathologica*, **13**, 217-239.

Ochs S, Brimijoin S (1993) Axonal transport. In: *Peripheral Neuropathy*, (Eds. Dyck PJ, Thomas PK, Griffin JW, Low PA, Poduslo JF), WB Saunders, Philadelphia, 331-360.

Olsson Y (1966) Studies on vascular permeability in peripheral nerves; II Distribution of circulating fluorescent serum albumin in rat sciatic nerve after local injection of histamine 5-hydroxy-tryptamine and compound 48/80. *Acta Physiologica Scandinavica*, **69**, suppl. 284, 1.

Ohta M, Offord K, Dyck PJ (1974) Morphometric evaluation of first sacral ganglia of man. *Journal of the Neurological Sciences*, **22**, 73-82.

Oldfors A (1980) Macrophages in peripheral nerves. An ultrastructural and enzyme histochemical study on rats. *Acta Neuropathologica*, **49**, 43-49.

Ouvrier RA (1989) Giant axonal neuropathy. A review. *Brain Development*, **11**, 207-214.

Pannese E (1974) The histogenesis of the spinal ganglia. *Advances in Anatomy, Embryology and Cell Biology*, **47**, 1-97.

Parhad IM, Clark AW, Griffin JW (1987) Effect of changes in neurofilament content on caliber of small axons: the ß-ß.-iminodipropionitrile model. *Journal of Neuroscience*, **7**, 2256-2263.

Pauling L, Robinson AB, Oxley SS (1973) Results of a loading test of ascorbic acid, niacinamide and pyridoxine in schizophrenic subjects and controls. In: *Orthomolecular Psychiatry: Treatment of Schizophrenia*, (Eds. Hawkins D, Pauling C) WH Freeman, San Francisco, 18-34.

Parry GJ, Bredesen DE (1985). Sensory neuropathy with low dose pyridoxine. *Neurology*, **35**, 1466-1468.

Pécot-Déchavassine M, Mina JC (1985) Effects of isaxonine on skeletal muscle reinnervation in the rat: an electrophysiologic evaluation. *Muscle and Nerve*, **8**, 105-114.

Pegum JS, (1952) Nicotinic acid and burning feet. *Lancet*, **2**, 536.

Perry MJ, Lawson SN, Robertson J (1991) Neurofilament immunoreactivity in populations of rat primary afferent neurons: a quantitative study of phosphorylated and non- phosphorylated sub-units. *Journal of Neurocytology*, **20**, 746-756.

Peyronnard J-M, Charron L (1982) Motor and sensory neurons of the rat sural nerve: a horseradish peroxidase study. *Muscle and Nerve* **5**, 654-660.

Phillips WEJ, Mills JHL, Charbonneau SM, Tryphonas L, Hatina GV, Zawidzka Z, Bryce FR, Munro IC (1978) Subacute toxicity of pyridoxine hydrochloride in the beagle dog. *Toxicology and Applied Pharmacology*, **44**, 323-333.

Pineda A, Maxwell DS, Kruger L (1967) The fine structure of neurons and satellite cells in the trigeminal ganglion of cat and monkey. *American Journal of Anatomy*, **121**, 461-488.

Pogell BM (1958) Enzymatic oxidation of pyridoxamine phosphate to pyridoxal phosphate in rabbit liver. *Journal of Biological Chemistry*, **232**, 761-766.

Powell HC, Koch T, Garrett R, Lampert PW (1978) Schwann cell abnormalities in 2,5-hexanedione neuropathy. *Journal of Neurocytology*, **7**, 517-528.

Price RL, Lasek RJ, Katz MJ (1990) Internal axonal cytoarchitecture is shaped locally by external compressive forces. *Brain Research*, **530**, 205-214.

Prineas J (1969a) The pathogenesis of dying back polyneuropathies: I. An ultrastructural study of experimental tri-ortho-cresyl phosphate intoxication in the cat. *Journal of Neuropathology and Experimental Neurology*, **38**, 571-597.

Prineas J (1969b) The pathogenesis of dying back polyneuropathy: II. An ultrastructural study of experimental acrylamide intoxication in the cat. *Journal of Neuropathology and Experimental Neurology*, **28**, 598-621.

Ramón y Cajal S (1928) Degeneration and Regeneration of the Nervous System (RM May, Trans.) Oxford University Press, London.

Reale E, Luciano L, Spitznas M (1975) Freeze-fracture faces of the perineurial sheath of the rabbit sciatic nerve. *Journal of Neurocytology*, **4**, 261-270.

Reese TS, Karnovsky MJ (1967) Fine structural localisation of a blood brain barrier to exogenous peroxidase. *Journal of Cell Biology*, **34**, 207-217.

Reynolds EH (1975) Chronic antiepileptic toxicity: A review. *Epilepsia*, **16**, 319-352.

Reynolds ES (1963) The use of lead citrate at high pH as an electron opaque stain in electron microscopy. *Journal of Cell Biology*, **17**, 208-212.

Reynolds RD, Leklem JE (1985) Vitamin B_6: its role in health and disease. Alan R Liss, New York.

Rimland B, Callaway E, Dreyfus P (1978) The effect of high doses of vitamin

B_6 on autistic children: a double blind crossover study. *American Journal of Psychiatry*, 472-475.

Roe DA (1973) Drug induced vitamin deficiencies. *Drug Therapy*, **3**, 23-32.

Roelofs RI, Hrushesky W, Rogin J, Rosenberg, L (1984) Peripheral sensory neuropathy and cisplatin chemotherapy. *Neurology*, **34**, 934-938.

Rordorf G, Koroshetz WJ, Bonventre JV (1991) Heat shock protects cultured neurons from glutamate toxicity. *Neuron*, **7**, 1043-1051.

Roots BI (1983) Neurofilament accumulation induced in synapses by leupeptin. *Science*, **221**, 971-572.

Rose DP, Braidman IP. Excretion of tryptophan metabolites as effected by pregnancy, contraceptive steroids and steroid hormones. *American Journal of Clinical Nutrition*, **24**, 673-683.

Rosen F, Mihich E, Nichol CA (1964) Selective metabolic and chemotherapeutic effects of vitamin B_6 metabolites. *Vitamins and Hormones*, **22**, 609-653.

Rosenfeld J, Dorman ME, Griffin JW, Sternberger LA, Sternberger NH, Price DL (1987) Distribution of neurofilament antigens after axonal injury. *Journal of Neuropathology and Experimental Neurology*, **46**, 269-282.

Rudman D, Williams P (1983) Megadose vitamins: use and misuse. *New England Journal of Medicine*, **309**, 488-490.

Sahenk Z, Mendell JR (1981) Acrylamide and 2,5-hexanedione neuropathies: abnormal bidirectional transport rate in distal axons. *Brain Research*, **219**, 397-406.

Santoro L, Ragno M, Nucciotti R, Barbieri F, Caruso G (1991) Pyridoxine neuropathy. A four-year electro-physiological and clinical follow-up of a severe case. *Acta Neurologica (Napoli)*, **13(1)**, 13-18.

Schaumburg H, Kaplan J, Windebank A, Vick N, Rasmus S, Pleasure D, Brown MJ (1983) Sensory neuropathy from pyridoxine abuse. A new megavitamin syndrome. *New England Journal of Medicine*, **309**, 445-448.

Schaumburg HH, Wisniewski HM, Spencer PS (1974) Ultrastructural studies of the dying back process. I. Peripheral nerve terminals and axon degeneration in systemic acrylamide intoxication. *Journal of Neuropathology and Experimental Neurology*, **23**, 260-284.

Schnapp BJ, Vale RD, Sheetz MP, Reese TS (1985) Single microtubules from squid axoplasm support bidirectional movement of organelles. *Cell*, **40**, 455-462.

Schröder JM (1972) Altered ratio between axon diameters and myelin sheath thickness in regenerated nerve fibres. *Brain Research*, **45**, 49-65.

Scudi JV, Unna K, Antopol W (1940) A study of the urinary excretion of Vitamin B_6 by a calorimetric method. *Journal of Biological Chemistry*, **135**, 371-376.

Seckel BR (1990) Enhancement of peripheral nerve regeneration. *Muscle and Nerve*, **13**, 785-800.

Seitz RJ, Reiners K, Himmelman F, Heininger K, Hartung HP, Toyka KV (1989) The blood-nerve barrier in Wallerian degeneration: a sequential long term study. *Muscle and Nerve*, **12**, 627-635.

Seppäläinen A M, Haltia M (1980) Carbon disulfide. In: *Experimental and Clinical Neurotoxicology* (Eds. Spencer PS, Schaumburg HH), Williams and Wilkins,Baltimore, 356-373.

Sihag RK, Nixon RA (1987) Evidence for site specific dephosphorylation of neurofilament proteins during axonal transport in RGC neurons. *Journal of Cell Biology*, **105**, 207 (abstract).

Smith DB, Gallagher BB (1970) The effect of penicillamine on seizure threshold: The role of pyridoxine. *Archives of Neurology*, **23**, 59-62.

Smith FR, Goodman DS (1976) Vitamin A transport and human vitamin A toxicity. *New England Journal of Medicine*, **294**, 805.

Smith KJ, Blakemore WF, Murray JA Patterson RC (1982) Internodal myelin volume and axon surface area. *Journal of the Neurological Sciences*, **55**, 231-246.

Smith RS (1973) Microtubule and neurofilament densities in amphibian spinal root nerve fibers: relationship to axoplasmic transport. *Canadian Journal of Physiology*, **51**, 798-806.

Snell E, Guirard B, Wiliams R (1942) Occurrence in natural products of a physiologically active metabolite of pyridoxine. *Journal of Biological Chemistry*, **143**, 519-530.

Spector R. (1978a) Vitamin B_6 transport in the central nervous system. In vitro studies. *Journal of Neurochemistry*, **30**, 881-887.

Spector R. (1978b) Vitamin B_6 transport in the central nervous system. In vivo studies. *Journal of Neurochemistry*, **30**, 889-897.

Spencer PS, Peterson ER, Madrid RA, Raine CS (1973) Effects of thallium salts on neuronal mitochondria in organotypic cord-ganglia-muscle combination cultures. *Journal of Cell Biology*, **58**, 79-95.

Spencer PS, Schaumburg HH (1975) Experimental neuropathology produced by 2,5-hexanedione - a major metabolite of the neurotoxic industrial solvent methyl n-butyl ketone. *Journal of Neurology, Neurosurgery and Psychiatry*, **38**, 771-775.

Spencer PS, Schaumburg HH (1978) Pathobiology of neurotoxic axonal degeneration. In: *Physiology and Pathobiology of axons*, (Ed. Waxman S), Raven Press, New York, 265-282.

Spencer PS, Schaumburg HH (1984) Experimental models of primary axonal disease induced by toxic chemicals. In: *Peripheral Neuropathy*, (Eds. PJ Dyck, PK Thomas, EH Lambert, R Bunge) WB Saunders, Philadelphia, 636-649.

Stelmack BM, Kiernan JA (1977) Effects of triiodothyronine on the normal and regenerating facial nerve of the rat. *Acta Neuropathologica*, **40**, 151-155.

Sterman AB (1983) Altered sensory ganglia in acrylamide neuropathy. Quantitaive evidence of neuronal reorganisation. *Journal of Neuropathology and Experimental Neurology*, **42**, 166-176.

Sternberger LA, Sternberger NH (1983) Monoclonal antibodies distinguish phosphorylated and nonphosphorylated forms of neurofilaments in situ. *Proceedings of the National Academy of Sciences USA*, **80**, 6126-6130.

Sternberger NH, Sternberger LA, Ulrich J (1985) Aberrant neurofilament phosphorylation in Alzheimer disease. *Proceedings of the National Academy of Sciences USA*, **82**, 4274-4276.

Stults VJ (1981) Nutritional hazards. In: *Food safety*. (Ed.Roberts HR), John Wiley & Sons, 67-134.

Sturman JA, Kremzner LT (1974) Regulation of ornithine decarboxylase synthesis: effect of a nutritional deficiency of vitamin B_6. *Life Science*,**14**, 977-983.

Thomas PK (1963) The connective tissue of peripheral nerve: an electron microscopic study. *Journal of Anatomy*, **97**, 35-44.

Thomas PK, Landon DN, King RHM (1992) Diseases of peripheral nerves. In: *Greenfield's Neuropathology*, (Eds: Adams JH, Duchen LW) Edward Arnold, London, 1116-1245.

Tokutake S (1990) On the assembly mechanism of neurofilaments. *International Journal of Biochemistry*, **22**, 1-6.

Tomiwa K, Nolan C, Cavanagh JB (1986) The effects of cisplatin on rat spinal ganglia: a study by light and electron microscopy and by morphometry. *Acta Neuropathologica*, **69**, 295-308.

Tomlinson DR (1988) Axonal transport and changes with ageing. *New*

Issues in Neurosciences **1**, 117-124.

Troncoso JC, Sternberger NH, Sternberger LA, Hoffman PN, Price DL (1986) Immunocytochemical studies of neurofilament antigens in the neurofibrillary pathology induced by aluminium. *Brain Research*, **364**, 295-300.

Towfighi J, Gonatas NK, McCree L (1973) Hexachlorophene neuropathy in rats. *Laboratory Investigation*, **29**, 428-436.

Tuellner HU (1987) Gangliosides and their influence on nerve regeneration. A short review of the experimental data. *Therapiewoche*, **37**, 990-996.

Tytell M, Black MM, Garner J, Lasek RJ (1981) Axonal transport: each rate component reflects the movement of distinct manomolecular complexes. *Science*, **214**, 179-181.

Tsukita S, Ishikawa H (1980) The movement of membranous organelles in axons. Electron microscopic identification of anterogradely and retrogradely transported organelles. *Journal of Cell Biology*, **84**, 513-530.

Unna K, Antopol W. (1940) Toxicity of vitamin B_6. *Proceedings of the Society of Experimental Biological Medicine*, **43**, 116-118.

U.S. Pharmacopeia XIX Edition (1975) Pharmacopeial Convention. Rockville. 429.

Vale RD, Reese TS, Sheetz MP (1985) Identification of a novel force-generating protein, kinesin, involved in microtubule-based motility. *Cell*, **42**, 39-59.

Waller A (1850) Experiments on the section of the glossopharyngeal and hypoglossal nerves of the frog, and observations on the alterations produced thereby in the structure of their primitive fibres. *Philosophical Transactions of the Royal Society*, London, B **140**, 423-429.

Watson DF, Griffin JW, Fittro KP, Hoffman PN (1989) Phosphorylation-dependent immunoreactivity of neurofilaments increases during axonal maturation and IDPN intoxication. *Journal of Neurochemistry*, **53(6)**, 1818-

1829.

Watson DF, Fittro KP, Hoffman PN, Griffin JW (1991) Phosphorylation-related immunoreactivity and the rate of transport of neurofilaments in chronic 2,5 hexanedione intoxication. *Brain Research*, **539**, 103-109.

Weinstein L (1975) Drugs used in the chemotherapy of tuberculosis and leprosy. In: *The Pharmacological Basis of Therapeutics* (Eds. Goodman LS, Wilman A), Macmillan, New York, 1204-1207.

Windebank AJ (1985) Neurotoxicity of pyridoxine analogs is related to co-enzyme structure. *Neurochemical Biochemistry*, **3**, 159-167.

Windebank AJ, Low PA, Blexnud MD, Schmelzer JD, Schaumburg HH (1985) Pyridoxine neuropathy in rats: specific degeneration of sensory axons. *Neurology*, **35**, 1617-1622.

Wood JN, Anderton BH (1981) Monoclonal antibodies to mammalian neurofilaments. *Bioscience Reports*. 1:263-268.

Woolliscroft J O (1983) Megavitamins; fact and fancy. *Disease a month*, **29**, 1-56.

Wyburn GM (1958) The capsule of spinal ganglion cells. *Journal of Anatomy*, **92**, 528-533.

Xu Y, Sladky J T, Brown M J (1989) Dose-dependent expression of neuronopathy after experimental pyridoxine intoxication. *Neurology*, **39**, 1077-1083.

Yahr MD, Duvoisin RC, Cote L, Cohen G (1972) Pyridoxine, dopa and parkinson. *Advances in Biochemistry and Pharmacology*, **4**, 185-194.

Yamamoto T (1991) Pathologic processes of lumbar primary sensory neurons produced by high doses of pyridoxine in rats - morphometric and electron microscopic studies. *Journal of the University of Occupational and Environmental Health* (Japan), **13**, 109-123.

Zenker W, Hohberg E (1973) A-α-nerve fibre: number of neurotubules in the stem fibre and in the terminal branches. *Journal of Neurocytology*, **2**, 143-148.